WATCH
Water and Global Change

Technical Report No. 43

DROUGHT AT THE GLOBAL SCALE IN THE 21ST CENTURY

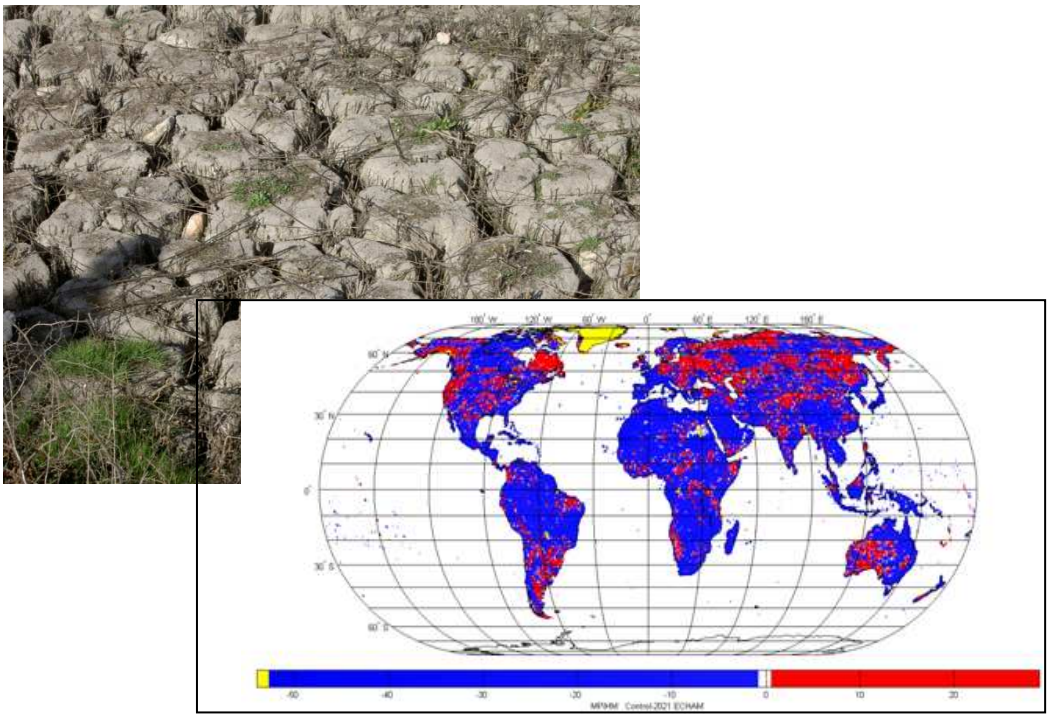

Gerald A. Corzo Perez, Henny A.J. van Lanen, Nathalie Bertrand, Cui Chen, Douglas Clark, Sonja Folwell, Simon N. Gosling, Naota Hanasaki, Jens Heinke & Frank Voβ

25 August 2011

WATCH is an Integrated Project Funded by the European Commission under the Sixth Framework Programme, Global Change and Ecosystems Thematic Priority Area (contract number: 036946).
The WACH project started 01/02/2007 and will continue for 4 years.

Title:	Drought at the global scale in the 21st Century
Authors:	Gerald A. Corzo Perez, Henny A.J. van Lanen, Nathalie Bertrand, Cui Chen, Douglas Clark, Sonja Folwell, Simon N. Gosling, Naota Hanasaki, Jens Heinke & Frank Voβ
Organisations:	- Wageningen University - Hydrology and Quantitative Water Management Group (WUR) - Laboratoire de Météorologie Dynamique (LMD), France - Max Planck Institute for Meteorology, Germany - Centre for Ecology and Hydrology, UK - University of Nottingham, UK - National Institute for Environment Studies, Japan - Potsdam-Institute for Climate Impact Research, Germany - University of Kassel, Germany
Submission date:	25 August 2011
Function:	This report is an output from Work Block 4; Task 4.3.1 Frequency, severity and extent of droughts in 21st century.
Deliverable	WATCH deliverables D 4.3.1 Assessment of the future change in major droughts (part 1) and their main physical aspects (likely frequency, severity, extent), D 4.3.2 Report on the sensitivity of future droughts and large-scale floods for climate change, and it contributes to M4.3-1 Future change of droughts.

Photo cover: Left: dry soil in the Upper-Guadiana Basin (2008)
Right: change in number of drought (2021-2050 vs CTRL) derived from the simulated runoff with the large-scale model MPI-HM, ECHAM A2 scenario

Table of Contents

Introduction

Drought is natural hazard that occurs everywhere across the globe, incl. both high and low rainfall areas. It can develop over short periods (weeks or months) or longer periods (seasons, years or even decades). Over the last decades, various regions in the world were regularly hit hard by drought (e.g. Horn of Africa, Australia, Amazon, USA and Europe). Droughts are complex large-scale phenomena involving numerous interacting climate processes and various land-atmosphere feedbacks. Different stores (e.g. soils, aquifers, lakes) in river basins lead to a complicated propagation of the climate signal into the water system. Although progress is made, the phenomena are still not well understood, which makes it difficult to adequately characterize, monitor and predict drought. Droughts do not directly cause fatalities in most regions across the globe, although poor people in the less-developed countries are very vulnerable and may die because of malnutrition and drinking unsafe water. Drought has large socio-economic and environmental impacts affecting many sectors. These multi-facetted impacts happen both in water-stressed areas, but also in regions where water availability has never before been a major concern. For example, data from Europe over the period 2000-2006 show that each year, on average 15% of the EU total area and 17% of the EU total population have suffered from the impact of droughts. Drought is a recurrent phenomenon in Europe that affects vast areas and millions of people (EEA, 2007; 2008; 2010). The total cost of droughts over the past 30 years amounts to 100 billion Euros (EC, 2007). Other continents also suffer from severe impact of drought (e.g. IPCC 2007b: 2007c; UN-ISDR, 2009; Dai et al., 2009; Bates et al., 2009; Sheffield et al., 2009; Lewis et al., 2011; Kirono et al., 2011).

Global climate change projections indicate that drought is likely to become more frequent and more severe in many regions across the world due to the increased temperatures (higher evaporation demand and less snow) together with decreases in precipitation (e.g. IPCC, 2007a; 2007b; 2007c; Bates et al., 2008; Sheffield & Wood, 2008; Dai 2010). Hence, there is an urgent need to improve drought preparedness through measures that reduce vulnerability to drought and the risks they pose world-wide, in particular considering the uncertain future.

This study intercompares global future hydrological drought (21st century) in a multi-model setting. The multi-model experiments of the EU-funded WATCH project (www.eu-watch.org) provide the opportunity for such analyses (Haddeland et al., 2011)]. We used a subset of the WATCH model ensemble (i.e. 7 large-scale models) with the aim to explore drought across the world through: (i) exploration of global hydrological models (GHMs) and land surface models (LSMs) driven by general circulation models (GCMs) which can provide information to answer the question if they are able to capture main features of historic drought (1970-2000), and (ii) intercomparison of drought in the 21st century derived from GHMs and LSMs driven by three GCMs for two scenarios (A2 and B1 scenarios) (impact of climate change). Figure 1 gives an outline of the study. Some models are classified as mass balanced based, whereas others belong to the energy balance or the LSMs. All 7 models were run over the period 1960-2100 on a global 0.5

degree grid and forced by the same weather data obtained from the WATCH Forcing Data (WFD , Weedon et al., 2011) and the driving forces obtained from three GCMs in both scenarios (i.e. CRNM, ECHAM, IPSL, A2 and B1 scenarios, 1960-2100, Chen et al., 2011). Monthly values were calculated as a cumulative sum of the daily values for the variables of interest. A comparative analysis of two drought characteristics have been performed (Number of drought events and Average deficit volume) for the monthly time step data set. The threshold method using an 80 percentile was applied in all the land cells available for the monthly data set of each cell. For the overall evaluation different types of visual as well as statistical analysis were performed. A discussion on each one of the results and the driven factors of important improvements in the analysis of the future scenarios are highlighted.

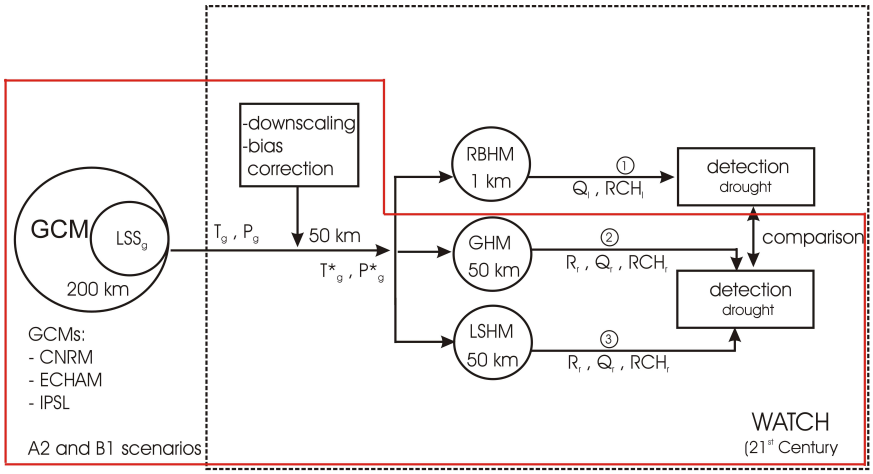

Figure 1: Flow chart showing the context of the multi-model intercomparison to assess future drought within WATCH.

This study is a follow-up of number of investigations on historic drought using WFD in the framework of the EU WATCH project. Hannaford et al. (2010); Stahl et al. (2011); and Prudhomme et al. (2011) compared low runoff or droughts obtained with some GHMs, LSMs or an RCM against observations from near-natural catchments in Europe. The GHMs and LSMs used in this study were also intercompared by Van Huijgevoort et al. (2011) at the global scale for the period 1963-2001 using WFD. At a much more detailed scale (WATCH Test Basins), Van Loon et al. (2011) compares the drought derived from grid cells of a set of GHMs and LSMs and the multi-model mean against those obtained with a more detailed river basin hydrological model (RBHM). These investigations contribute to the understanding on whether the GHMs and LSMs selected within WATCH are able to capture drought, which is relevant to assess their potential to be used to predict future drought.

First we will briefly summarize the main properties of the suite of large-scale models (GHMs and LSMs) that has been used in this study followed by a description of the common forcing data (three GCMs, i.e. CRNM, ECHAM, IPSL) and the drought

identification approach (Chapter 2). Then we will explore for the control period (1971-2000) whether these models fed by climate forcing of three GCMs (i.e. CRNM, ECHAM, IPSL) can reproduce the number of droughts and the durations derived from the same model, but then forced by WFD (reanalysis data). We also will intercompare the models on the number of land grids that have a large number of days with zero runoff. Next we will describe global future drought in a multi-model setting (Chapter 3). Chapter 4 describes a correlation analysis. Finally, we will draw some conclusions (Chapter 5).

Models and methods

The analysis of the 21st century focus on the quantification and characterization of drought in the 20th century (control period) and the analysis of the variability of the global hydrological and land surface models (future droughts). The main characteristics of the models and data used for the analyses are described in the following sections.

2.1 Large-scale models

To investigate the dryness of a regions conventionally droughts characteristics are evaluated. In a global analysis data availability is restricted to average of regions as well as the modelling of cells as hydrological units. Global models that integrate the interaction of atmosphere-land General Circulation Models, (GCMs) are preferred, but their spatial scale is still too coarse to simulate sufficiently reliable land surface processes, including hydrological extremes. Therefore, combined observational-modelling frameworks are implemented. These combined modelling approaches are based on using off-line models. Multiple models have been developed over the last decades, which include GHMs and LSMs that simulate the global and continental terrestrial water cycle. The GHMs and LSMs operate at a more detailed scale than the GCMs, which allows a better representation of the hydrological processes at the land surface, which likely will lead to a better identification of hydrological extremes. These models are forced with global reanalysis meteorological datasets to simulate the past water cycle or with downscaled, bias-corrected future meteorological data derived from GCMs to generate possible future water cycles.

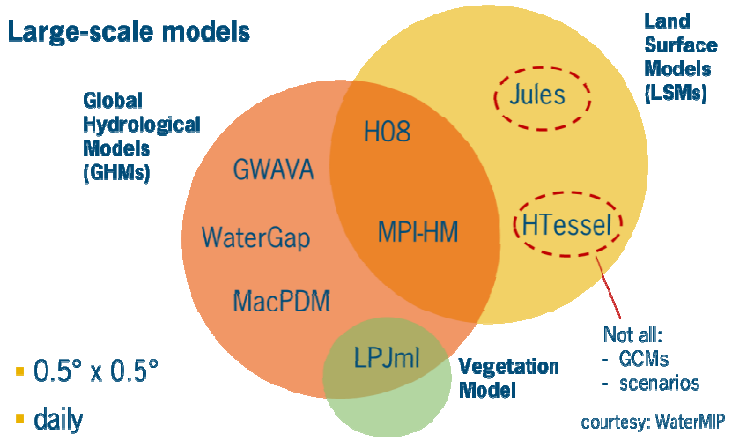

Figure 2 Large-scale models that were intercompared.

This report is based on the analysis of eight hydrological models as presented in Figure 2. All models were run at 0.5° spatial resolution for the global land areas for a 53 year period (1958—2001) using a newly-developed global meteorological dataset

(WATCH Forcing Data WFD, Weedon et al., 2011). Haddeland et al., 2011 described the intercomparison setup and the first results of the multi-model global water balance, which are the source of the modelling setup of this report.

These models have been grouped in GHMs and LSMs. From the WaterMIP (Haddeland et al., 2011) most global properties have been studied. A protocol for the intercomparison of these models have been applied defining among other things: a resolution of the model results for each hydrological variable is 0.5 latitude by 0.5 longitude, the use of land areas defined by the CRU (Climate Research Unit of the University of East Anglia) land mask. The CRU mask is characterized in this analysis over 67,420 cells (total land area is 146.7 million km²). The total land area above the equator represents around 78% of the total land area. For this report only the runoff components Qs and Qsb; totalized to Qst (monthly time scale) have been studied.

2.2 Climate forcing

We needed forcing for the control period and the future (21th century). These data are explained in the next sections.

2.2.1 WATCH Forcing Data (WFD)

The WATCH forcing variables are taken from the ERA-40 reanalysis product of the European Centre for Medium Range Weather Forecasting (ECMWF) as described by Uppala et al. (2005), and are interpolated to 0.5o spatial resolution, including elevation corrections as well as different methods for bias and/or under catch corrections. For detailed information on the forcing variables see Weedon et al. (2010, 2011).

2.2.2 Future climate

The models runs are based on 3 GCM and 2 climate scenarios (A2 and B1). The models are the Institute Pierre Simon Laplace (IPSL), the Centre National de Recherches Météorologiques (CNRM) and the ECHAM5 from Max Plank Institute.

Table 1: The fourth Special Report on Emissions Scenarios scenario part of the Fourth Assessment Report

AR4	More economic focus	More environmental focus
Globalisation (homogeneous world)	A1 rapid economic growth (groups: A1T; A1B; A1Fl) 1.4 - 6.4 °C	**B1** **global environmental sustainability 1.1 - 2.9 °C**
Regionalisation (heterogeneous world)	**A2** **regionally oriented economic development** **2.0 - 5.4 °C**	B2 local environmental sustainability 1.4 - 3.8 °C

Based on the IPCC fourth Special Report on Emissions Scenarios scenario it is selected scenarios A2 (Extreme change) and B1 (mild changes) (Table 1).

The large-scale models are described in Table 2. The data available from the 9 models forced with the 3 GCMs under different scenarios is presented. Some models did not run under scenario B2 due to time constrains. For the first part of this report only three models have been selected. In the annexes of this document the other 6 model results and graphs are presented. General observations of the other model might be mentioned and the respective reference to the annex will be given.

Table 2: Large-scale models and forcing datasets

Model	type	WFD	GCM and scenarios					
			ECHAM		IPSL		CNRM	
			A2	B1	A2	B1	A2	B1
WaterGAP	GHM	+	+	+	+	+	+	+
MPI-HM	GHM	+	+	+	+	+	+	+
Htessel	LSM	+	+	+	+	+	+	+
GWAVA	GHM	+	+	+	+	+	+	+
LPJLM	GHM	+	+	+	+	+	+	+
Jules	LSM	+	+		+		+	
H08	LSM	+	+		+		+	
Orchidee	GHM	+	+		+		+	
MacPDM	GHM	+	+		+		+	

For this study a number of conventions have been used to be able to understand and compare the different possible models, periods of time analysed, scenarios and GCMs.

WFD = Watch Forcing Data (only the period 1971-2000 was used, control)

GCM= Can be either IPSL, CNRM or ECHAM (available for scenarios A2 and B1), on three different periods of time. This is an example of some of the main convention used.

For the probabilistic analysis

- nd2021A2i = Number of Droughts in the period 2021, scenario A2, GCM i = IPSL
- nd1971c = Number of Droughts in the control period 1971, GCM c= CNRM

For the overall statistics simple, self-descriptive abbreviations of the models are used

- WFD 1971-2000
- GCM-A2 2021-2050
- GCM-A2 2071-2100
- GCM-B1 2021-2050

2.3 Drought identification

Drought is defined as a sustained and regionally extensive occurrence of below average water availability (Tallaksen et al., 2004). It is triggered by low or non-rainfall, often in combination with high evaporation rates. Analysis of drought is performed by identifying anomalies determined and characterized by time series statistics (e.g., percentiles). Overall statistical information of the events are grouped, and then the spatial analysis is done.

A detailed analysis of the model outcome allows improving the understanding of how hydrological droughts evolve at large scales. For this, in addition to the normal statistical analysis to obtain hydrological regimes, a compensated unit is elaborated and some remarks are done on the results obtained.

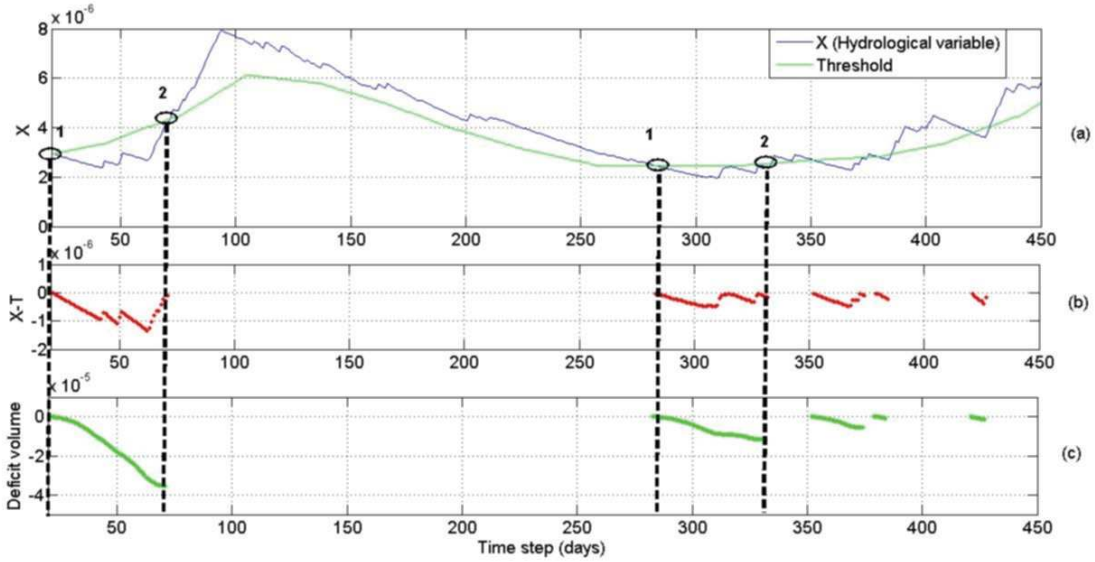

Figure 3 Threshold method for the calculation of drought characteristics. (a) daily time series and monthly variable threshold (Smoothed). (b) Deficit at each time step. (c) Deficit volume (accumulated).

To determine droughts from the modelling results the threshold level method (Hisdal et al., 2004) is applied. With this method, a drought occurs when the variable of interest (e.g., precipitation, soil moisture, groundwater storage, or discharge) is below a predefined threshold (Figure). The start of a drought event is indicated by the point in time when the variable falls below the threshold and the event continues until the threshold is exceeded again. Hence, each drought event can be characterised by its beginning, end and duration. Other commonly used drought characteristics are: deficit volume, calculated by summing up the differences between actual flow and the threshold level over the drought period, and minimum flow during an event (Hisdal et al., 2004). Both a fixed and a variable (seasonal, monthly, or daily) threshold can be used. In this study, a monthly threshold derived from the frequency duration curves of daily data are taken. For cells with a perennial runoff relatively low thresholds in the range from the 70 to 95 percentile can be considered reasonable. In this study the 80-percentile is selected, meaning that subsurface runoff values are exceeded 80 percent of the time. Although it is possible to think on more fuzzy bounds for the drought identification of a cell, this is not contemplated in this study. For cells with an intermittent or ephemeral runoff having a majority of zero flow, the 80-percentile could easily be zero in one or more months, and hence no drought events would be selected for these months. For these dry regions a higher threshold (low percentile) can be chosen as proposed by Fleig et al., 2006, or the region can be excluded because drought in streamflow is not so meaningful. The later has been done in this study, although the proposed methodology can handle higher thresholds. Dry regions were excluded from the drought analysis when in more than 80% of the time the simulated runoff is zero. If the percentage of zero flow is lower than 80%, but the time series presents one single event, it is considered as arid region, and it is also studied independently.

From the identification of drought events using the variable threshold method we extract the drought characteristics of each cell. The drought characteristics that fit our purpose are the average drought duration (*ADD*), average drought deficit volume (*ADV*) and number of events (*nd*). These drought characteristics are calculated as follows.

The drought duration (*DD*) is determined by the period of time the variable is under the drought threshold. *DD* is the total drought duration at cell c of a particular event.

$$ADD = \frac{\sum_{i=1}^{nd} DD}{N}$$

where *ADD* is the average drought duration at cell c and Nd is the number of droughts per cell.

The deficit volume (*DV*) is calculated by accumulating the daily deficit (X-T) as visualized in Figure. X represents the value of the simulated variable (in this study the subsurface runoff Qsb).

$$DV_i = \sum_{t_s}^{t_e} (X_t - T_t)$$

where DV_i is the deficit volume of the event *i*. The initial and final time steps are represented by t_s and t_e respectively. T_t is the threshold per time step.

$$RADV = \frac{\sum_{i=1}^{i=Nd} DV_i}{\sigma_X}$$

where *RADV* is the relative average deficit volume at cell *c*. The division by the standard deviation of the series (σ_X) is implemented since in the spatial analyses it is required to compare relative (standardized) and not absolute values.

$$ADI = \frac{\sum_{i=1}^{i=nd} DV_i}{N} / ADD(X)$$

where *ADI* is the Average Drought Intensity per cell.

Droughts characteristics are calculated using as reference the thresholds found on the control period. With this it is expected to have a clear relation on the changes of the model respect to its representation of the 20th century. For this number of drought events have been selected as a measure of droughts changes and similarities. The hypothesis is that similar statistical variability should lead to similar thresholds and similar number of events. However, some steps presented here discussed the drought durations as an important measure to complement the spatial analysis and the understanding of model differences.

2.4 Drought Equivalent as a measure of considering arid cells and drought characteristics

Dryness of a region (cell) can be characterized by an average number of drought events. However, in (semi-) arid regions there are no such events, because there is no runoff or only for a short period. Cells with such runoff conditions are called hereafter “arid cells”. In this global analysis arid cells cannot simply be excluded because the number is different for each of the situations. Likely, the number deviates, for instance, for a particular large-scale model using WFD and the GCM for the CTRL, but also for a particular model when we compare the projections with the CTRL (e.g. change from a wet to an arid state).

Since we cannot exclude arid cells and if we assume that the Number of drought events (*nd*) tends to be higher when the cell becomes arid. Then the critical instability or maximum possible *nd* will mean an equivalent situation of dryness (arid). For this we

propose a coefficient of dryness (*Cd*), which will be help the representation of arid cell in terms of nds. For this we assume that the equivalent number of drought events for one particular arid cell resembles the extreme situation of number of events in the model results. Figures 4, 5 and 7 show that the maximum number of droughts can vary from the CTRL situation (n=87) to the end of the 21st century (n=95 for some projections). A visual inspection of probability distributions for all large-scale models shows that the maximum *nd* is about 100 in most cases.

2.5 Approach to analyse 21st drought in a multi-model context

The steps used in this study can be described as follows:

a. Analysis of the 20th century control using WFD and GCM. A mask of arid and non-arid regions was generated and the calculation of the average number of drought events for each model and each period of time was performed. An inter-comparison of modelling results for the 20th century and the observed WFD results was performed. Having these results it is possible to look for other dimensions of the problem in terms of arid regions, number of drought events and the drought durations.

b. The analysis of modelling results without the mask was performed to determine the difference in-between each model forced by the observed WFD in 20th century data control period and 21st century in each scenario in each period of time. The statistical distribution of the results were plotted and discussed. Then overall average statistical information was compared for the three periods of time. This contemplates the use of simple averaging, the analysis of arid regions and the analysis of a drought equivalent concept to compensate for the effect of the arid regions in the averaging process.

c. A panel of results was compiled to evaluate extreme drought conditions (spatial distribution) and how many events are expected along the globe.

d. Arid regions on different continents were evaluated to analyse the spatial changes expected.

e. Correlation analysis between each model and each period of time was done to identify which models provide similar number of drought events.

Number of droughts and durations

3.1 Non-arid regions and number of droughts

Arid regions in the calculation of drought characteristics give a zero value as average of the time series or as an indeterminate value in the number of drought events. The indeterminate value can be related to the start of an event that never ends or the event that never started but end above the threshold. In this respect it is important to compare the control period. So an arid cell present at a location in one model will not be contemplated in any other model. For this a mask of non-arid cells was created with all the models available. The masks used are shown in
Figure .

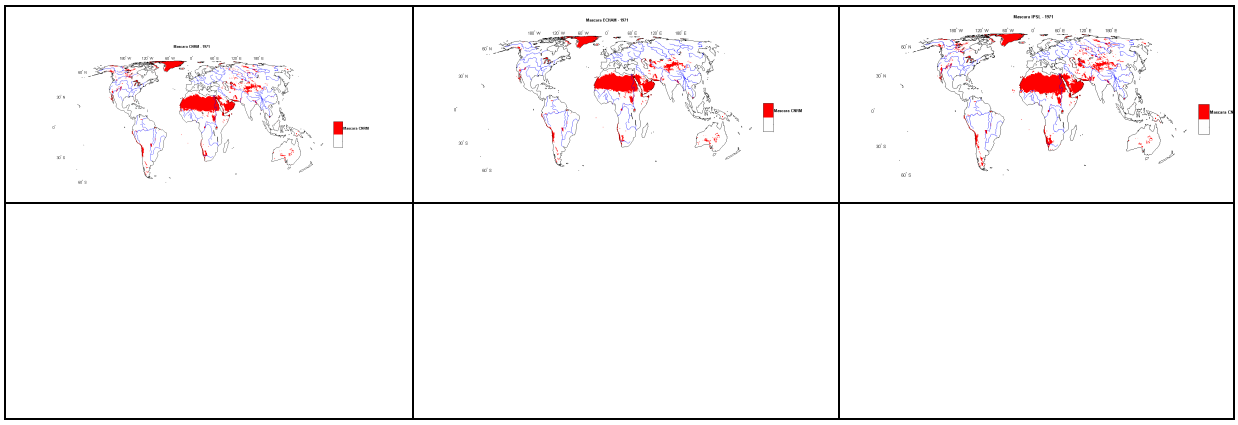

Figure 4 Mask of arid cells (zero values) in all models for the control period per each GCM (left: CNRM, middle: ECHAM5, and right: IPSL).

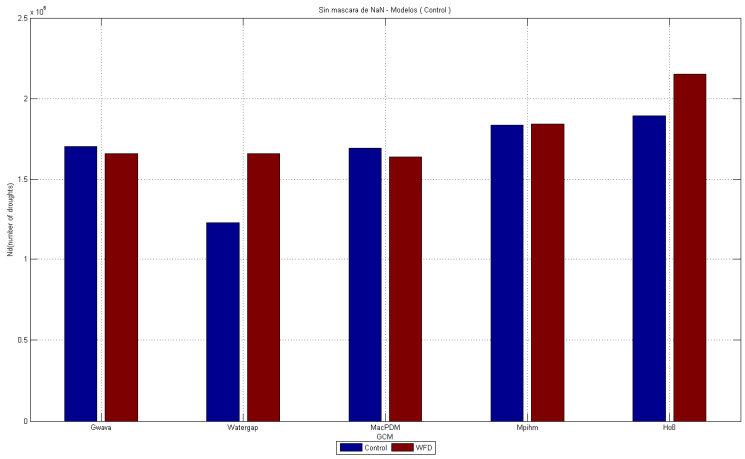

Figure 2: Comparison of number of droughts for the control period after the removal of all arid regions.

Number of droughts have been determined for the non-arid cells in the control period. This has been done for five large-scale models (Figure 5). In general there is a rather good agreement between the GCM climate and the forcing data for the control period in the 20th century.

Since the number of results are beyond the limits of this report, results have been only discussed for some modelling results. However, conclusions are based upon the results of most models, scenarios and periods of time (Sections 2.1 and 2.2). The annexes of this report include most of the graphical results of the other models.

3.2 Drought events in the control period and in the 21st century

A first exploratory analysis was done by looking at the number of drought events for the GWAVA model. The normal probability plot is created for the number of drought for the three GCMs (Figure 6, upper row). The model shows deviations from the three that GCM inputs to the models on the upper and lower tails, having higher values of drought events for IPSL. There is a line of similar patterns in all periods of time with slightly increase in probability while the time period considers is higher. The probability distribution shows that almost all the results have more variance than what could be expected on a normal distribution. The control period for the ECHAM seem to have the highest deviation and without a clear distribution. On the IPSL case it is possible to see that the distribution is pretty similar but the lower tale has important differences. This was identified as well on the analysis of the other models. This is attributed to the number of zero events presented in the three GCM models.

A further comparison on the distributions plots show the difference between the models run under the three GCM A2 scenarios for three models. For this each of the probability distribution of the number of drought event in the control period show to have a clear

discrepancy on the extreme events and on the very low number of events. Figure 6 also shows the results of number of drought events for 3 other large-scale models. The three models have a very similar response on the WFD with a slightly change in the shape on 30 events, where all three models agree on 50 percent of the events are above this value. The control period in all models have very similar responses, however, it is also possible to see a high difference in the curve between control and 21st century scenarios. It is also important to notice that above 30 events there is a good agreement between the MPI-HM and H08 on the 21st century and clear displacement of the event towards low number of events in the 21st century.

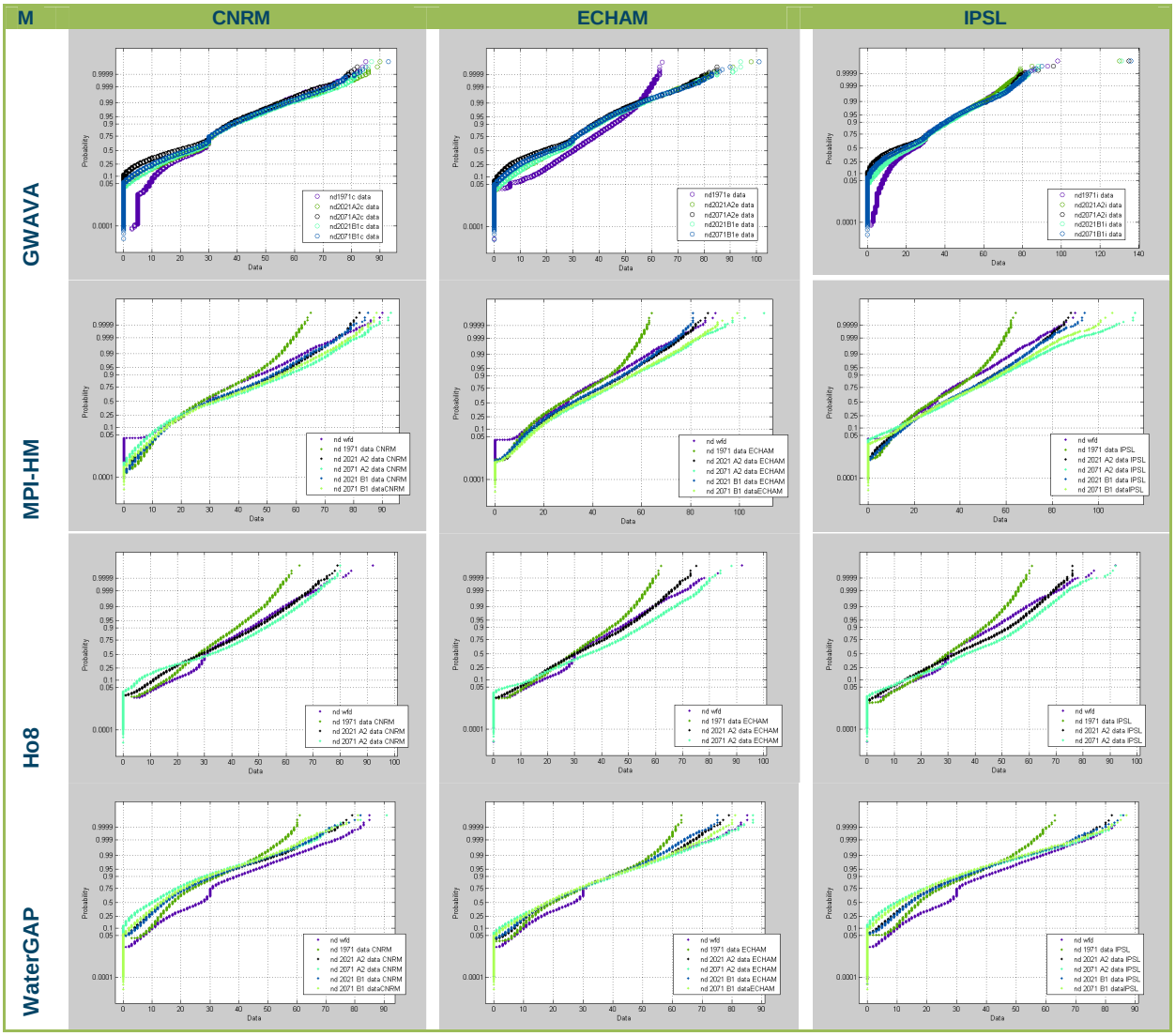

Figure 6 Probability distribution functions of the number of drought events for four large-models with three GCMs and A2 and B1 scenarios as input.

The regions seem to become arid on the three selected models with the increase of the number of events is significantly above the GCM forced models (Figure 8). In almost all models the number of arid cells increases, and the second part of the 21st century shows the highest values.

A second analysis was performed with the MPI-HM model, where the spatial distribution of the number of droughts is plotted in a map (Figure 7). The spatial distribution of events has predominant critical values on the western USA, Western Europe, Northern Asia, Amazonia high elevation regions and some small regions in Africa and Indonesia.

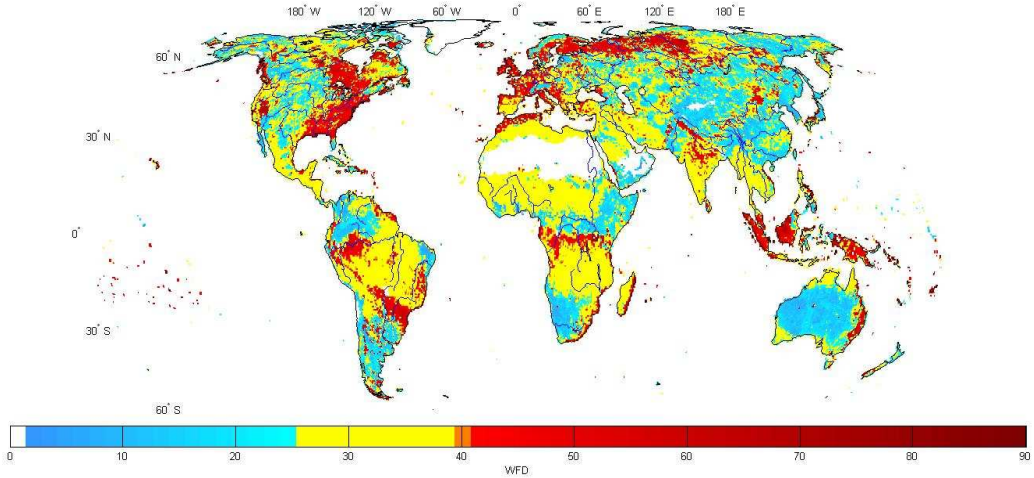

Figure 7 Distribution of the number of droughts obtained for the MPI-HM model.

Most models with low drought numbers have an important number of samples with zero (arid) events. This zero events are generated when or either there is no events at all (being threshold equal zero), or that 80% of the samples is zero, or when an event starts and does not end on the whole time series. This has the implication on the number of events. It can be shown that the anomaly of some areas however, due to the spatial context of each model, a different representation or response to the forcing will lead to different regions becoming zero. As stated earlier, a way to deal with this on the space of solutions of the number of drought event is to consider a drought equivalent on arid cell using a dryness coefficient of 100 (Section 2.4). With this the arid cells become equivalent to the maximum number of events.

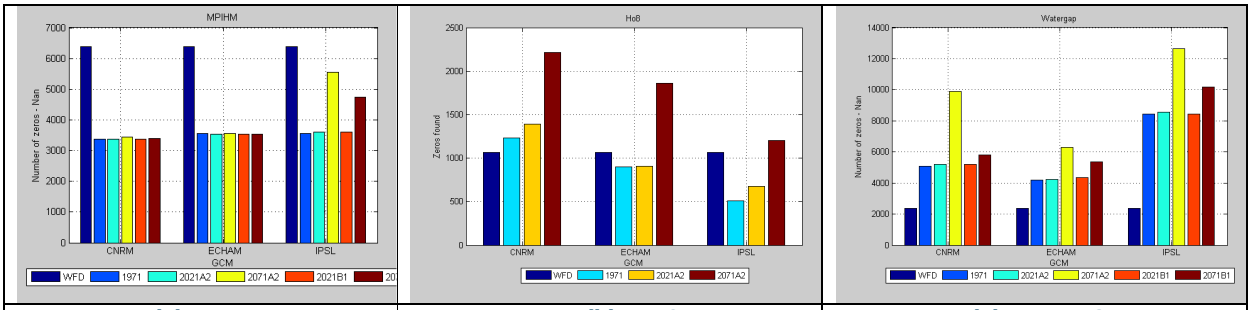

(a) MPI-HM (b) Ho8 (c) WaterGAP

Figure 8 Number of zero and Nan cells obtained per model.

Figure 9 shows the results of applying a drought equivalent on the arid (zero) event cells present in all possible scenarios. The analysis shows that using a dryness coefficient of 100 (based on the PDF of the models) it is possible to get a picture of how the spatial relation of drought in fact increases.

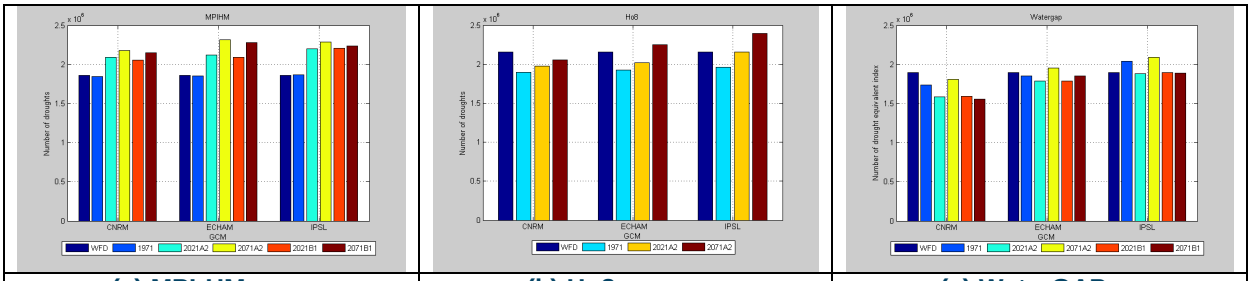

(a) MPI-HM (b) Ho8 (c) WaterGAP

Figure 9 Analysis of number of drought events including arid regions by drought equivalent on arid cell using a dryness coefficient of 100.

3.3 Drought durations in the control period and in the 21st century

The results of presented as PDFs show not clear results for the different models under the different scenarios. The MPI-HM has a close agreement on the distribution of control and WFD, and the percentage of high durations is increasing for scenarios A2 on both periods of the 21st century. The most significant increase of events seems to be present using the IPSL forcing. This also is similar on what is found on arid cells in most of the models that used this forcing.

On the other hand for the H08 model there is a clear reduction on the number of events (Figure 10). However, it is clear from
Figure that the number of arid cells is highly significant and therefore it is the main reason of this apparent reduction on the accumulated value of drought durations. This is

also correlated with the high percentage of zero values present in the lower tail of the graphs. WaterGAP presents a very similar behaviour as the H08 but with a weaker transition on the low values and zeros.

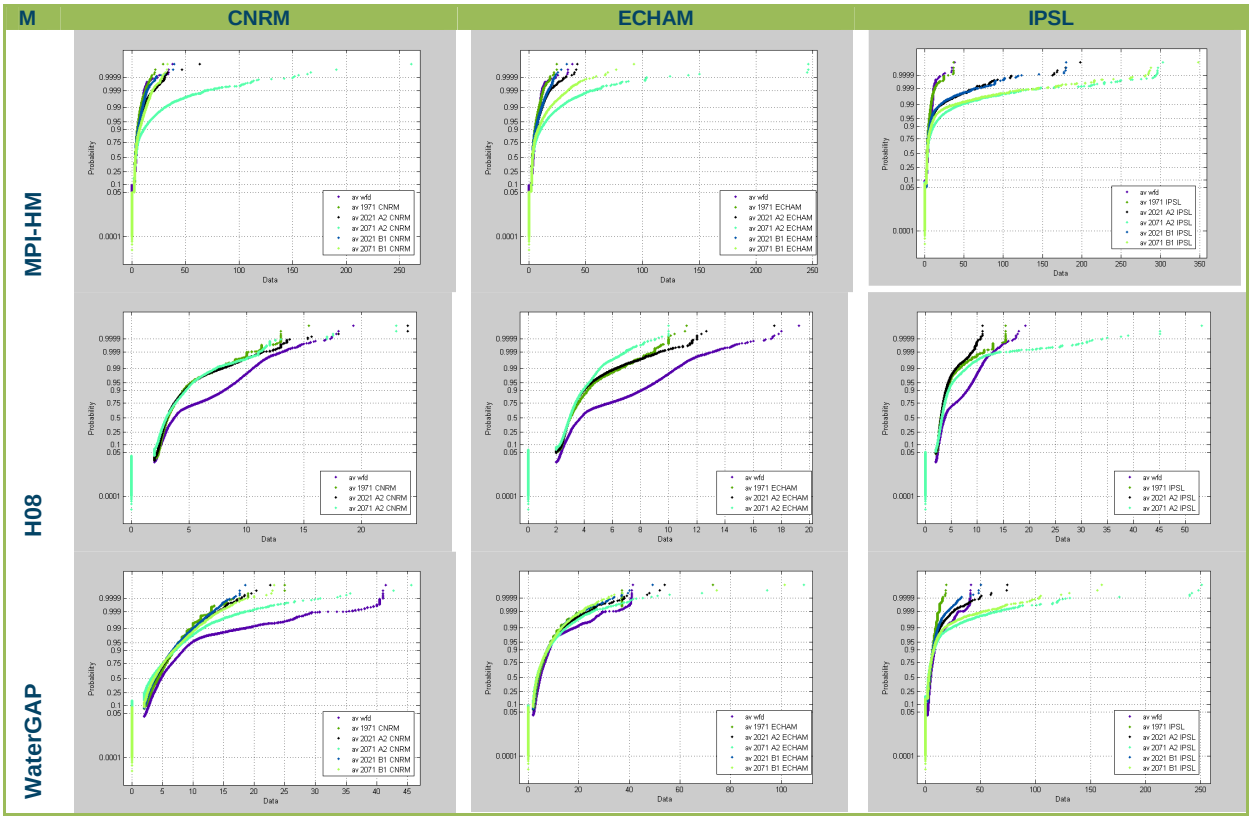

Figure 10 Probability distribution function representation of the spatial cumulative average drought durations for 3 models in three GCM in a A2 and B1 scenario.

3.4 Spatial analysis of drought events and arid regions for the control period and 21st Century

3.4.1 Spatial distribution of drought events

For spatial analysis of drought it is important to investigate the overall spatial distribution of events and arid regions. In this sense an overall analysis of the regions, and their distribution have been explored. A panel of drought results shows how the overall distribution of the drought critical regions (Figure 11). Drought events seem to be more dominant in the late part of the 21st century. The results of the three large-scale models show that America, Africa and Indonesia are the continents with higher changes. The region that seems to reduce its number of events is the northern part of Asia, however,

these regions are considered to have a weak representation in most of the global hydrological models.

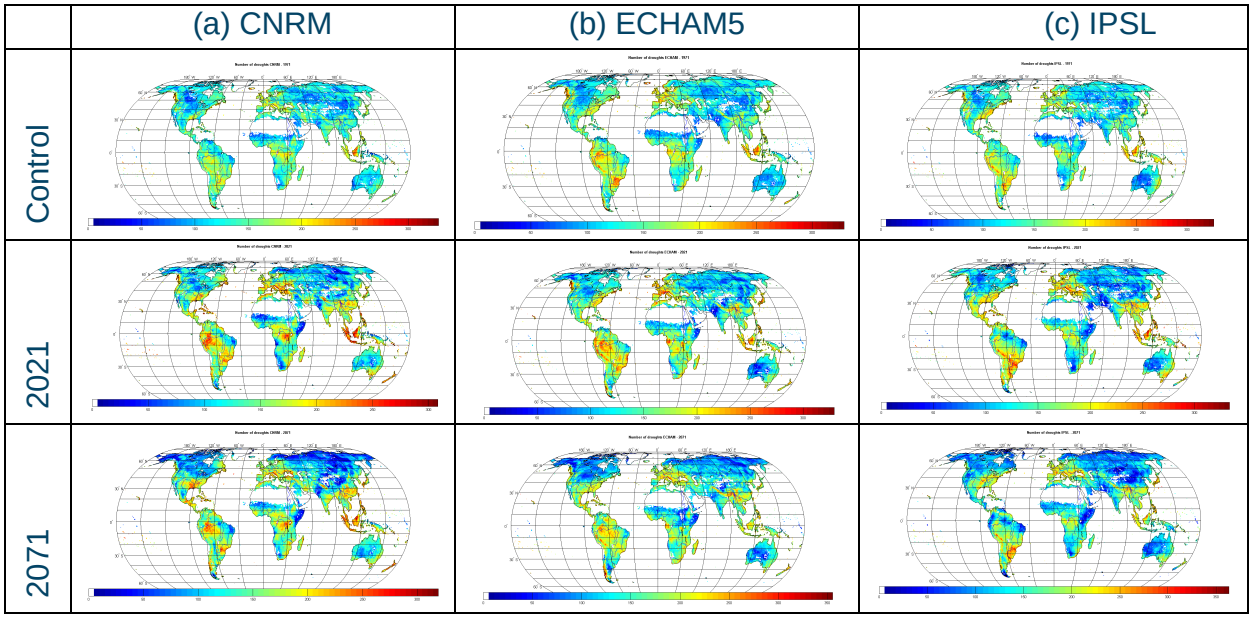

Figure 11 Ensemble of number of drought events on the control period.

Drought events seem for be more predominant in the late part of the 21st century. The results between models show that pattern in America, Africa and Indonesia are the ones with higher changes. The region that seems to reduce its number of event is the northern part of Asia, however, these regions are considered to have a weak representation on most of the global hydrological models.

3.4.2 Spatial distribution of arid regions

WaterGAP has been selected here to show the distribution of arid cells for each continent per time period. The European region has a clear minor increase in the mid-21st century arid cells, but a critical on the late 21st century (Figure 12). In this respect cold region seems to be the more affected and near the equator in Northern Africa there is almost no increase in arid cells. In the southern part of America almost no change in arid regions is projected, with the exception of a few regions on the southern part of the Amazonia basin (Figure 13).

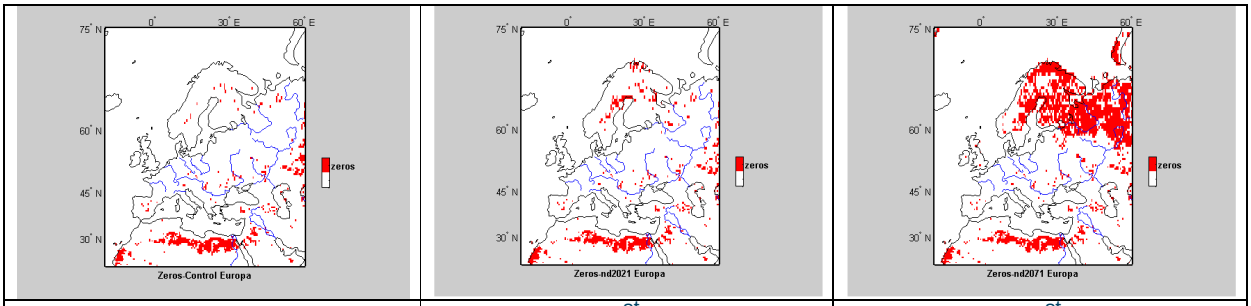

(a) Control | (b) Mid-21st century | (c) Late 21st century

Figure 12: Maps with the spatial location of arid cells for Europe as obtained from the WaterGAP model (CNRM, A2.)

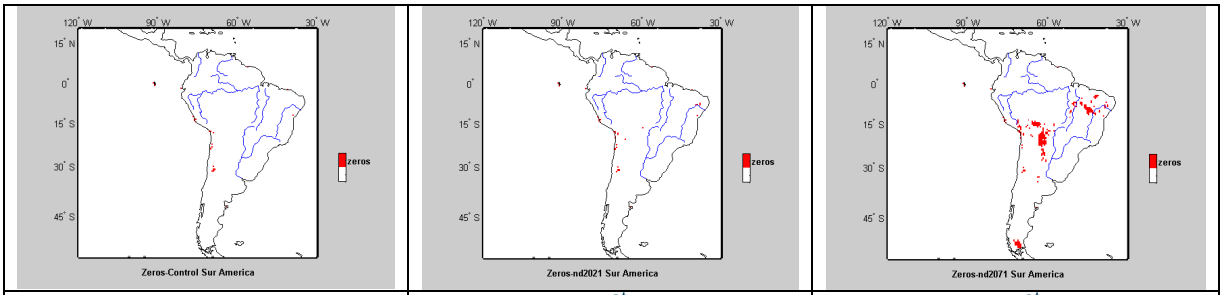

(a) Control | (b) Mid-21st century | (c) Late 21st century

Figure 13 Maps with the spatial location of arid cells for South America as obtained from the WaterGAP model (CNRM, A2).

Figures 14, 15 and 16 give the spatial distribution of the arid regions for North America, Asia and Africa, respectively, for the control period and the mid and late 21st century.

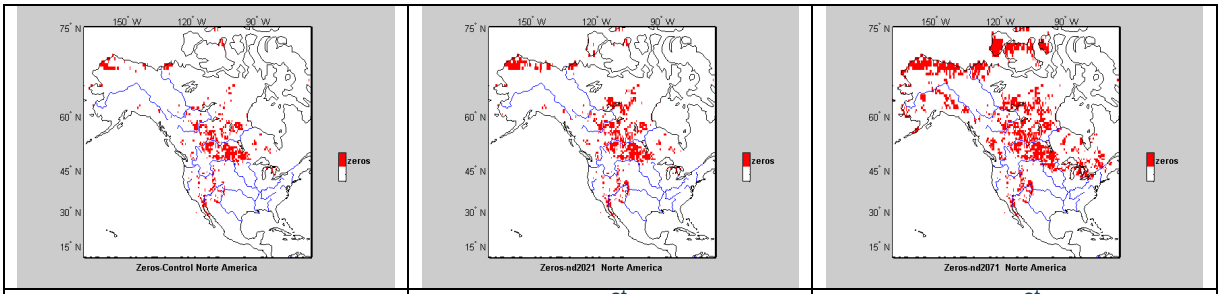

(a) Control | (b) Mid-21st century | (c) Late 21st century

Figure 14 Maps with the spatial location of arid cells for North America as obtained from the WaterGAP model (CNRM, A2).

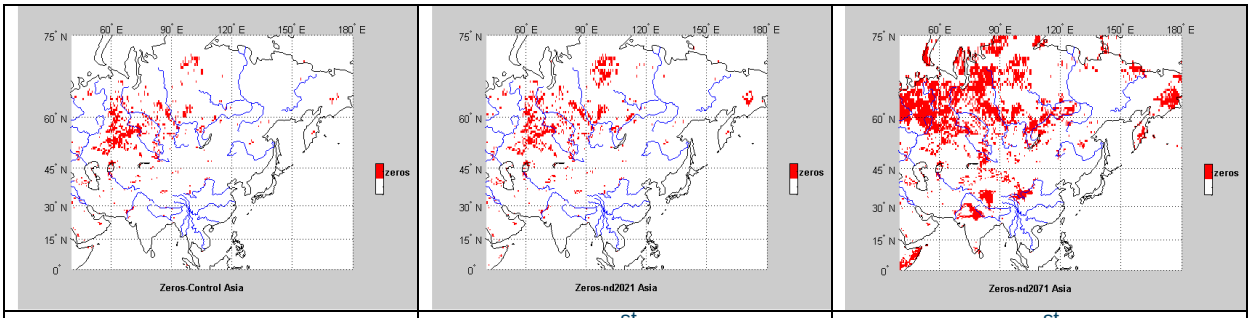

(a) Control	(b) Mid-21st century	(c) Late 21st century

Figure 15 Maps with the spatial location of arid cells for Asia as obtained from the WaterGAP model (CNRM, A2).

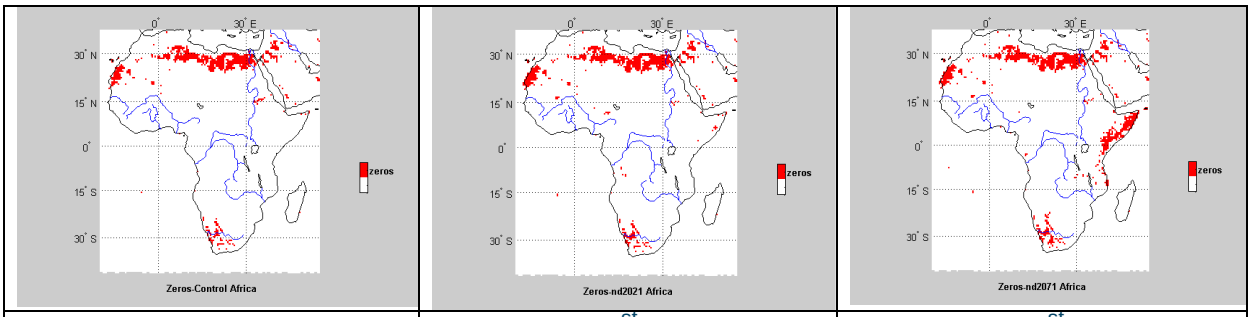

(a) Control	(b) Mid-21st century	(c) Late 21st century

Figure 16 Maps with the spatial location of arid cells for Africa as obtained from the WaterGAP model (CNRM, A2).

4. Correlation analysis of number of drought events

Number of droughts as obtained from seven large-scale models with CNRM climate input were correlated for three periods (control period, mid and late 21st century) (Table 3). The correlation analysis shows clear similarities between GWAVA, LPJLm and MacPDM for the control period. For the mid-21st century simulation Jules is also close with a high correlation of 0.52 with MPI-HM. However, for the late 21st century none of the models have a clear relation in their drought events correlation analysis.

Table 3 Correlation of number of drought events for a number of large scale models with CNRM as climate input (upper: control period, 1971-2000, 2021-2050, and 2071-2100)

Control - CNRM							
	Gwava	Watergap	Macpdm	Mpihm	Ho8	Lpjml	Jules
Gwava	1	0.197927	0.706601	0.267635	0.030094	0.360939	0.426633
Watergap	0.197927	1	0.149736	0.313476	0.037727	0.285117	0.008219
Macpdm	0.706601	0.149736	1	0.182602	0.008107	0.253753	0.516007
Mpihm	0.267635	0.313476	0.182602	1	0.031233	0.433933	0.191206
Ho8	0.030094	0.037727	0.008107	0.031233	1	0.044247	-0.10252
Jules	0.360939	0.285117	0.253753	0.433933	0.044247	1	0.183708
Lpjml	0.426633	0.008219	0.516007	0.191206	-0.10252	0.183708	1

2021-2050, A2 - CNRM							
	Gwava	Watergap	Macpdm	Mpihm	Ho8	Lpjml	Jules
Gwava	1	0.281683	0.63485	0.339777	-0.00173	0.394999	0.355693
Watergap	0.281683	1	0.255265	0.390954	-0.06486	0.404327	0.059014
Macpdm	0.63485	0.255265	1	0.270196	-0.04012	0.355976	0.412797
Mpihm	0.339777	0.390954	0.270196	1	-0.10655	0.525644	0.199298
Ho8	-0.00173	-0.064863	-0.04012	-0.10655	1	-0.06968	-0.15444
Jules	0.394999	0.404327	0.355976	0.525644	-0.06968	1	0.185821
Lpjml	0.355693	0.059014	0.412797	0.199298	-0.15444	0.185821	1

2071-2100, A2 - CNRM							
	Gwava	Watergap	Macpdm	Mpihm	Ho8	Lpjml	Jules
Gwava	1	0.366161	0.666776	0.279192	-0.10115	0.421034	0.167652
Watergap	0.366161	1	0.367999	0.346594	-0.14708	0.429455	0.077742
Macpdm	0.666776	0.367999	1	0.22802	-0.11985	0.427795	0.218182
Mpihm	0.279192	0.346594	0.22802	1	-0.04948	0.362443	-0.09761
Ho8	-0.10115	-0.147084	-0.11985	-0.04948	1	-0.10451	-0.14158
Jules	0.421034	0.429455	0.427795	0.362443	-0.10451	1	-0.0394
Lpjml	0.167652	0.077742	0.218182	-0.09761	-0.14158	-0.0394	1

For the ECHAM GCM similar correlations with high values between MPI-HM, LPJLM, MacPDM are found in the control period (Table 4). For the mid-21st century the correlation shows better agreement between models. The second part of the 21st century seems to have no clear correlations, as CNRM.

Table 4 Correlation of number of drought events for a number of large scale models with ECHAM as climate input (upper: control period, 1971-2000, 2021-2050, and 2071-2100)

Control - ECHAM							
	Gwava	Watergap	Macpdm	Mpihm	Ho8	Lpjml	Jules
Gwava	1	0.307473	0.723291	0.332003	0.046988	0.335191	0.358398
Watergap	0.307473	1	0.230694	0.505418	0.044651	0.365986	0.41579
Macpdm	0.723291	0.230694	1	0.220241	0.027942	0.223629	0.235729
Mpihm	0.332003	0.505418	0.220241	1	0.035943	0.41998	0.571535
Ho8	0.046988	0.044651	0.027942	0.035943	1	0.0788	0.029627
Jules	0.335191	0.365986	0.223629	0.41998	0.0788	1	0.653735
Lpjml	0.358398	0.41579	0.235729	0.571535	0.029627	0.653735	1

2021-2050, A2 – ECHAM							
	Gwava	Watergap	Macpdm	Mpihm	Ho8	Lpjml	Jules
Gwava	1	0.33233	0.604779	0.324592	0.006117	0.362607	0.348183
Watergap	0.33233	1	0.231937	0.519514	-0.0069	0.421703	0.483035
Macpdm	0.604779	0.231937	1	0.208826	-0.02359	0.279124	0.257144
Mpihm	0.324592	0.519514	0.208826	1	-0.00426	0.435259	0.508375
Ho8	0.006117	-0.0069	-0.02359	-0.00426	1	0.011684	0.00736
Jules	0.362607	0.421703	0.279124	0.435259	0.011684	1	0.692778
Lpjml	0.348183	0.483035	0.257144	0.508375	0.00736	0.692778	1

2071-2100, A2 - ECHAM							
	Gwava	Watergap	Macpdm	Mpihm	Ho8	Lpjml	Jules
Gwava	1	0.357948	0.681578	0.215878	-0.03552	0.386117	0.433515
Watergap	0.357948	1	0.287974	0.434589	0.002501	0.460888	0.524552
Macpdm	0.681578	0.287974	1	0.158086	-0.06098	0.378673	0.426466
Mpihm	0.215878	0.434589	0.158086	1	0.009544	0.324264	0.297985
Ho8	-0.03552	0.002501	-0.06098	0.009544	1	0.02296	-0.00779
Jules	0.386117	0.460888	0.378673	0.324264	0.02296	1	0.687534
Lpjml	0.433515	0.524552	0.426466	0.297985	-0.00779	0.687534	1

5. Concluding remarks

This study has explored differences between seven different large-scale models forced with WATCH Forcing Data (WFD) and different GCMs (CNRM, ECHAM and IPSL) to investigate different climate change scenarios (A2 and B1). The number and spatial distribution of drought events do not clearly show a consistent change (increase or decrease) due to the variation on number of arid cells (cells with zero flow in most cases) that are present in different simulation periods (control, mid and late 21st century). After exploring approaches, i.e. introduction of an equivalent drought measure, to remove arid cells it seems that control period and WFD have relatively similar statistical values and therefore similar statistical properties. An increase in number of drought events was identified over the 21st century. However, the equivalent drought measure requires a more comprehensive elaboration to achieve a better physical interpretation. The use of a panel of number of drought events seems to reveal homogeneity for the three GCMs and therefore could be a way to include all model results and its uncertainty, but this was beyond the scope of this study. A breakdown of the spatial distribution in continents can lead to clearer outcome that can improve the understanding of the similarities and capabilities of models.

Acknowledgements

This research was undertaken as part of the European Union (FP6) funded Integrated Project 515 Water and Global Change (WATCH, contract 036946). The research is part of the programme of the Wageningen Institute for Environment and Climate Research (WIMEK-SENSE). The study contributes to the UNESCO IHP-VII programme (Cross-cutting programme FRIEND and Theme 1 Adapting to the impacts of global changes on river basins and aquifer systems).

References

Bates, B.C., Kundzewicz, Z.W., Wu, S. & Palutikof, J.P. (Eds.) (2008): Climate Change and Water. Technical Paper of the Intergovernmental Panel on Climate Change, IPCC Secretariat, Geneva, [available at: http://www.ipcc.ch/pdf/technical-papers/climate-change-water-en.pdf].

Chen, C., Hagemann, S., Clark, D., Folwell, S., Gosling, S., Haddeland, I., Hanasaki, N., Heinke, J. & Ludwig, F. and Voβ, F. (2011): Evaluation of projected hydrological changes in the 21st century obtained from a multi-model ensemble. WATCH Technical Report No. 45. [available at: http://www.eu-watch.org/publications/technical-reports]

Dai, A. (2010): Drought under global warming: a review. Wiley Interdisciplinary Reviews: Climate Change, n/a. doi: 10.1002/wcc.81.

Dai, A.G., Qian, T.T., Trenberth, K.E. & Milliman, J.D. (2009): Changes in Continental Freshwater Discharge from 1948 to 2004. Journal of Climate, 22, 2773-2792.

EC (2007): Communication Addressing the challenge of water scarcity and droughts in the European Union, COM(2007) 414 final, European Commission, Brussels.

EEA (2007): The pan-European environment: glimpses into an uncertain future. European Environmental Agency. EEA Report No 4/2007.

EEA (2008): Impacts of Europe's changing climate - 2008 indicator-based assessment. Joint EEA-JRC-WHO report, EEA Report No 4/2008, Copenhagen.

EEA (2010): EEA (2010) Mapping the impacts of natural hazards and technological accidents in Europe. An overview of the last decade. EEA Technical report No 13/2010, Copenhagen, 2010.

Haddeland, I., Clark, D., 560 Franssen, W., Ludwig, F., Voss, F., Arnell, N., Bertrand, N., Best, M., Folwell, S., Gerten, D., Gomes, S., Gosling, S. N., Hagemann, S., Hanasaki, N., Harding, R., Heinke, J., Kabat, P., Koirala, S., Oki, T., Polcher, J., Stacke, T., Viterbo, P., Weedon, G. P., and Yeh, P. (2011): Multi-model estimate of the global water balance: setup and first results, J. Hydrometeor., DOI:10.1175/2011JHM1324.1.

Hannaford, J., Lloyd-Hughes, B., Keef, C., Parry, S., and Prudhomme, C. (2010): Examining the large scale spatial 565 coherence of European drought using regional indicators of precipitation and streamflow deficit, Hydrol. Process., doi:10.1002/hyp.7725.

IPCC (2007a): Climate Change 2007: Climate Change 2007: The Physical Science Basis. Contribution of Working Group I to the Fourth Assessment Report of the Intergovernmental Panel on Climate Change, S. Solomon, D. Qin, M. Manning, Z. Chen, M. Marquis, K. B. Averyt, M. Tignor and H. L. Miller (Eds.), Cambridge University Press, Cambridge.

IPCC (2007b): Climate Change 2007: Impacts, Adaptation and Vulnerability. Contribution of Working Group II to the Fourth Assessment Report of the Intergovernmental Panel on Climate Change, M.L. Parry, O.F. Canziani, J.P. Palutikof, P.J. van der Linden and C.E. Hanson (Eds.), Cambridge University Press, Cambridge.

IPCC (2007c): Climate Change 2007: Mitigation. Contribution of Working Group III to the Fourth Assessment Report of the Intergovernmental Panel on Climate Change, B. Metz, O. Davidson, P.Bosch, R. Dave and L. Meyer (Eds.), Cambridge University Press, Cambridge.

Kirono, D.G.C., Kent D.M., Hennessy K.J. & Mpelasokaet F. (2011): Characteristics of Australian droughts under enhanced greenhouse conditions: Results from 14 global climate models, Journal of Arid Environments, doi:10.1016/j.jaridenv.2010.12.012.

Lewis, S.L., Brando, P.M., Phillips, O.L., van der Heijden, G.M.F., Nepstad, D. (2011): The 2010 Amazon Drought. Science (31): 554.

Peters E, Van Lanen HAJ, Alvarez J & Bradford RBB (2001) Groundwater droughts: evaluation of temporal variability of recharge in three European groundwater catchments. ARIDE Technical report no.11, Wageningen, 124 pg.

Prudhomme, C., Parry, S., Hannaford, J., Clark, D.B., Hagemann, S. & Voss, F. (2011) How well do large-scale models reproduce regional hydrological extremes in Europe? J Hydrometeo., doi: 10.1175/2011JHM1387.1.

Sheffield, J. & Wood, E.F. (2008): Projected changes in drought occurrence under future global warming from multi-model, multi-scenario, IPCC AR4 simulations. Clim Dyn., 31: 79–105.

Sheffield, J., Andreadis, K., Wood, E. & Lettenmaier, D. (2009): Global and continental drought in the second half of the twentieth century: Severity-area-duration analysis and temporal variability of large-scale events. J. Climate, 22: 1962–1981.

Stahl, K., Tallaksen, L.M., Gudmundsson, L. & Christensen, J.H. (2011): Streamflow data from small basins: a challenging test to high resolution regional climate modelling. J Hydrometeo., doi: 10.1175/2011JHM1356.1.

Tallaksen, L. M. and & Van Lanen, H. A. J. (2004): Hydrological drought: processes and estimation methods for streamflow and groundwater, Developments in Water Science, 48, Elsevier Science B.V.

UN-ISDR (2009): Global Assessment Report on Disaster Risk Reduction. UNITED NATIONS, Geneva, Switzerland.

Van Huijgevoort, M.H.J., Loon, A.F., van, Hanel, M., Haddeland, I., Horvát, O., Koutroulis, A., Machlica, A., Weedon, G., Fendeková, M., Tsanis, I. & Lanen, H.A.J. van (2011) Simulation of low flows and drought events in WATCH test basins: impact of climate forcing datasets. WATCH Technical Report No. 25, 44 pg., [available at: http://www.eu-watch.org/publications/technical-reports]

Van Loon, A.F., van, Lanen, H.A.J. van, Tallaksen, L.M., Hanel, M., Fendeková, M., Machlica, M., Sapriza, G., Koutroulis, A., Huijgevoort, M.H.J. van, Jódar Bermúdez, J., Hisdal, H. & Tsanis, I. (2011): Propagation of drought through the hydrological cycle. WATCH Technical Report No. 32, 97 pg., [available at: http://www.eu-watch.org/publications/technical-reports]

Weedon, G., Gomes, S., Viterbo, P., Shuttleworth, J., Blyth, E., Sterle, H., Adam, J., Bellouin, N., Boucher, O.,and Best, M. (2011): Evidence of changing evaporation in the late twentieth century from the WATCH Forcing Dataset, J. Hydrometeorol., doi: 10.1175/2011JHM1369.1.

Annexes General drought analysis of 21st century

Annex 1: Analysis based on number of drought events

ANNEX 1.1 MPI-HM

1.1.1 Analysis of number of drought events

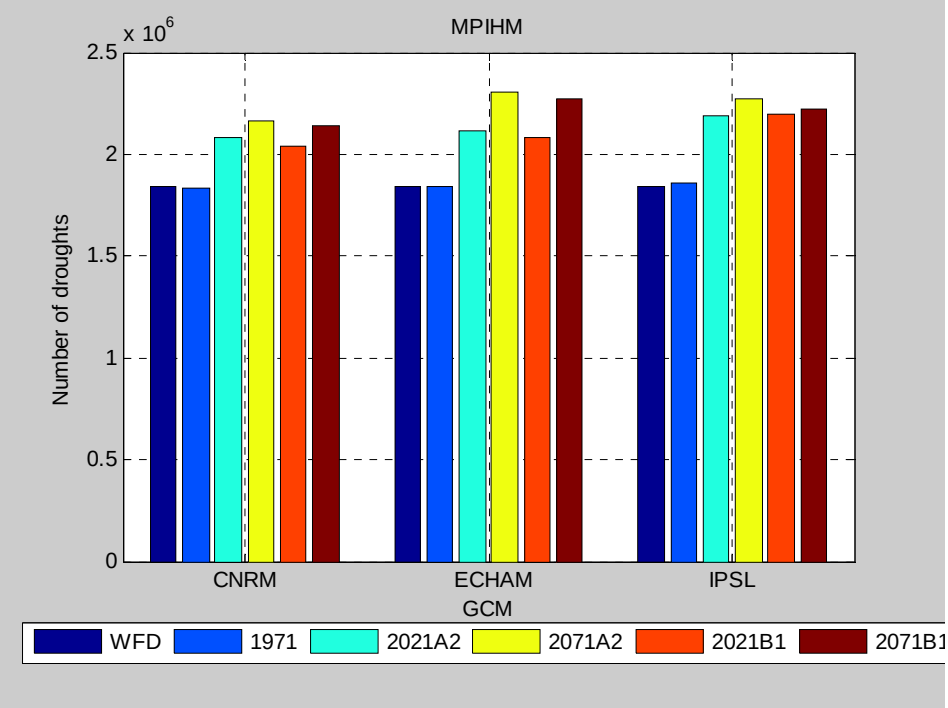

Number of drought events for control, mid and late 21st century (not corrected for arid regions).

1.1.2 Number of arid regions

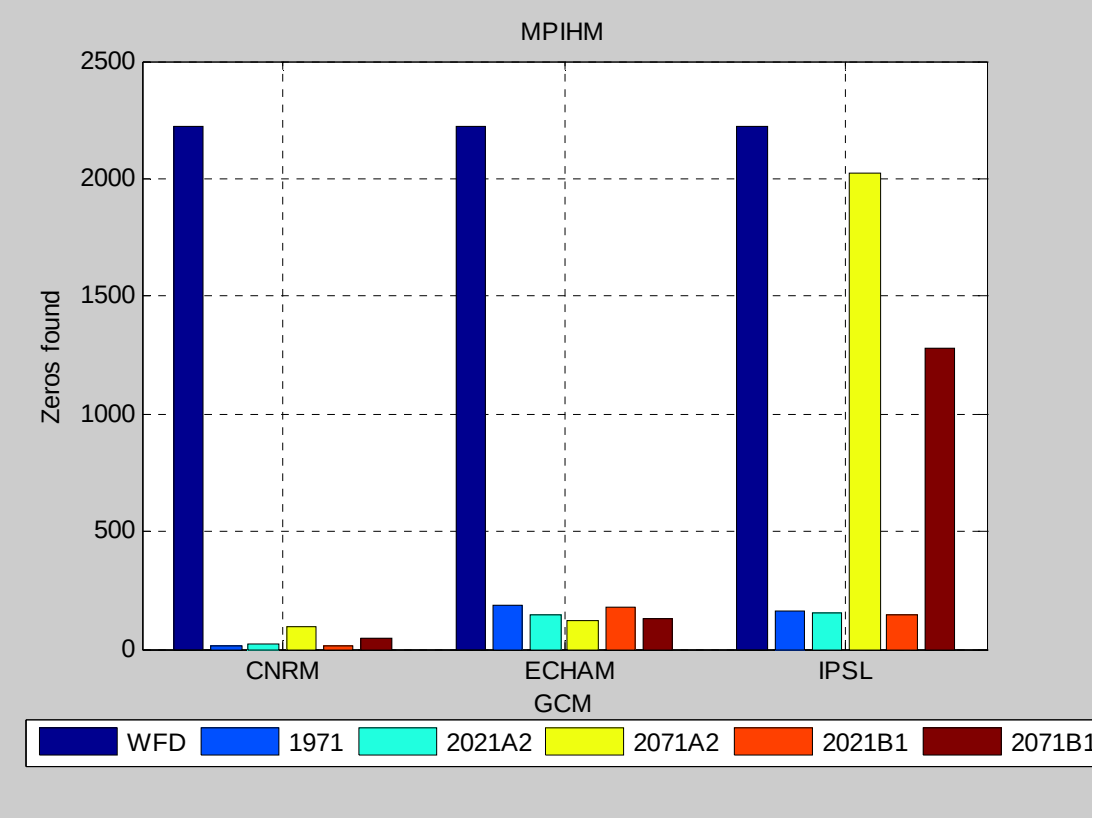

Number of Zeros

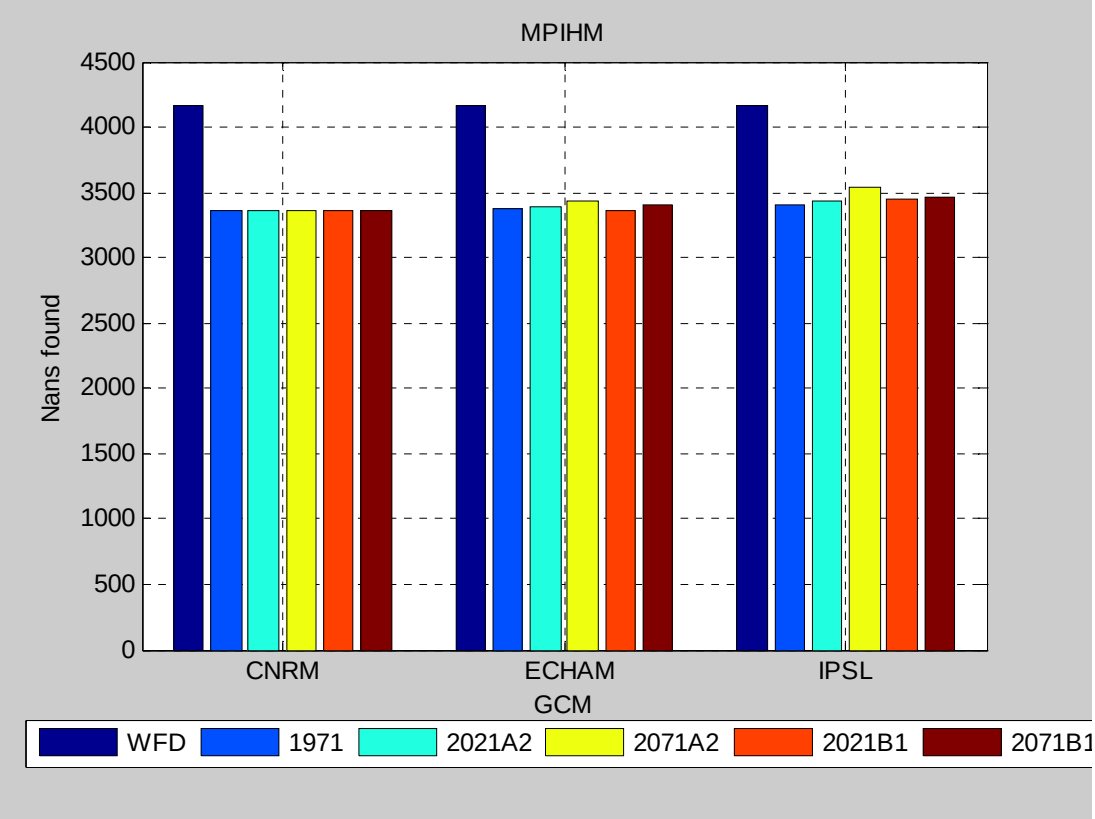

Number of Nans

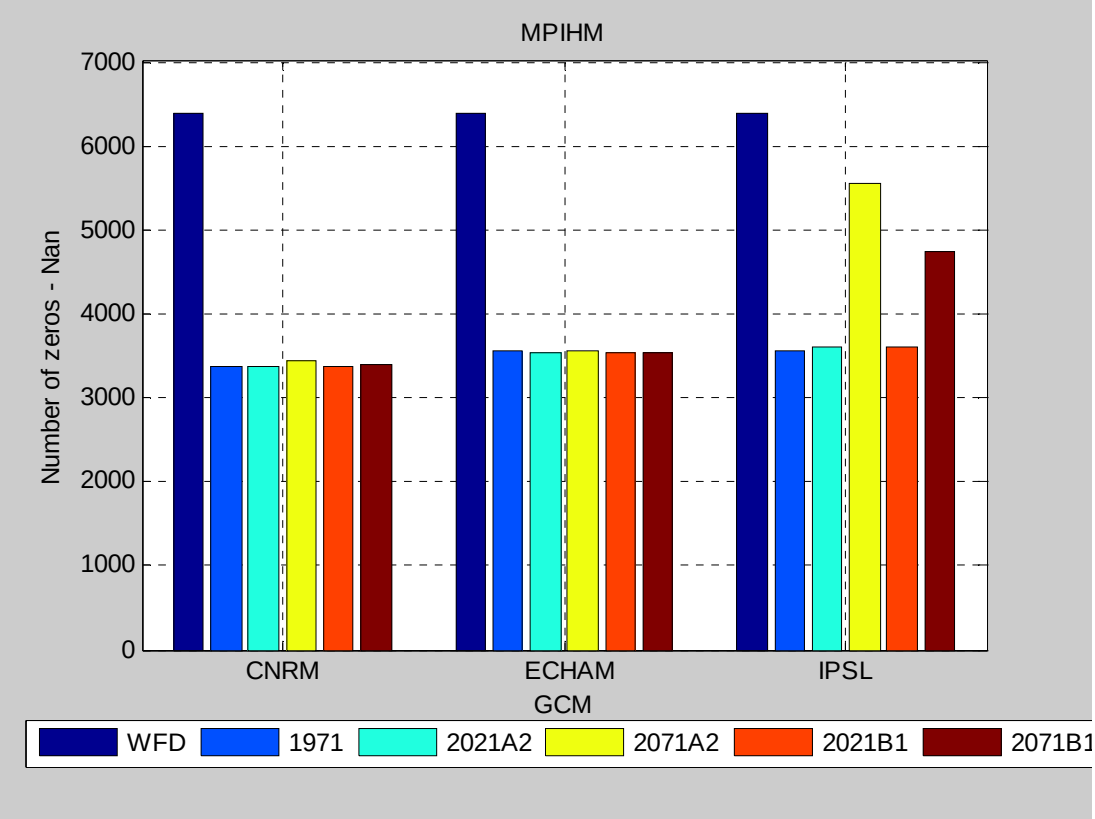

Number of arid regions (zeros + Nans) for control, mid and late 21st century.

1.1.3 PDF Number of drought events for three GCMs

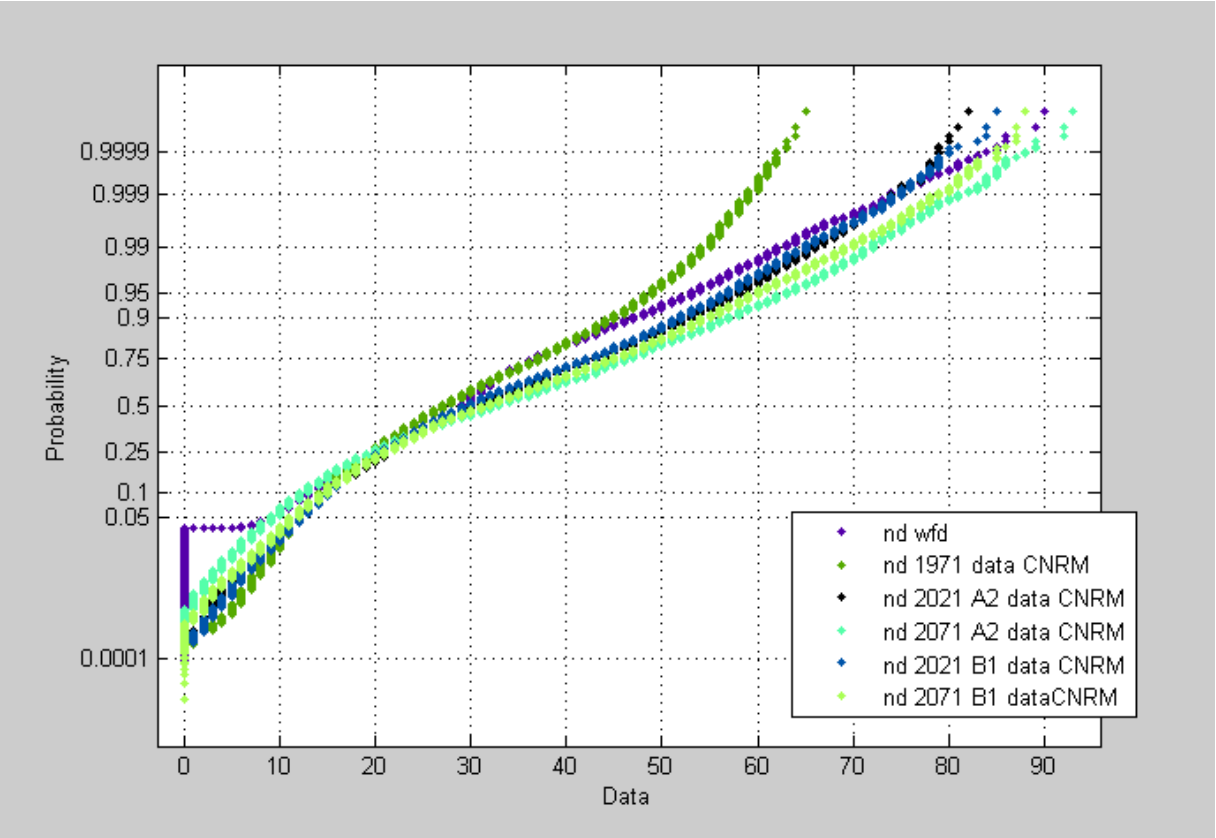

Probability density funtions of drought events for control, mid and late 21st century (not corrected for arid regions) as obtained with MPI-HM and CNRM climate input.

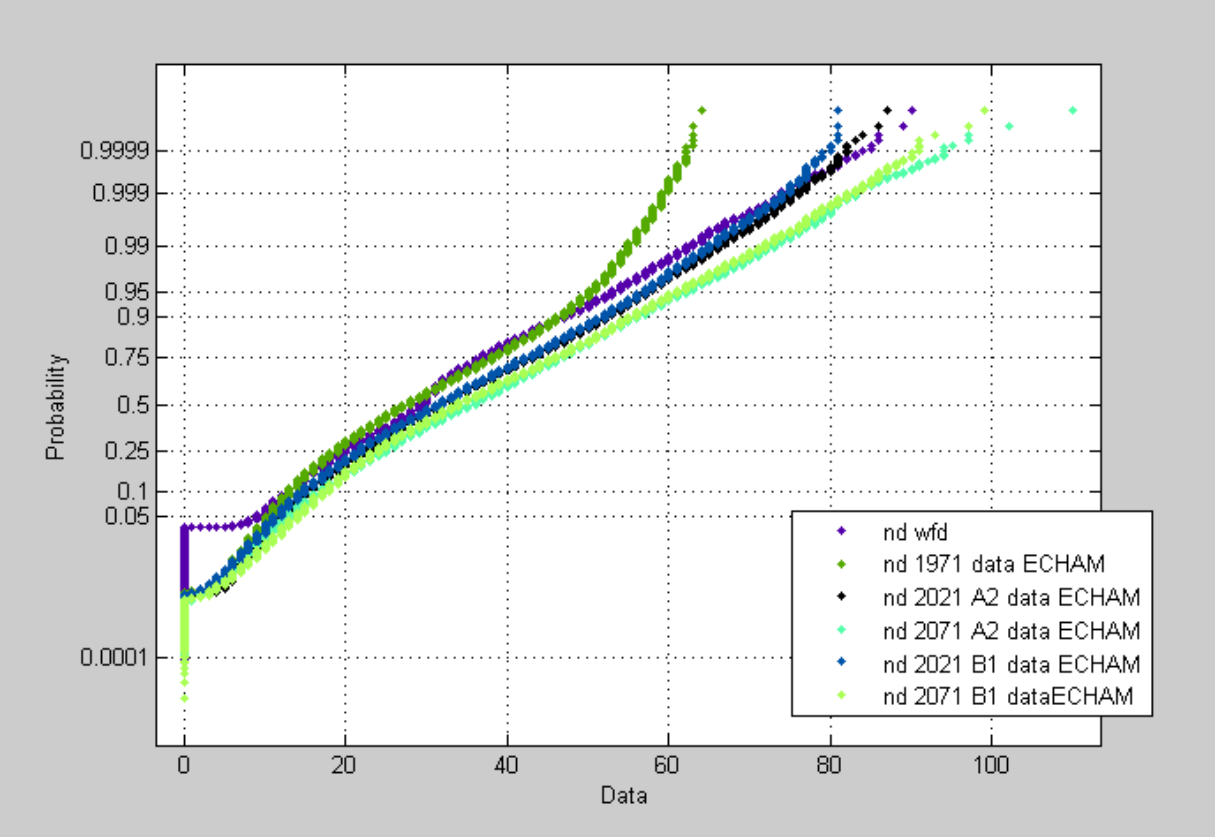

Probability density funtions of drought events for control, mid and late 21st century (not corrected for arid regions) as obtained with MPI-HM and ECHAM input.

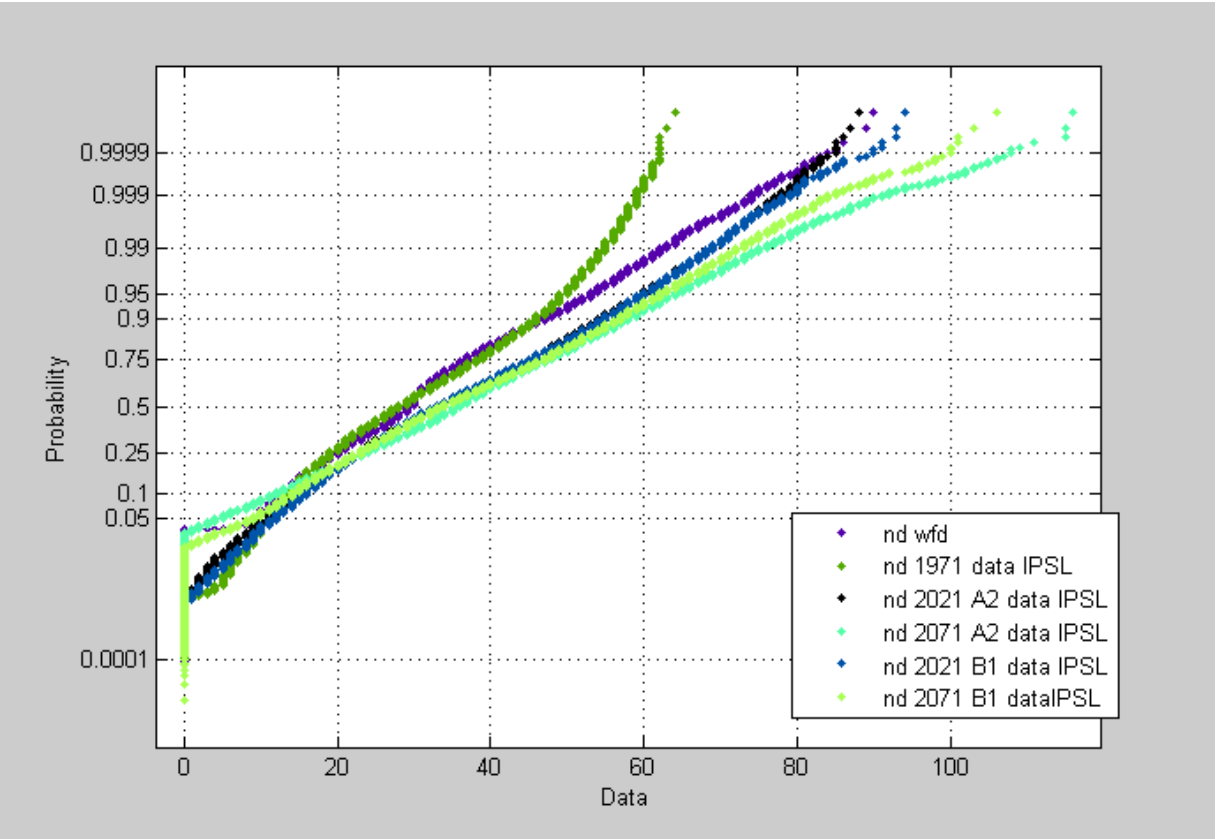

Probability density funtions of drought events for control, mid and late 21st century (not corrected for arid regions) as obtained with MPI-HM and IPSL climate input.

1.1.4 Analysis of MPI-HM with a drought equivalent index

ANNEX 1.2 GWAVA

1.2.1 Analysis of number of drought events

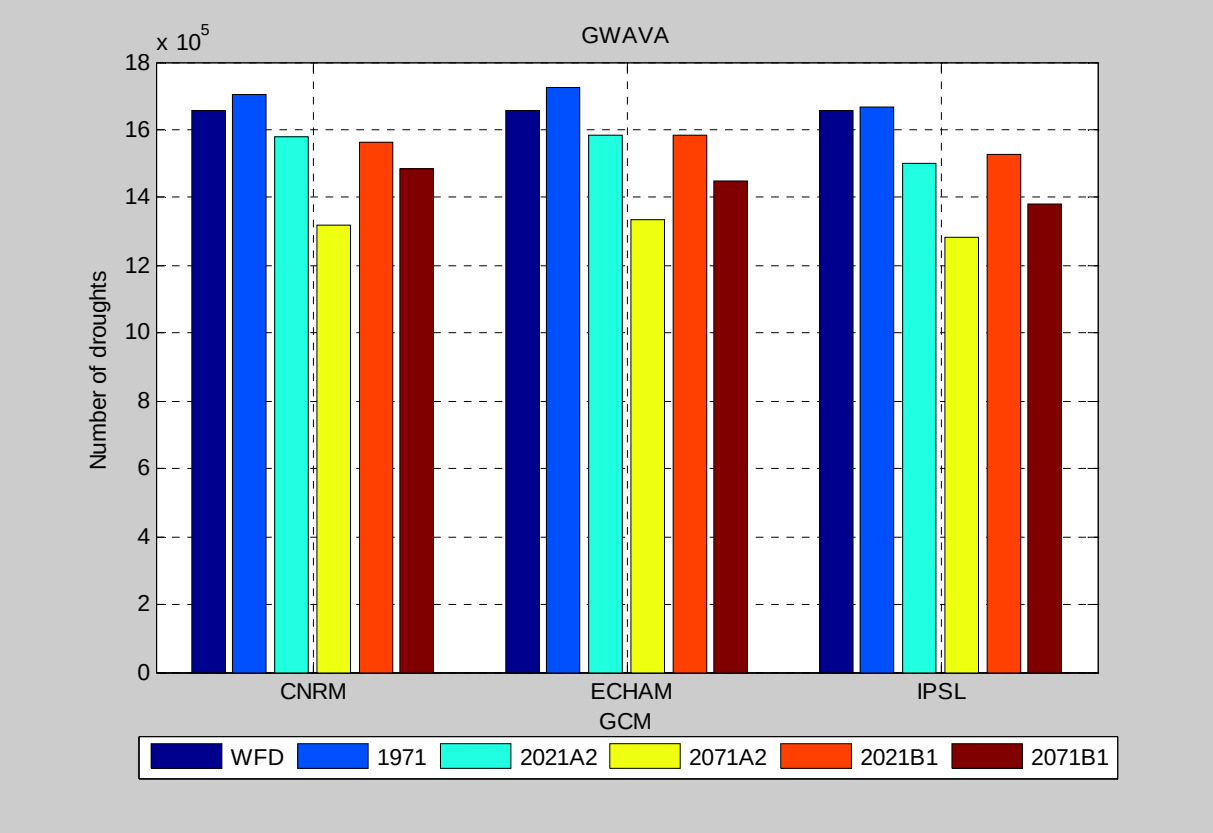

Number of drought events for control, mid and late 21st century (not corrected for arid regions).

1.2.2 Number of arid regions

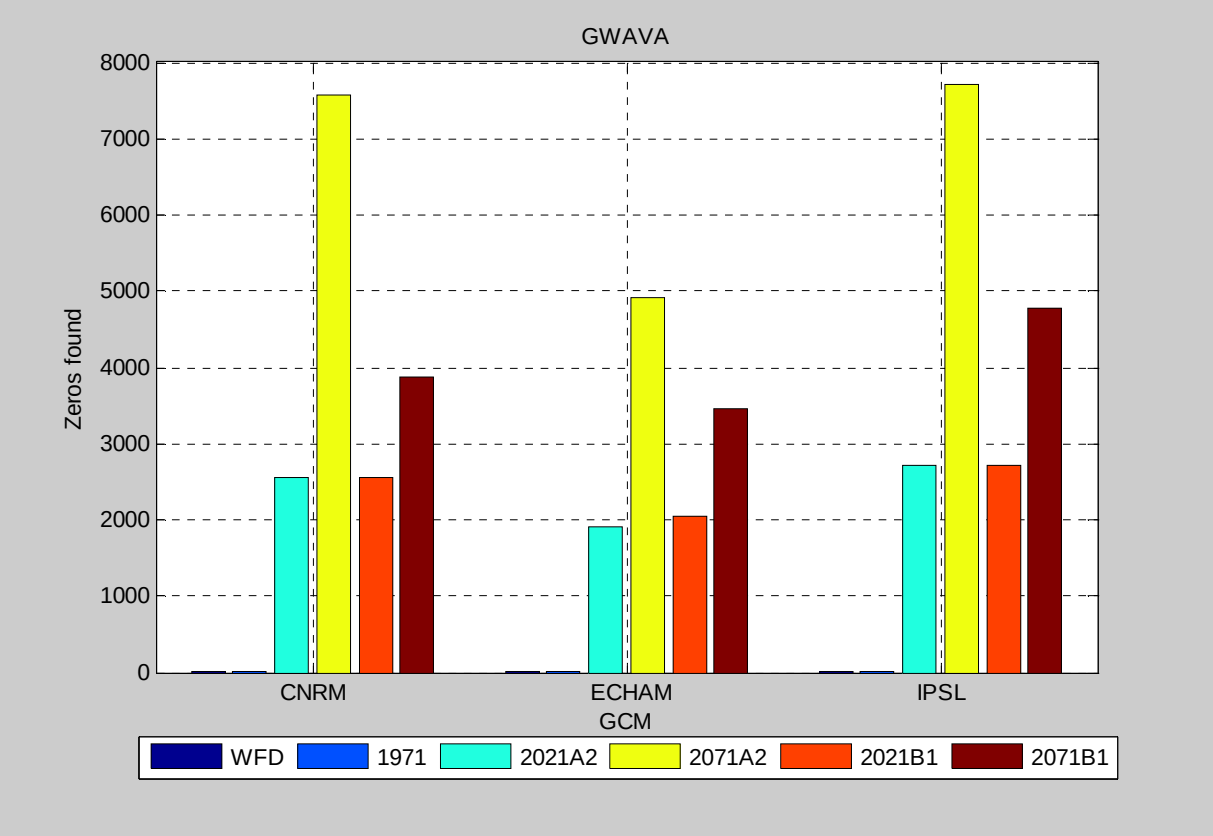

Number of Zeros

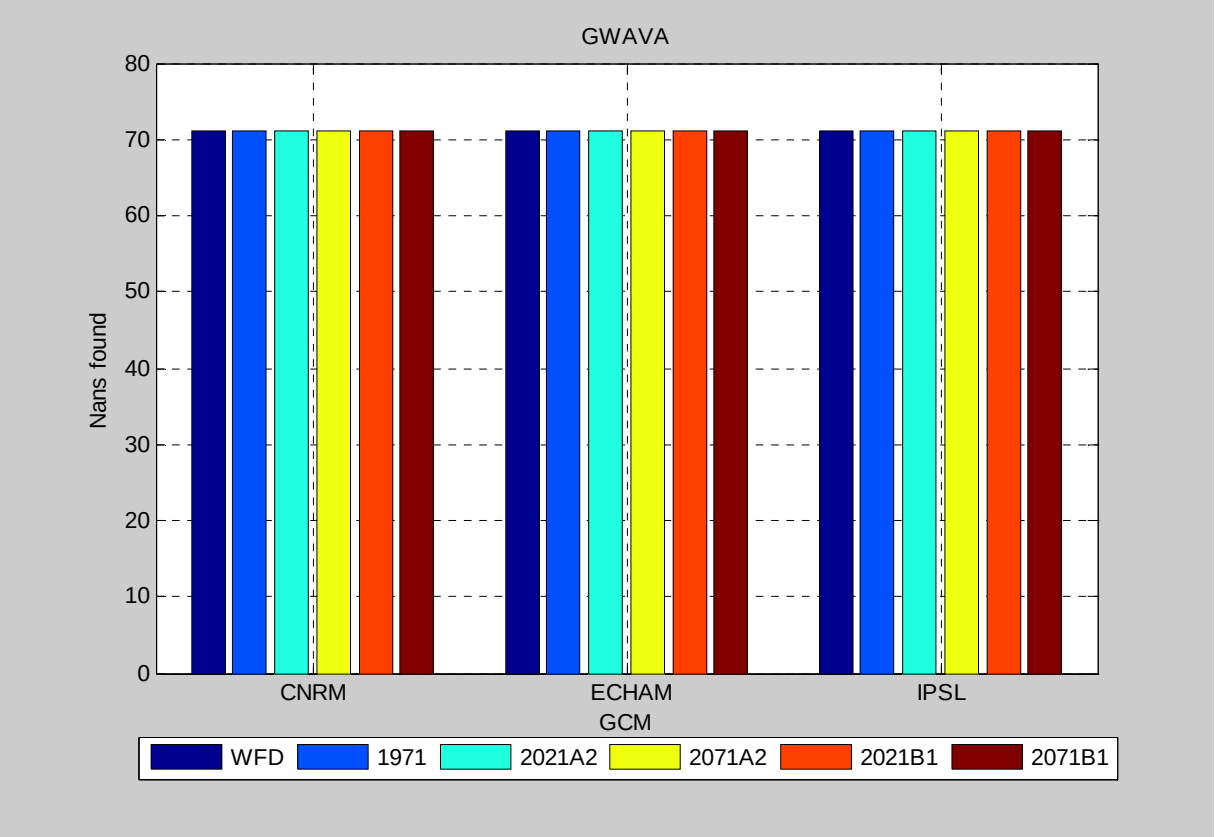

Number of Nans

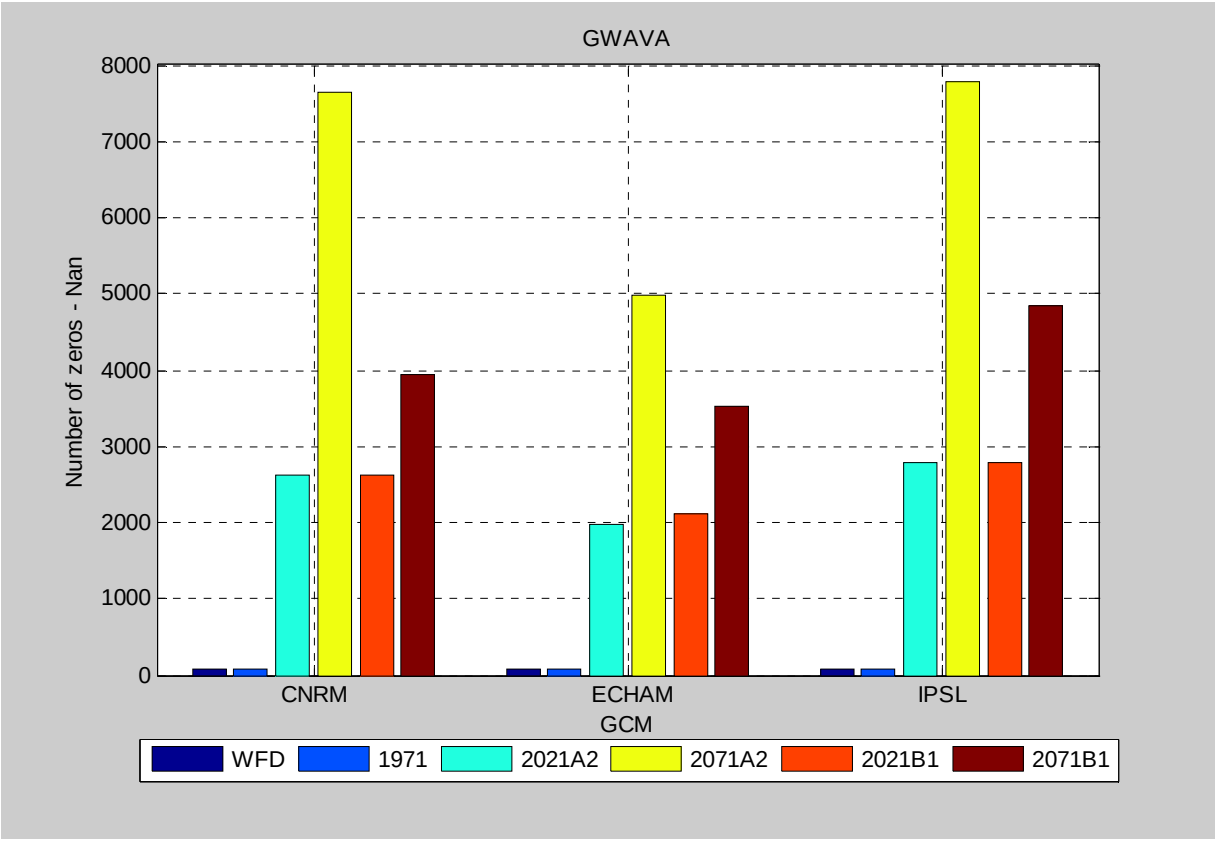

Number of arid regions (zeros + Nans) for control, mid and late 21st century.

1.2.3 PDF Number of drought events for three GCMs

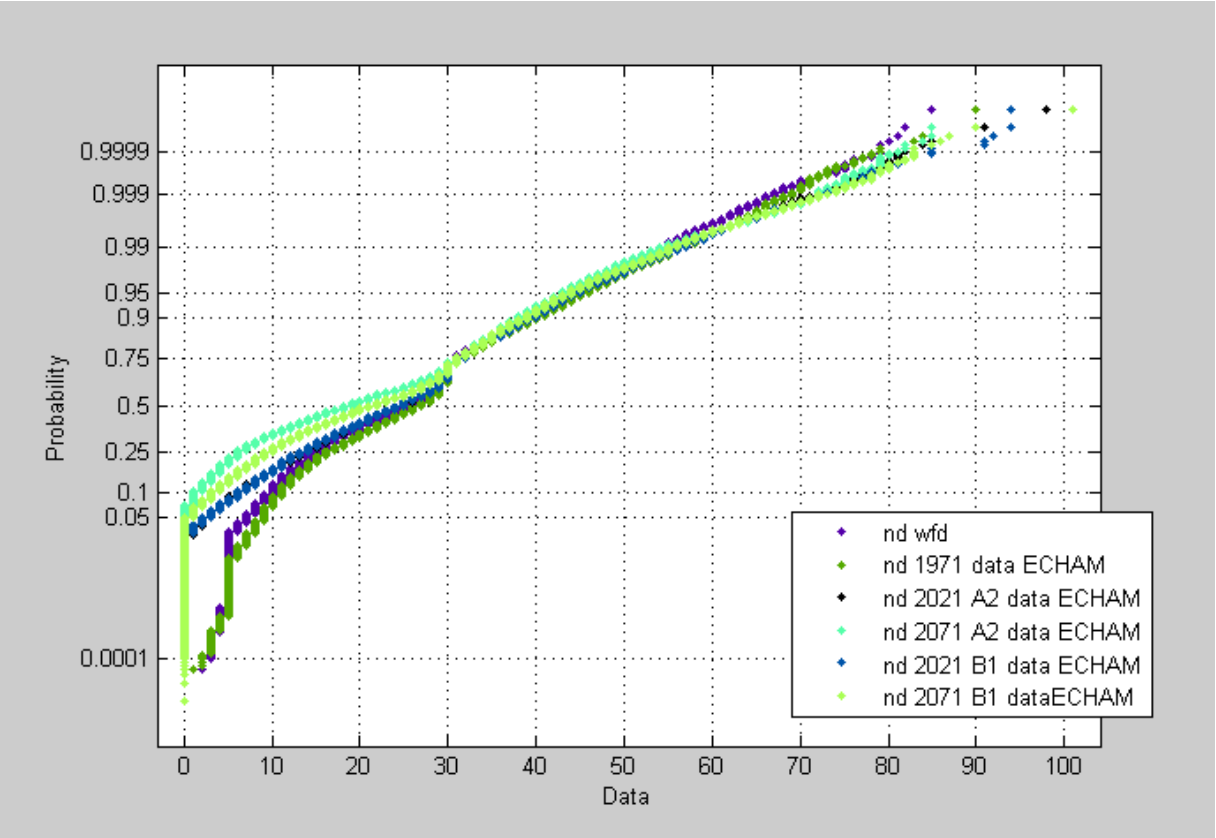

Probability density funtions of drought events for control, mid and late 21st century (not corrected for arid regions) as obtained with GWAVA and ECHAM climate input.

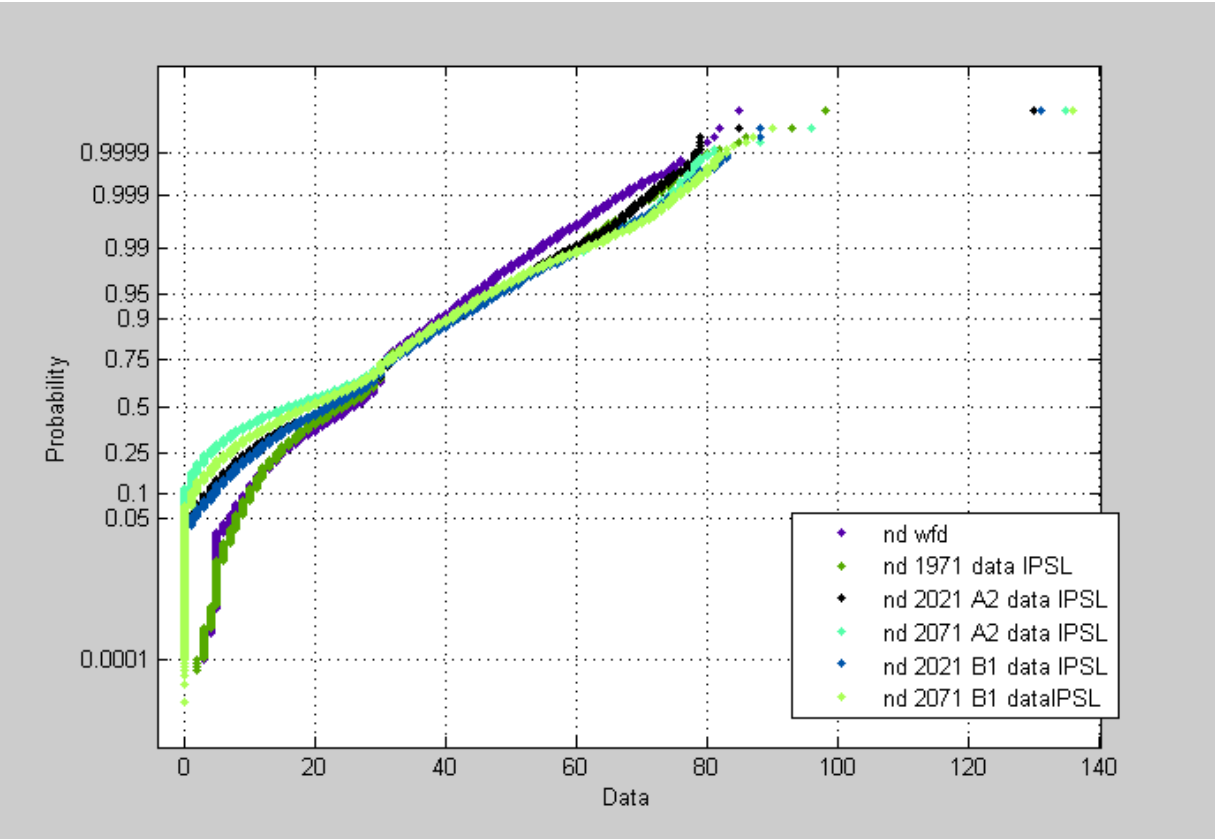

Probability density funtions of drought events for control, mid and late 21st century (not corrected for arid regions) as obtained with GWAVA and IPSL climate input.

1.2.4 Analysis of GWAVA with a drought equivalent index

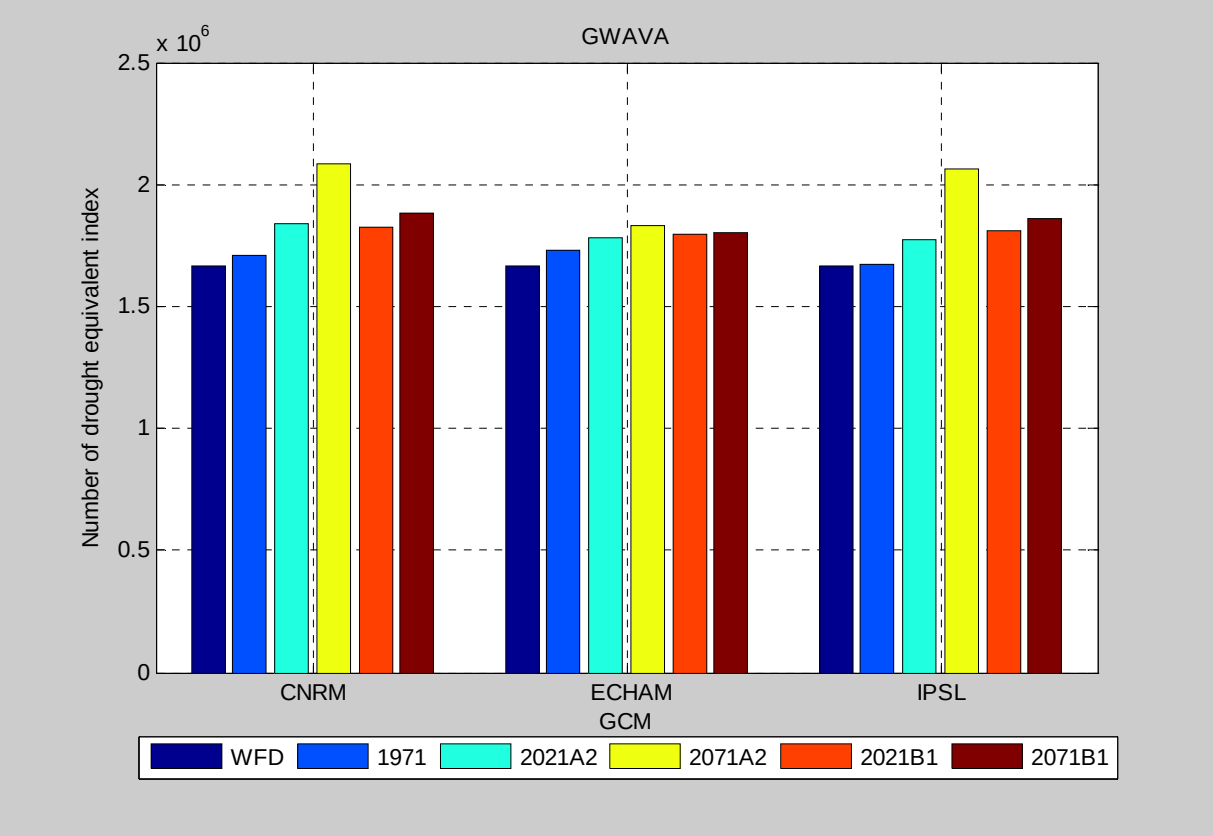

Number of drought events for control, mid and late 21st century (corrected for arid regions).

ANNEX 1.3 H08

1.3.1 Analysis of number of drought events

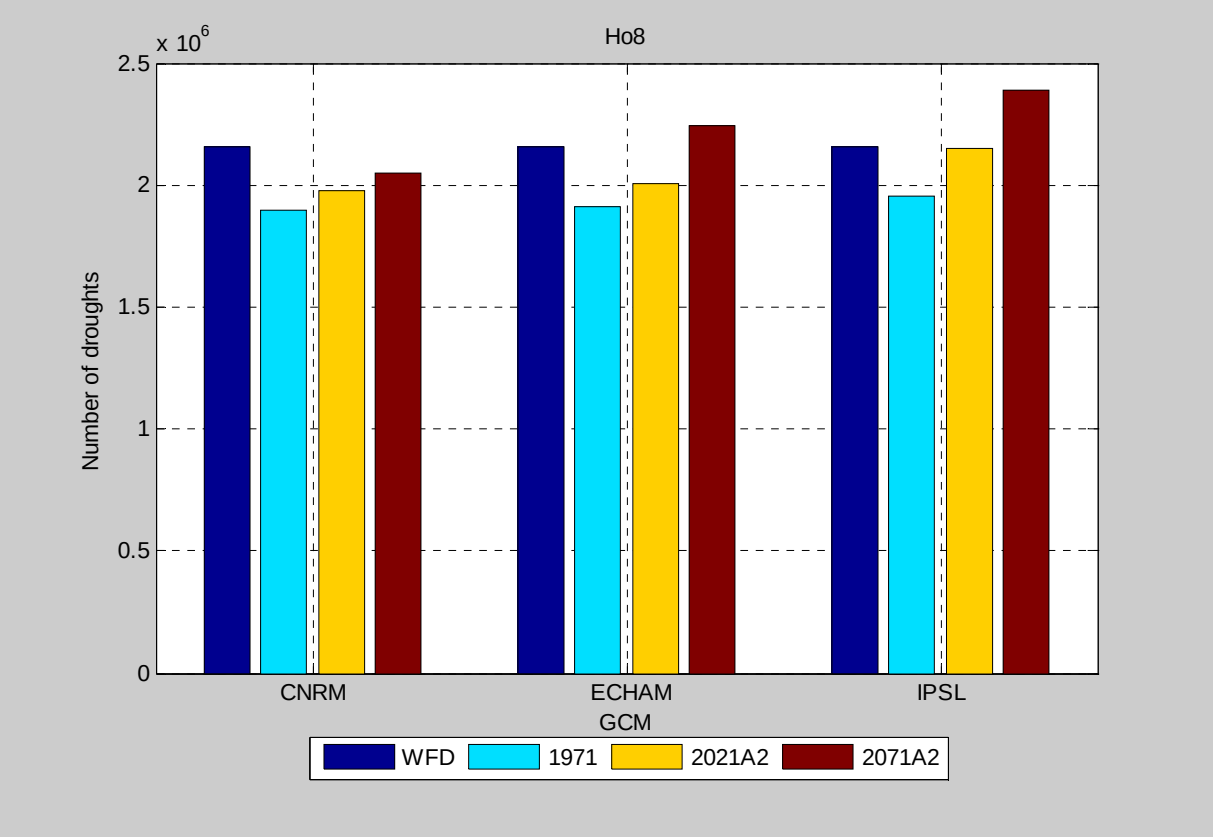

Number of drought events for control, mid and late 21st century (not corrected for arid regions).

1.3.2 Number of arid regions

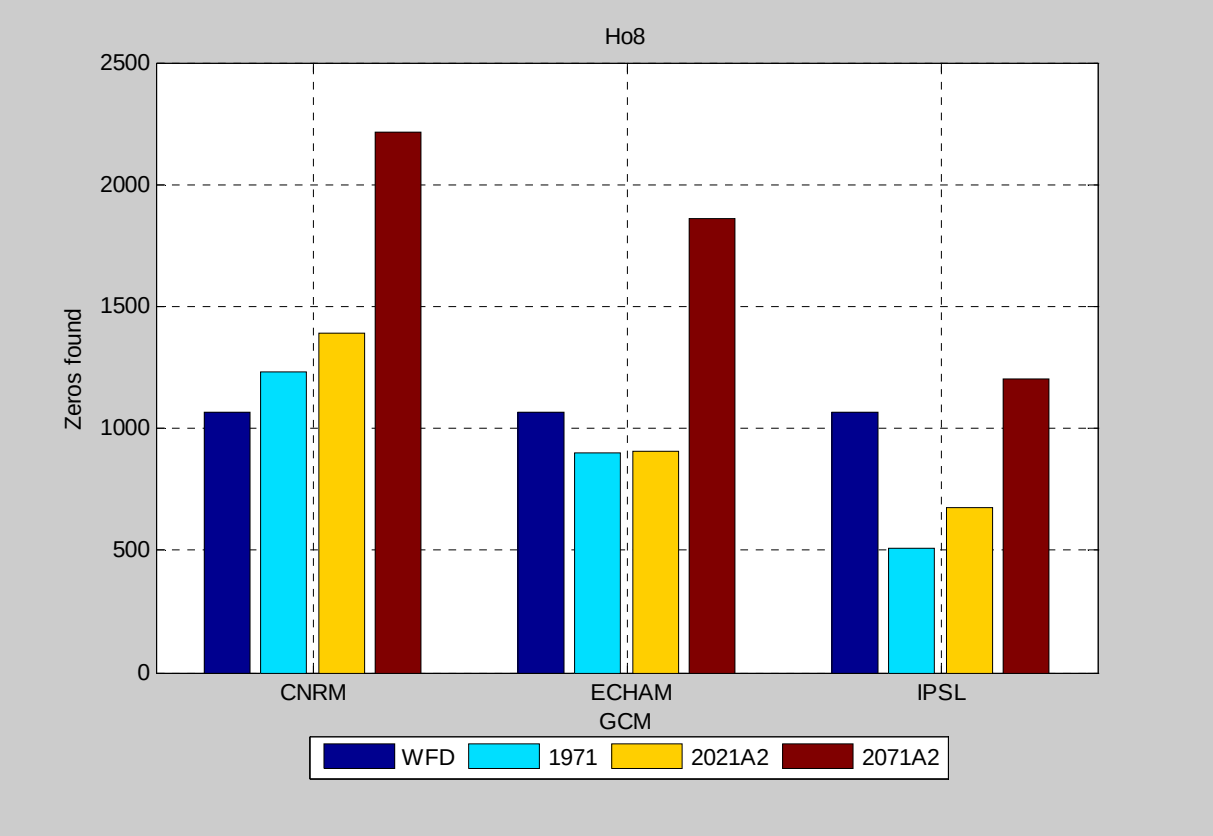

Number of Zeros.

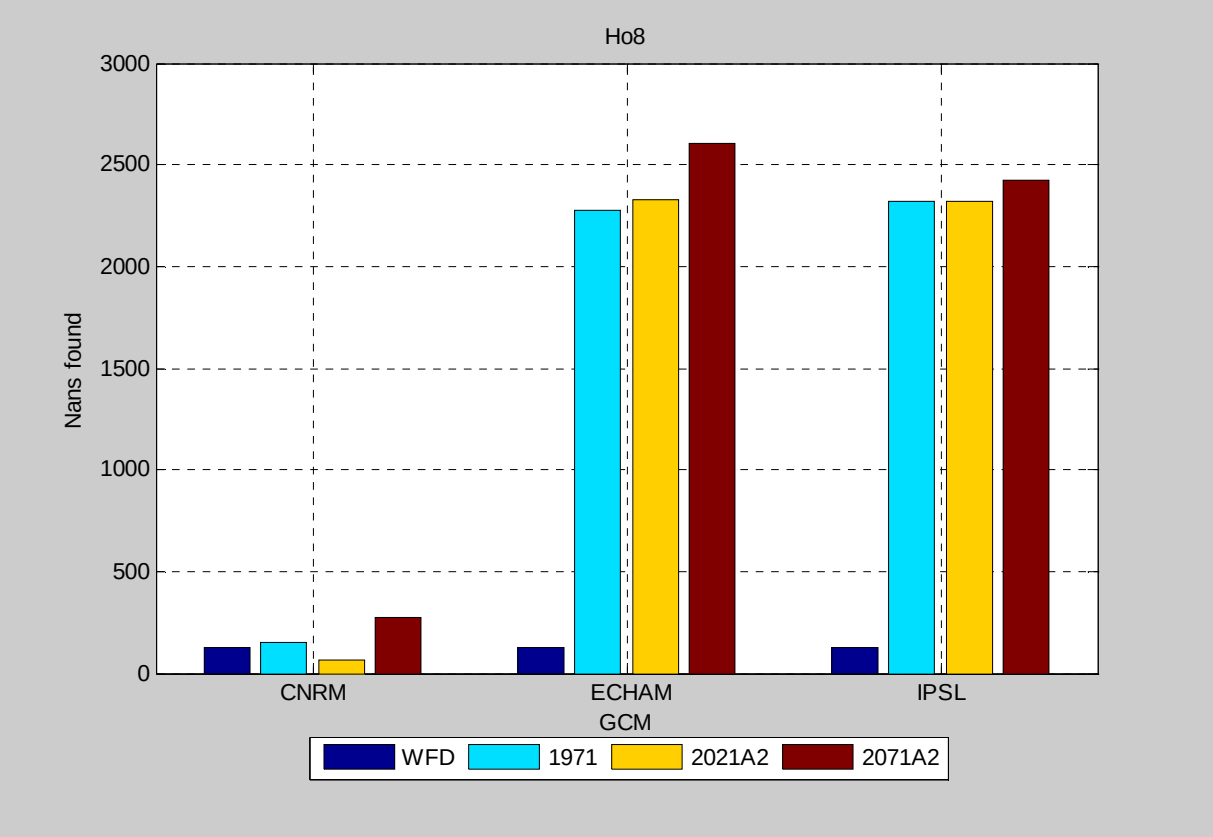

Number of Nans.

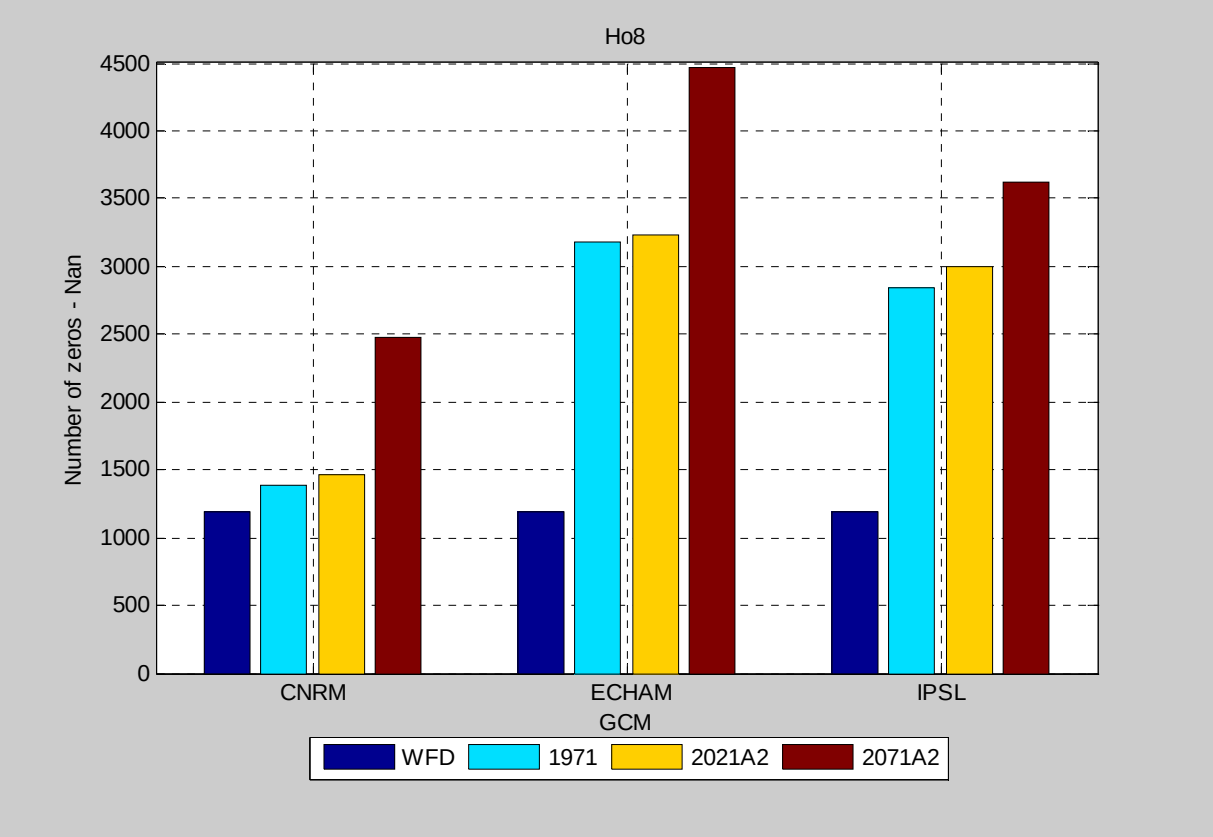

Number of arid regions (zeros + Nans) for control, mid and late 21st century.

1.3.3 PDF Number of drought events for three GCMs

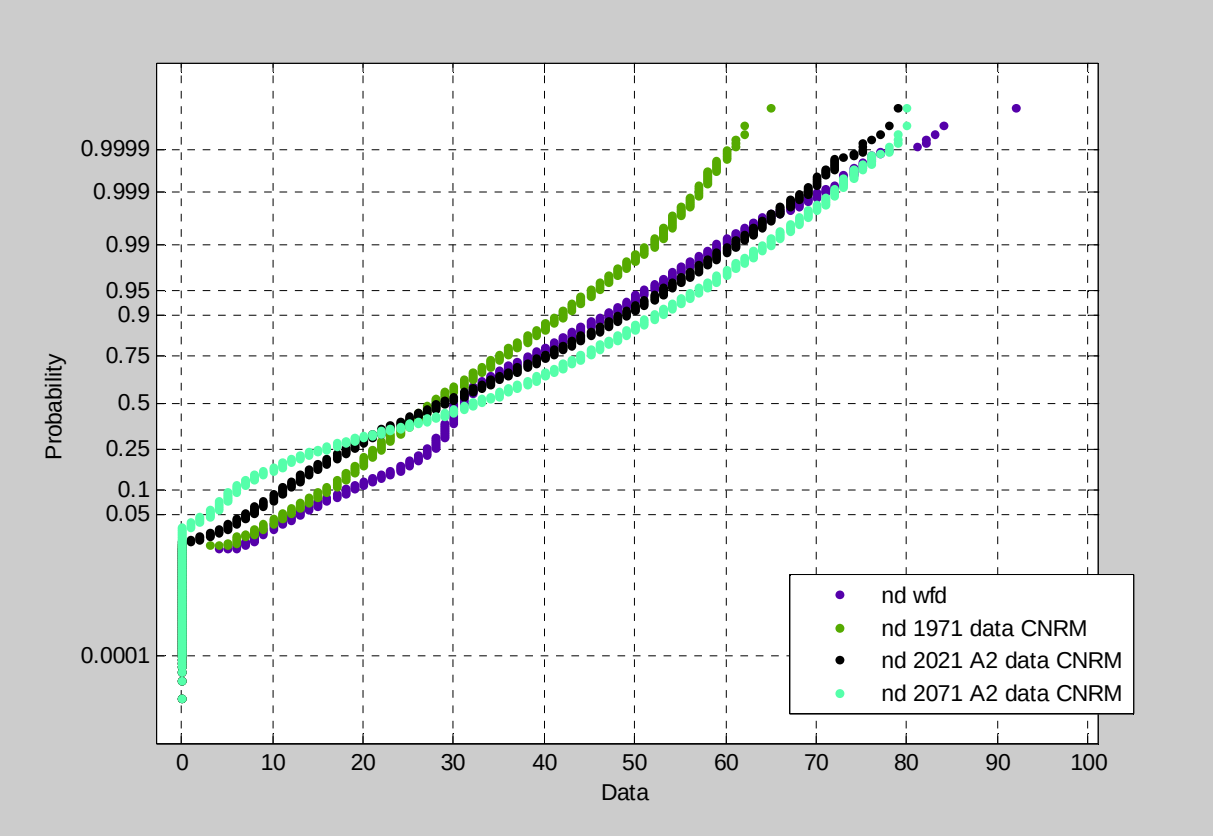

Probability density funtions of drought events for control, mid and late 21st century (not corrected for arid regions) as obtained with H08 and CNRM climate input.

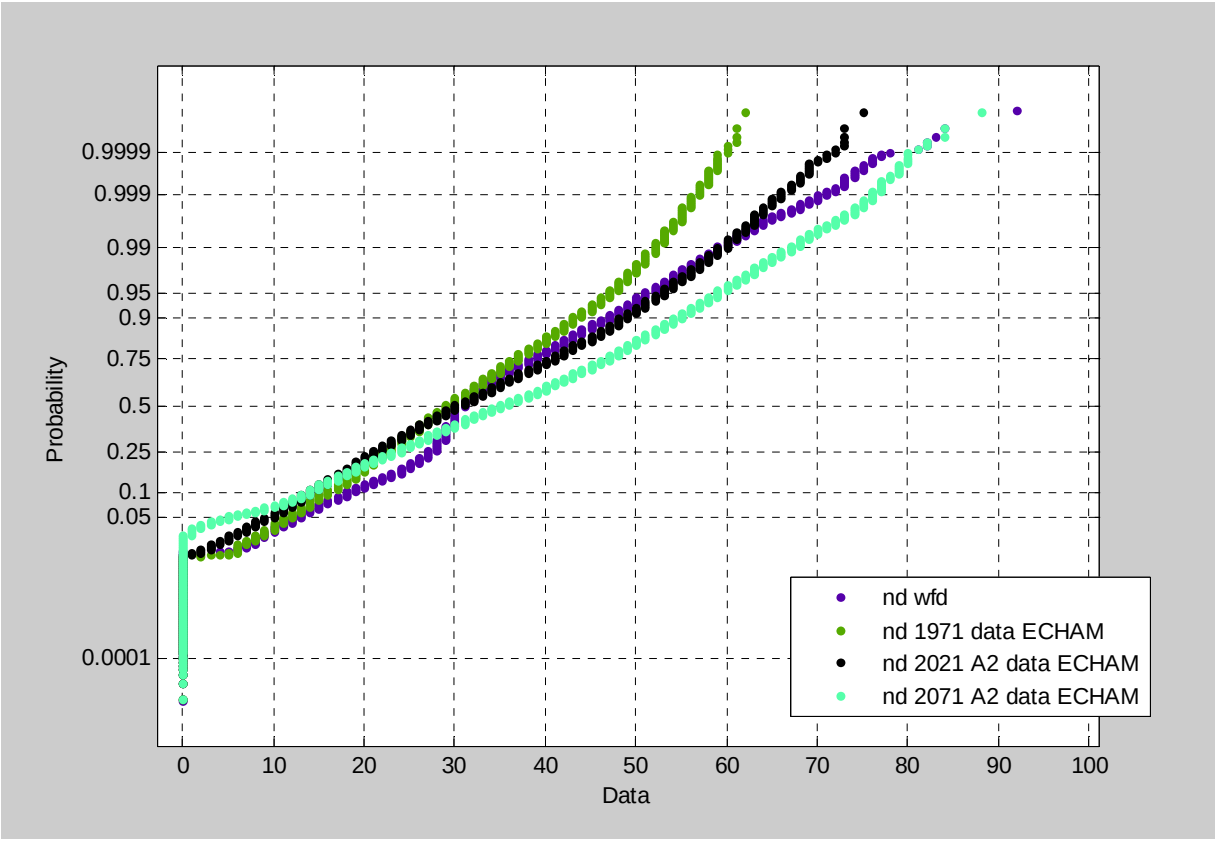

Probability density funtions of drought events for control, mid and late 21st century (not corrected for arid regions) as obtained with H08 and ECHAM climate input.

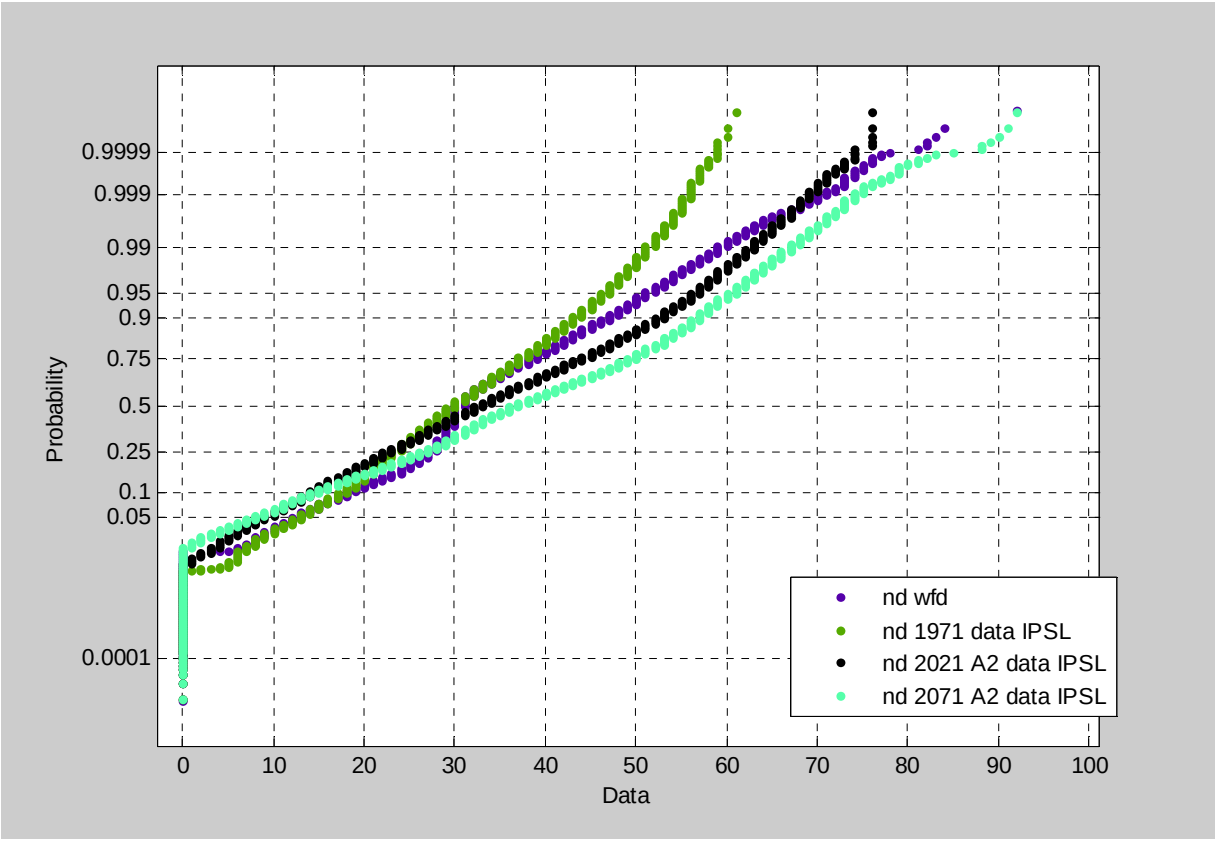

Probability density funtions of drought events for control, mid and late 21st century (not corrected for arid regions) as obtained with H08 and IPSL climate input.

1.3.4 Analysis of H08 with a drought equivalent index

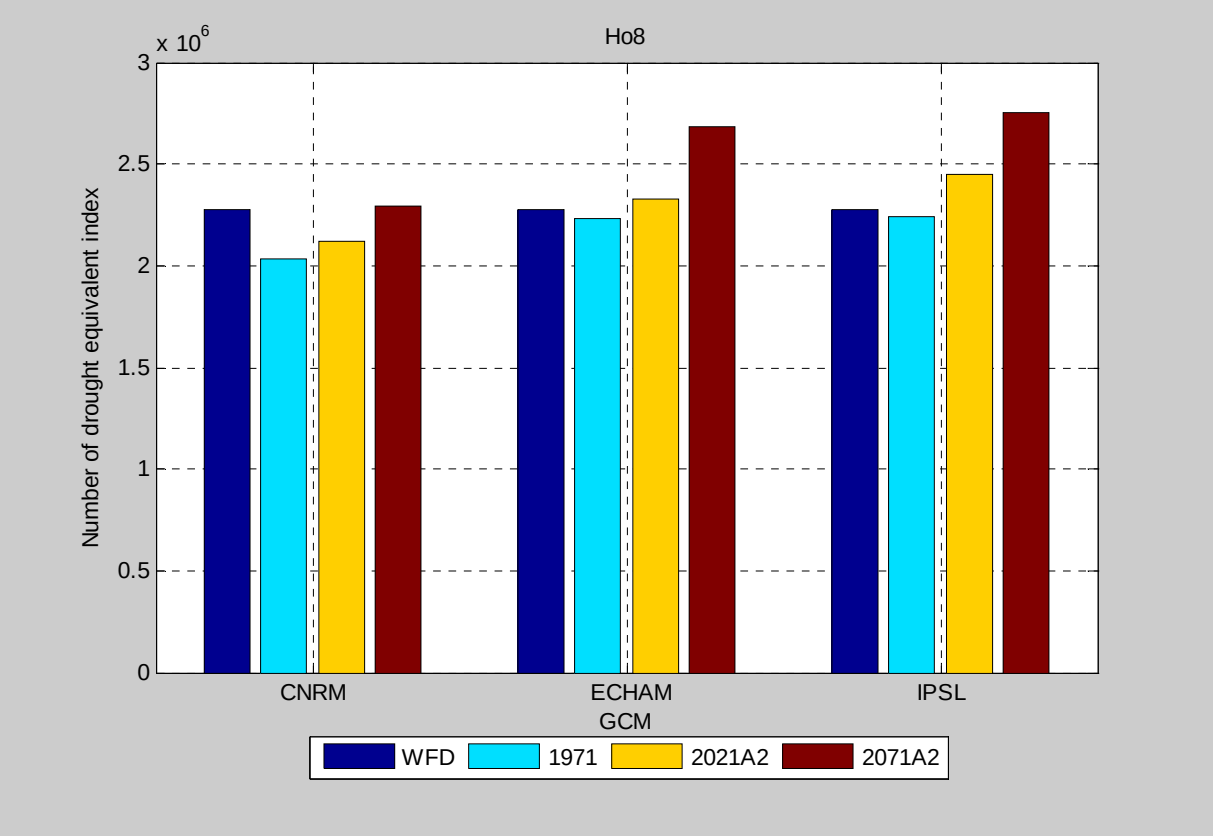

Number of drought events for control, mid and late 21st century (corrected for arid regions).

ANNEX 1.4 MACPDM

1.4.1 Analysis of number of drought events

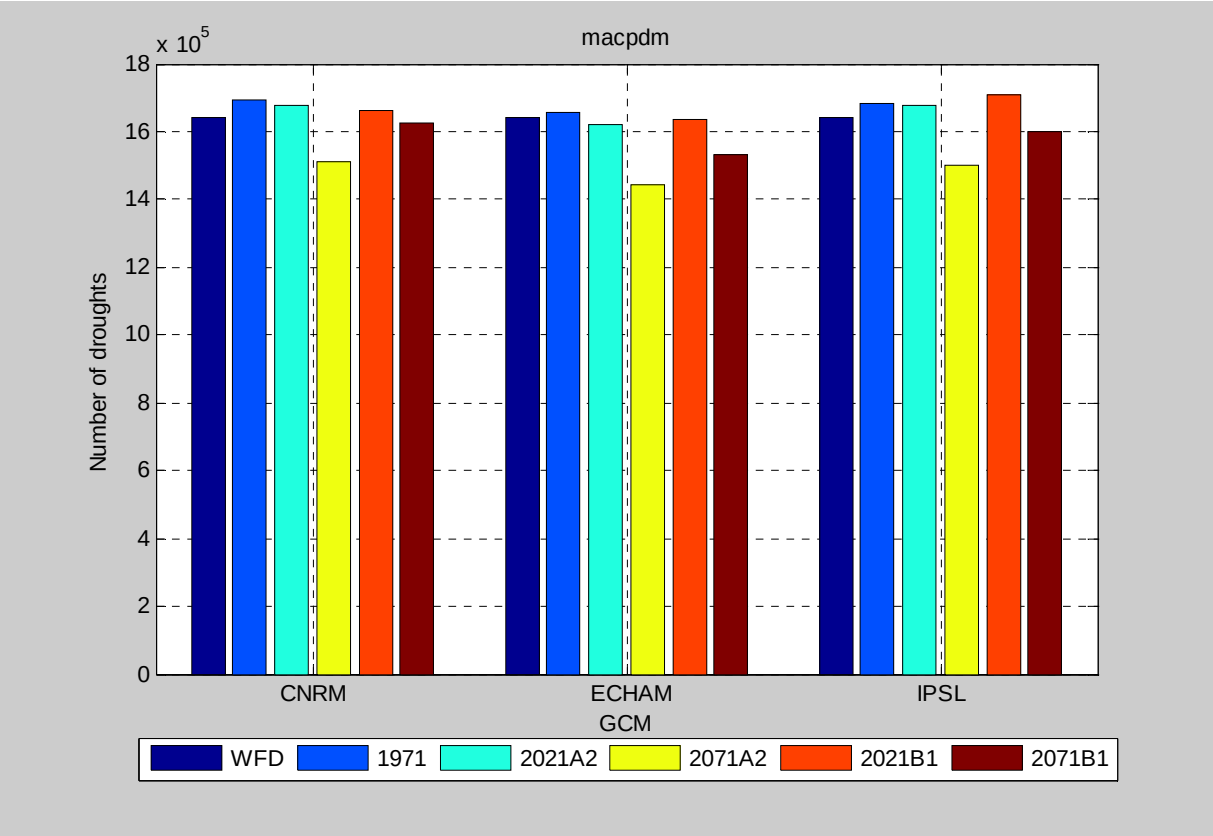

Number of drought events for control, mid and late 21st century (not corrected for arid regions).

1.4.2 Number of arid regions

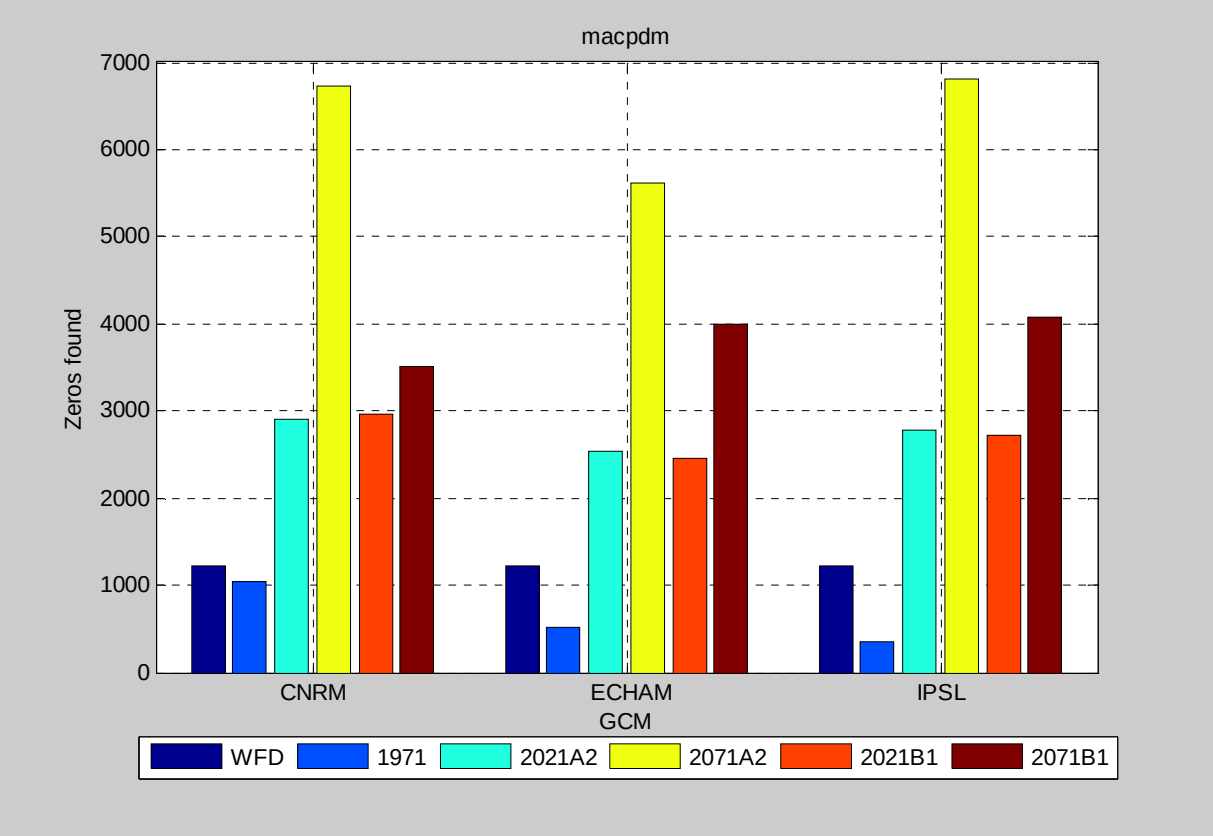

Number of Zeros.

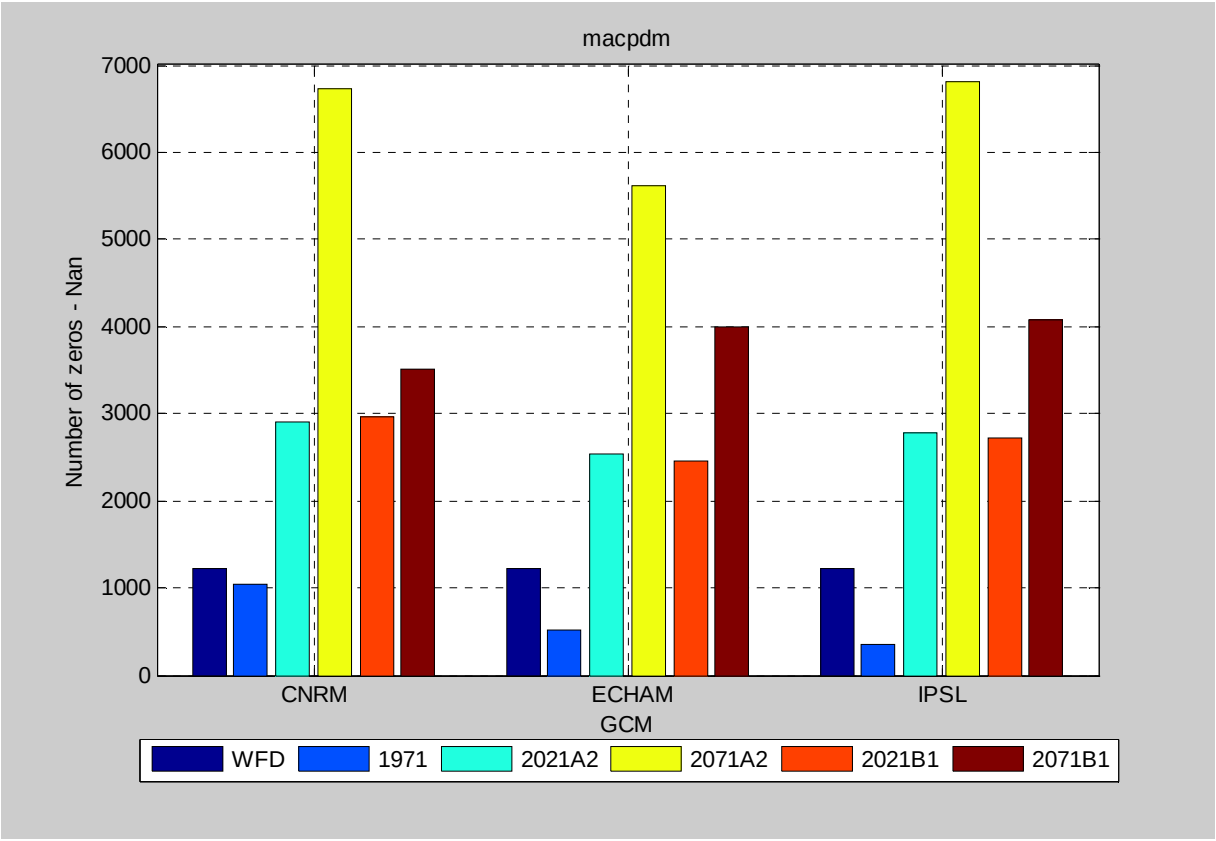

Number of arid regions (zeros + Nans) for control, mid and late 21st century.

1.4.3 PDF Number of drought events for three GCMs

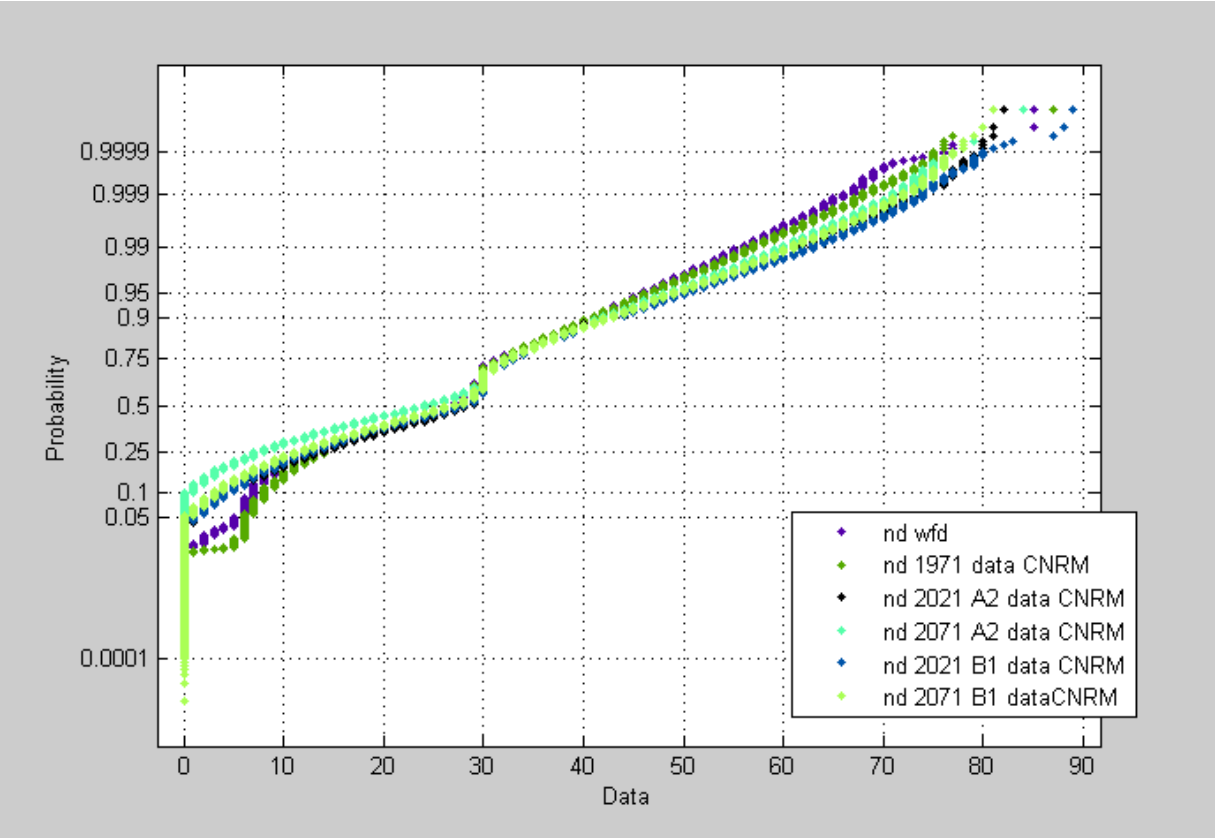

Probability density funtions of drought events for control, mid and late 21st century (not corrected for arid regions) as obtained with MACPDM and CNRM climate input.

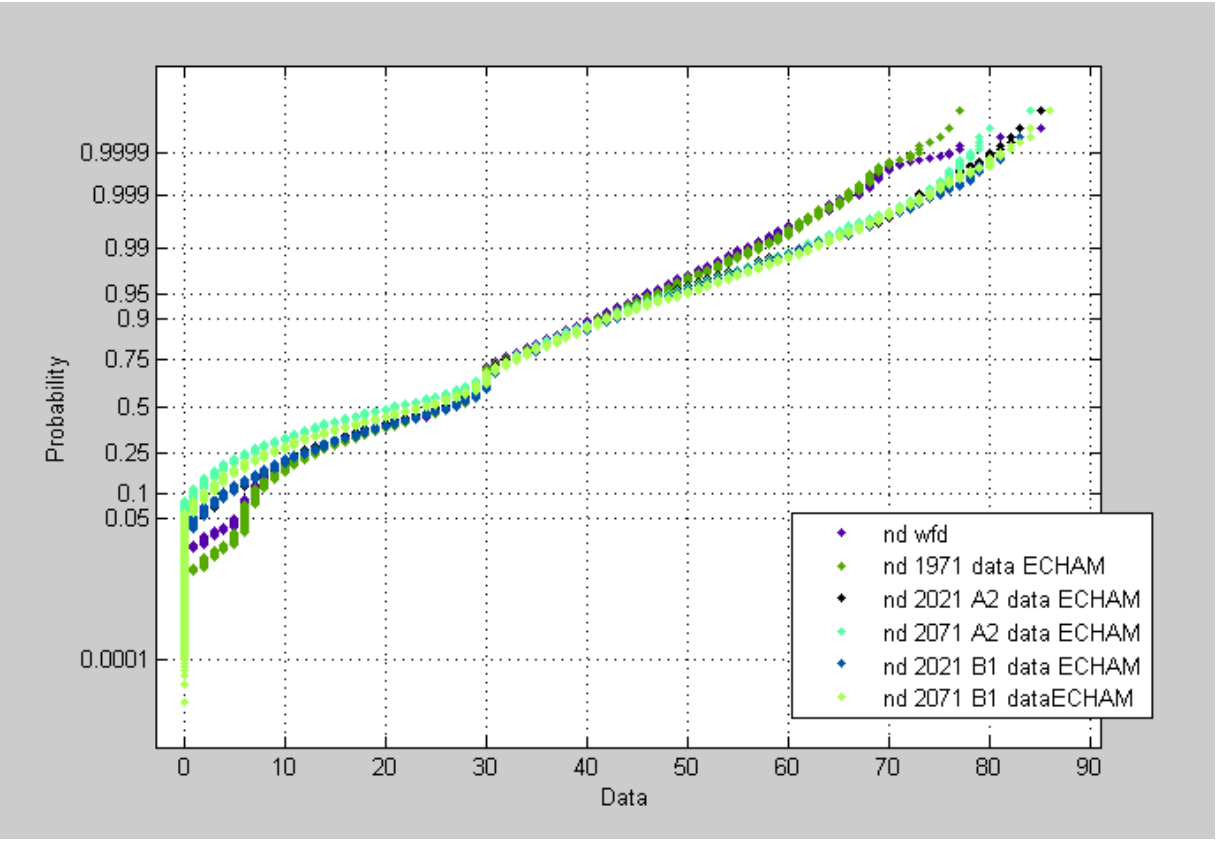

Probability density funtions of drought events for control, mid and late 21st century (not corrected for arid regions) as obtained with MACPDM and ECHAM climate input.

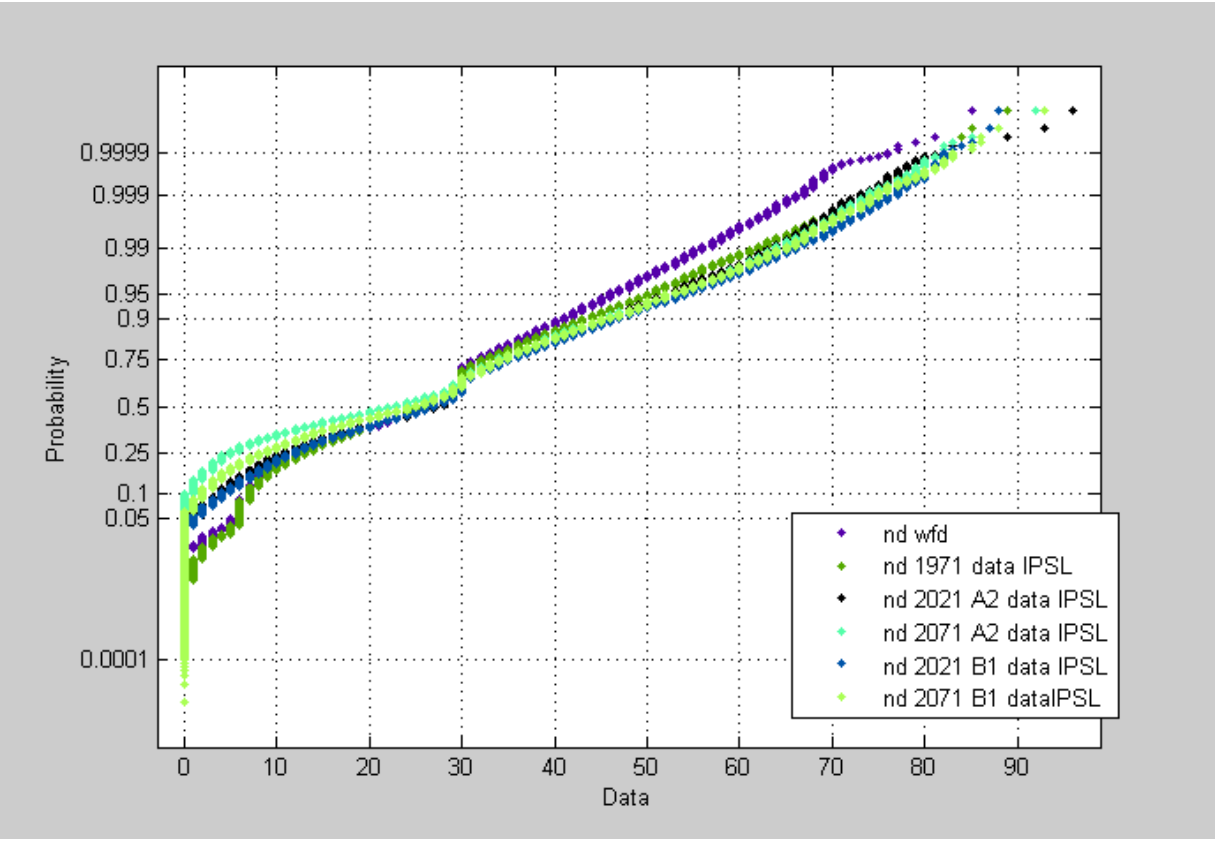

Probability density funtions of drought events for control, mid and late 21st century (not corrected for arid regions) as obtained with MACPDM and IPSL climate input.

1.4.4 Analysis of MacPDM with a drought equivalent index

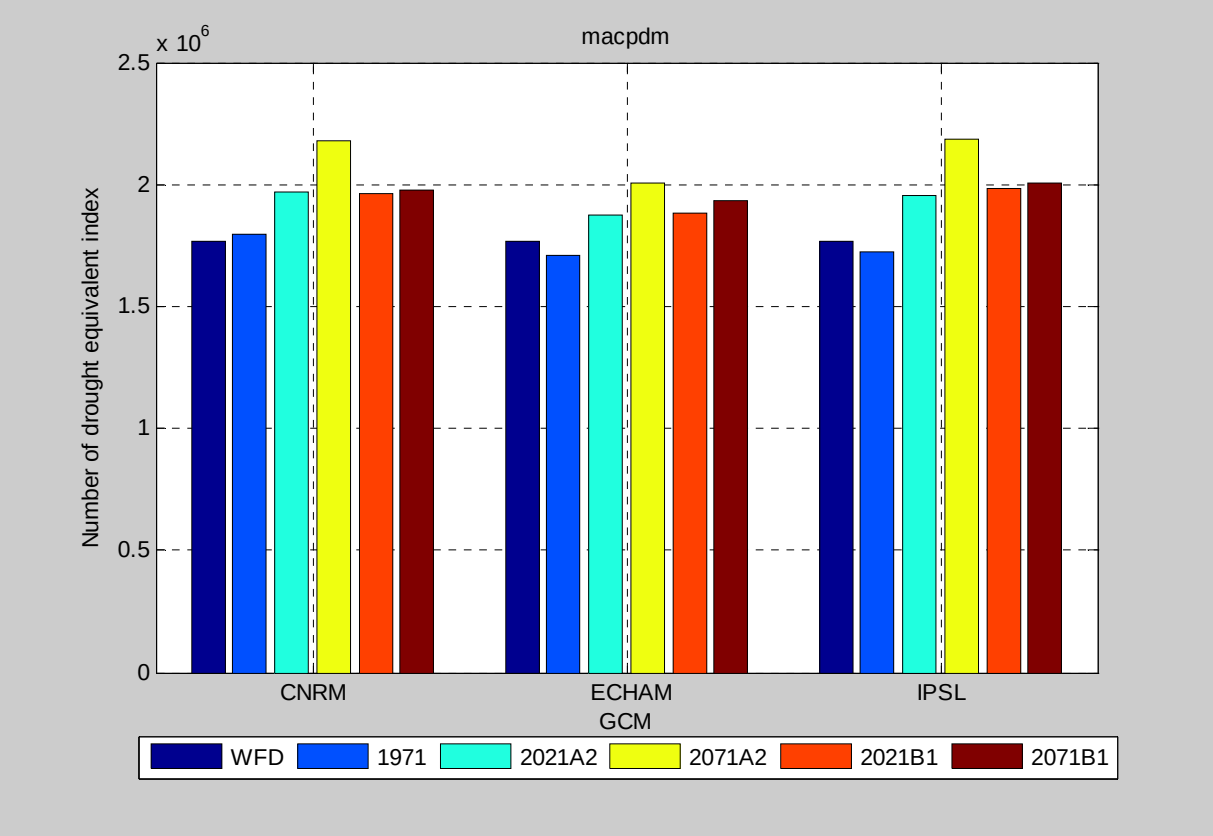

Number of drought events for control, mid and late 21st century (corrected for arid regions).

ANNEX 1.5 LPJML

1.5.1 Analysis of number of drought events

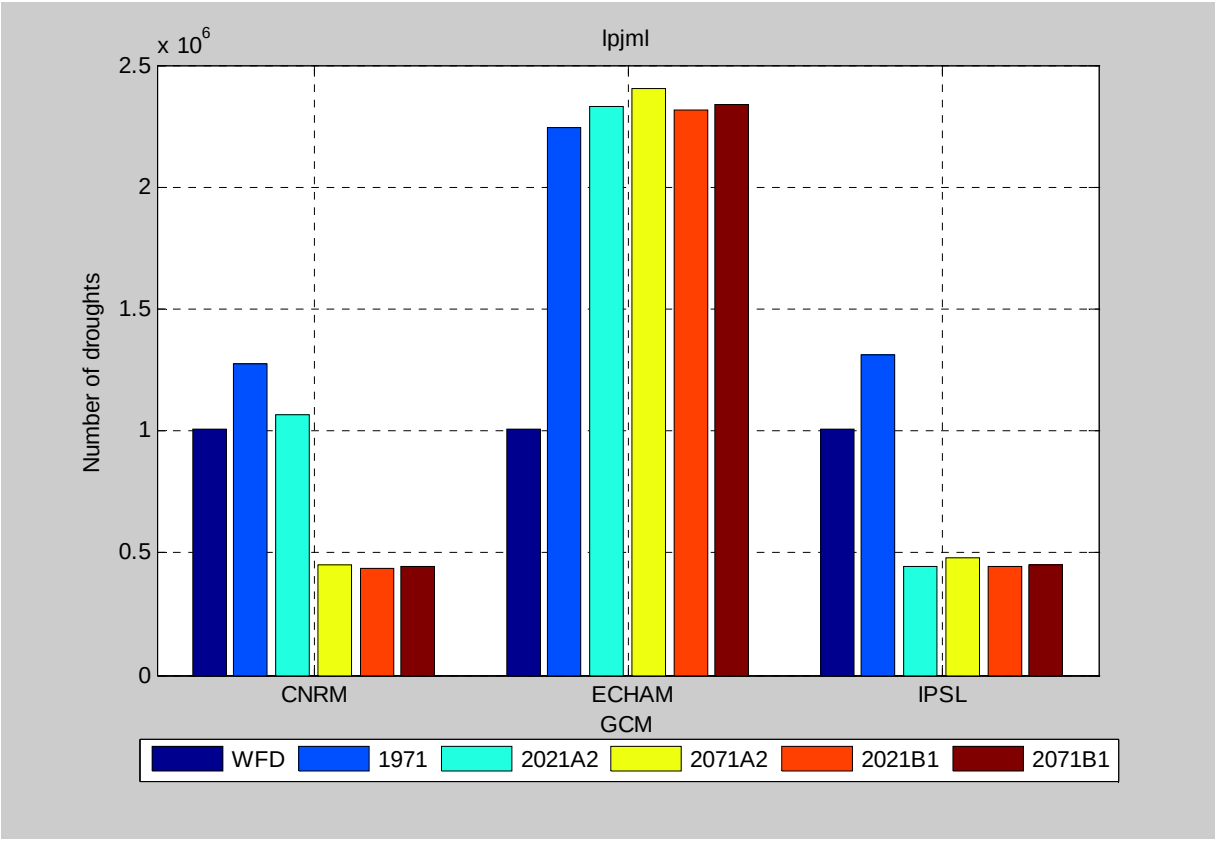

Number of drought events for control, mid and late 21st century (not corrected for arid regions).

1.5.2. Number of arid regions

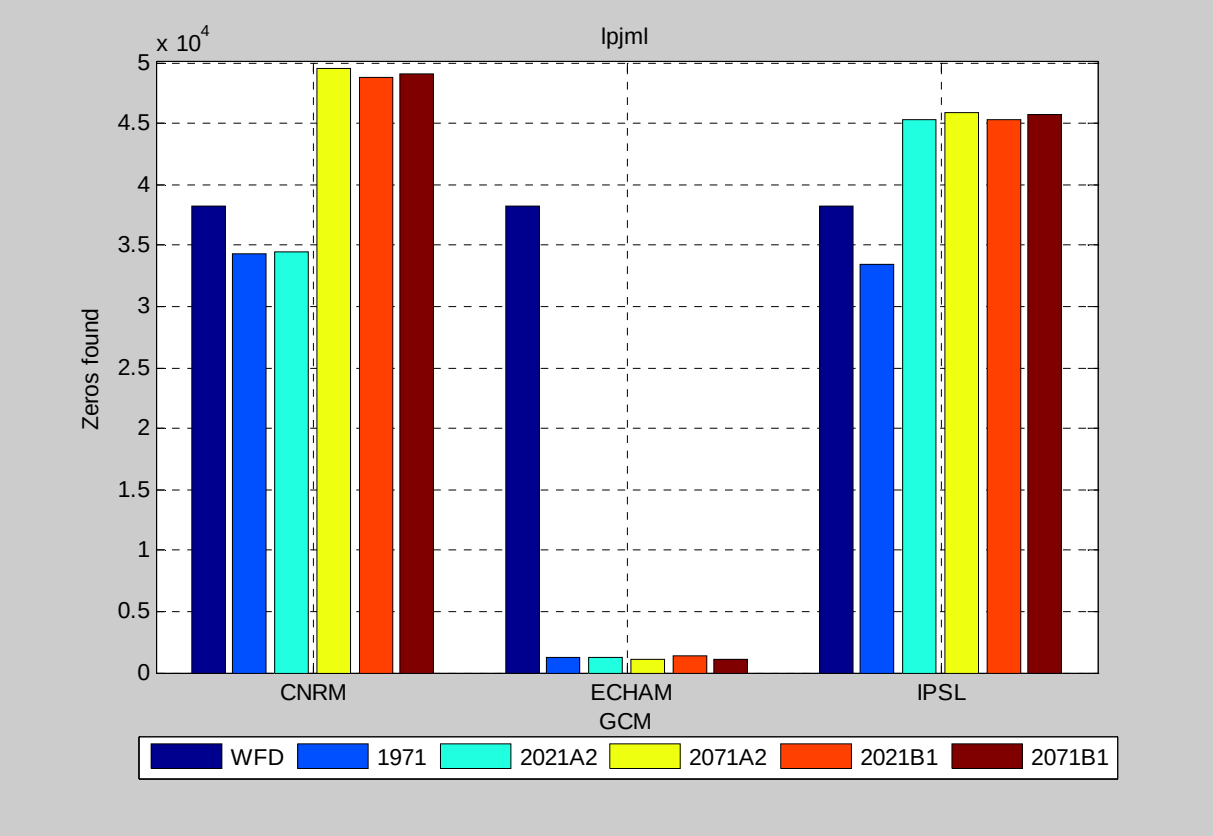

Number of Zeros.

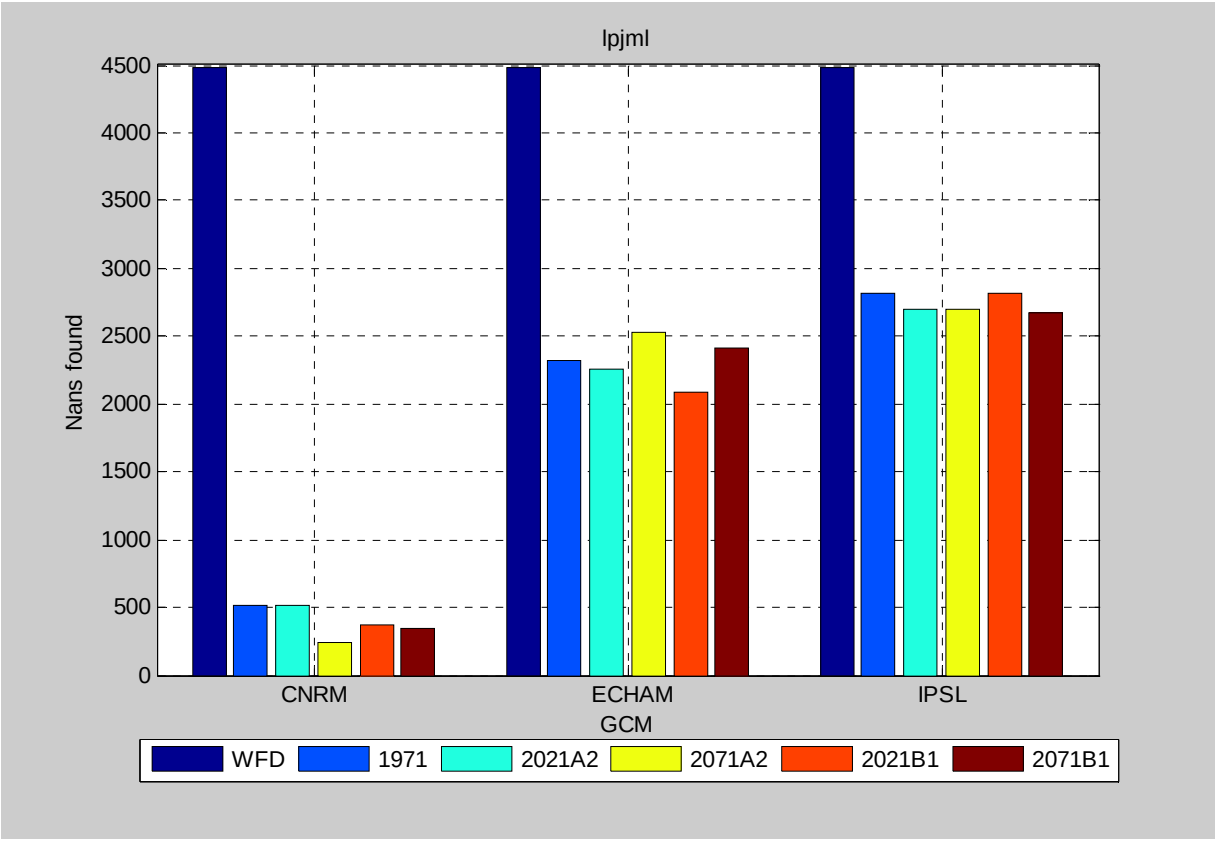

Number of Nans.

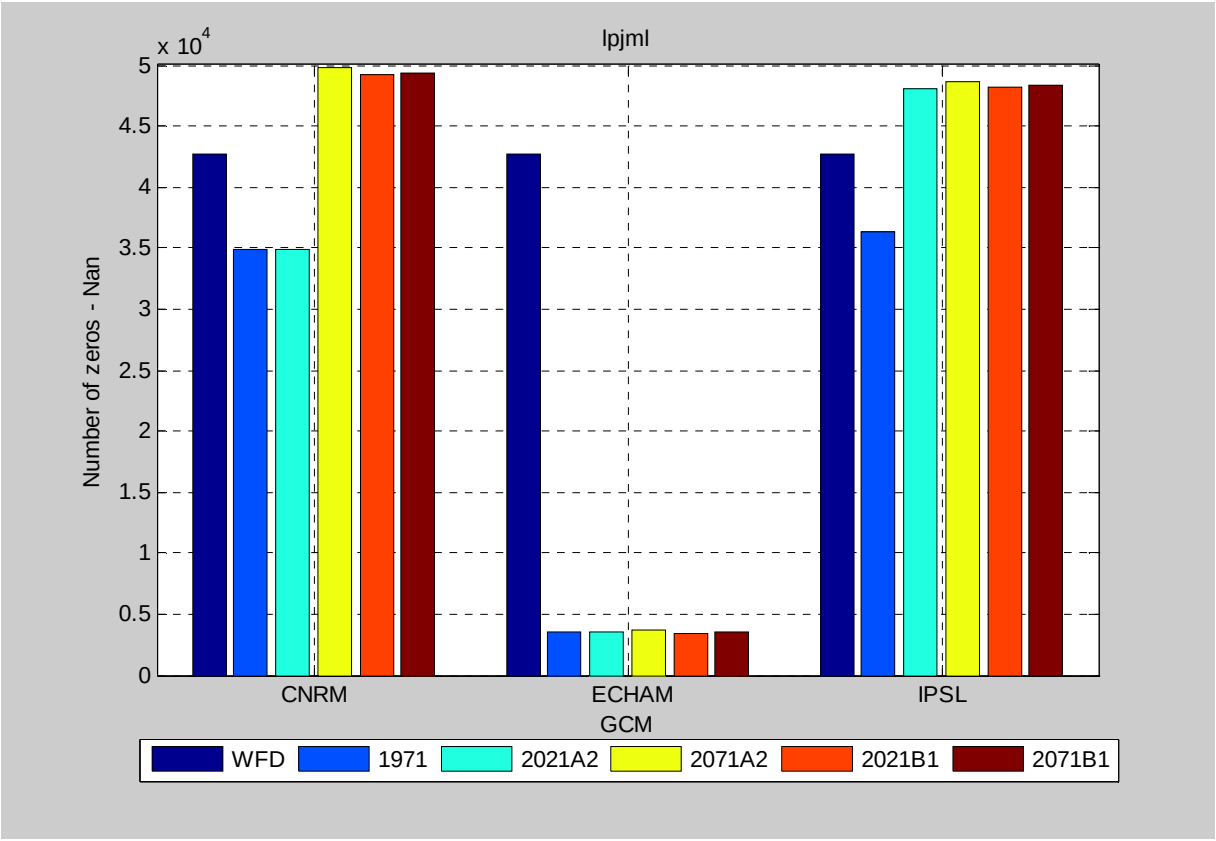

Number of arid regions (zeros + Nans) for control, mid and late 21st century.

1.5.3 PDF Number of drought events for three GCMs

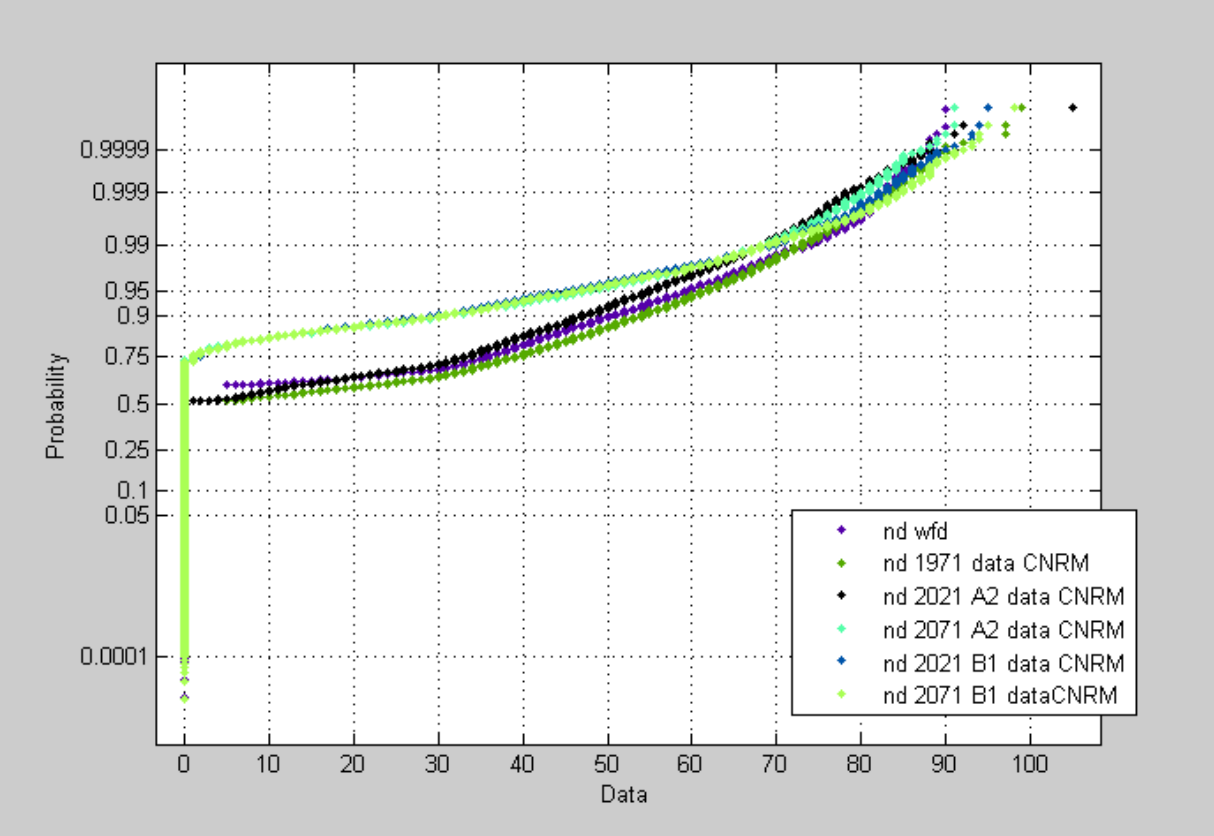

Probability density funtions of drought events for control, mid and late 21st century (not corrected for arid regions) as obtained with LPJlm and CNRM climate input.

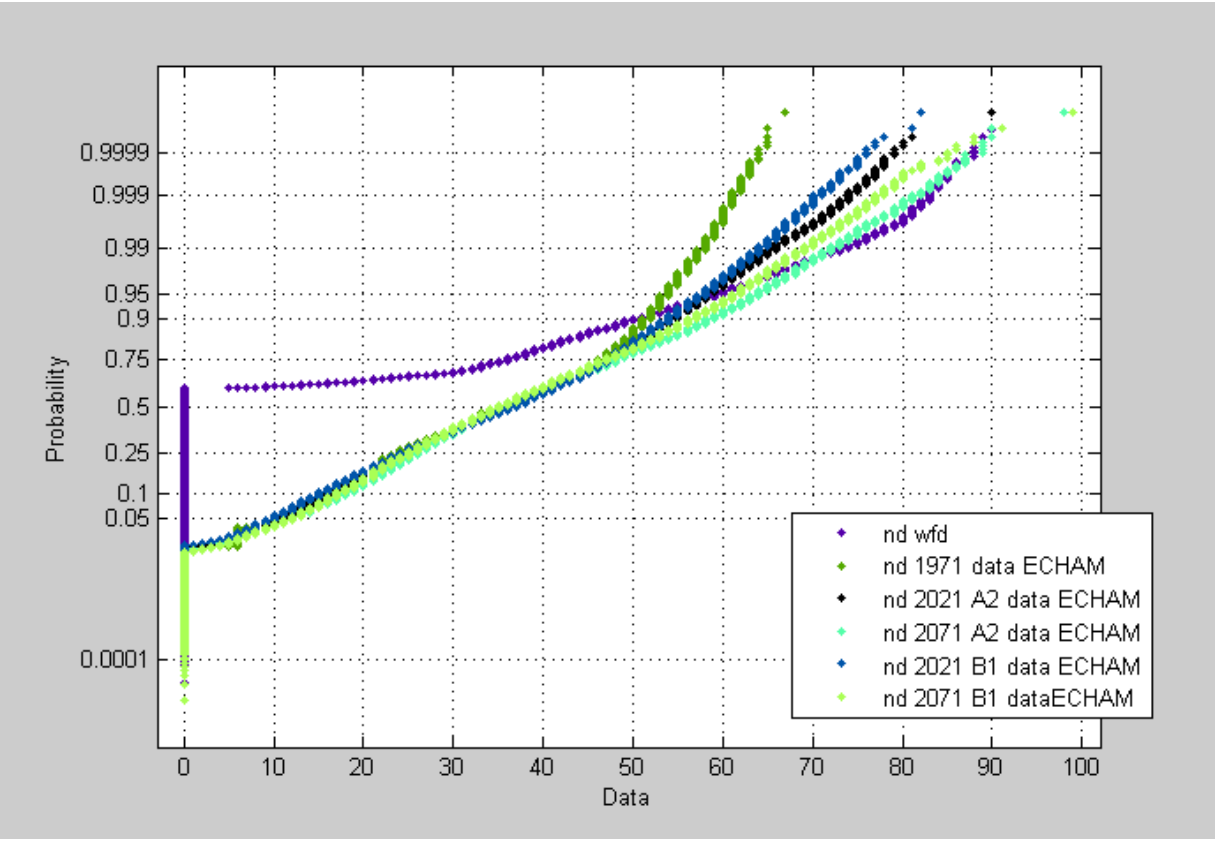

Probability density funtions of drought events for control, mid and late 21st century (not corrected for arid regions) as obtained with LPJlm and ECHAM climate input.

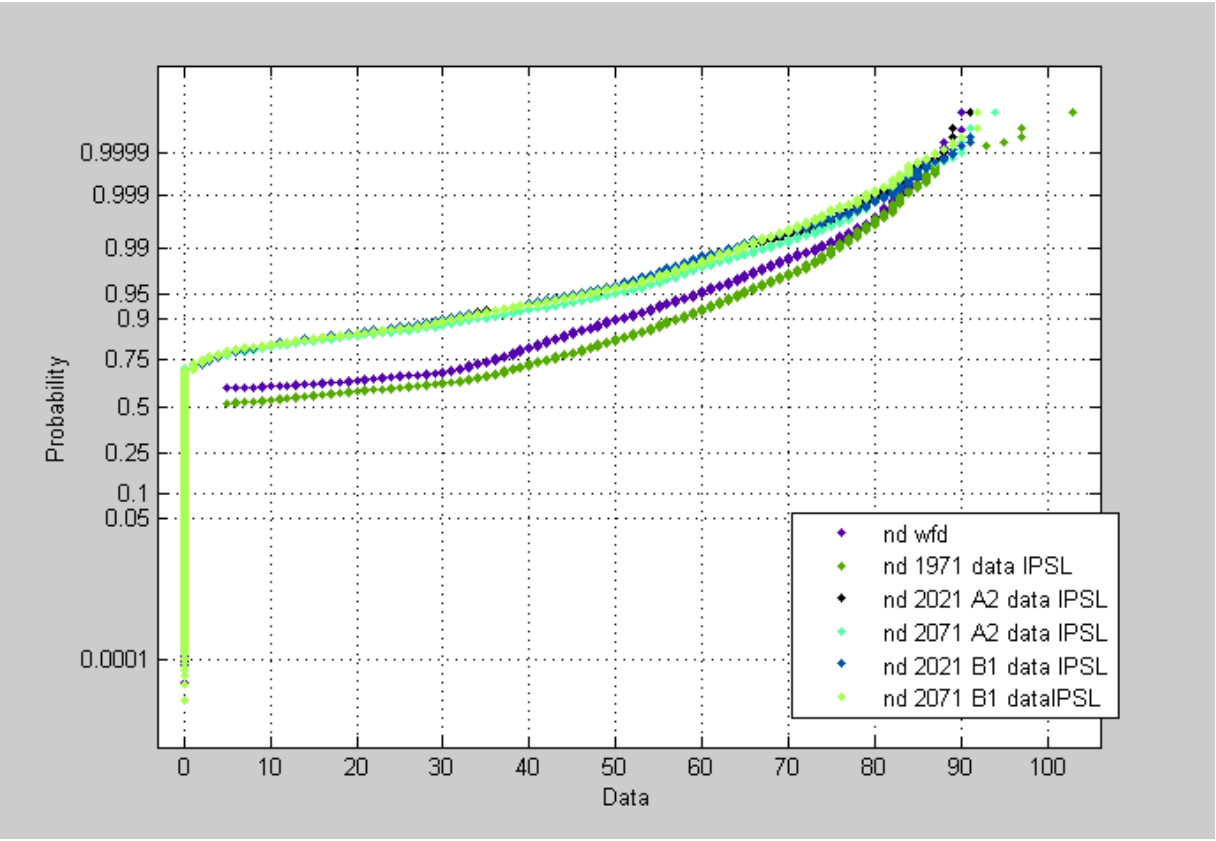

Probability density funtions of drought events for control, mid and late 21st century (not corrected for arid regions) as obtained with LPJlm and IPSL climate input.

1.5.4 Analysis of LPJml with a drought equivalent index

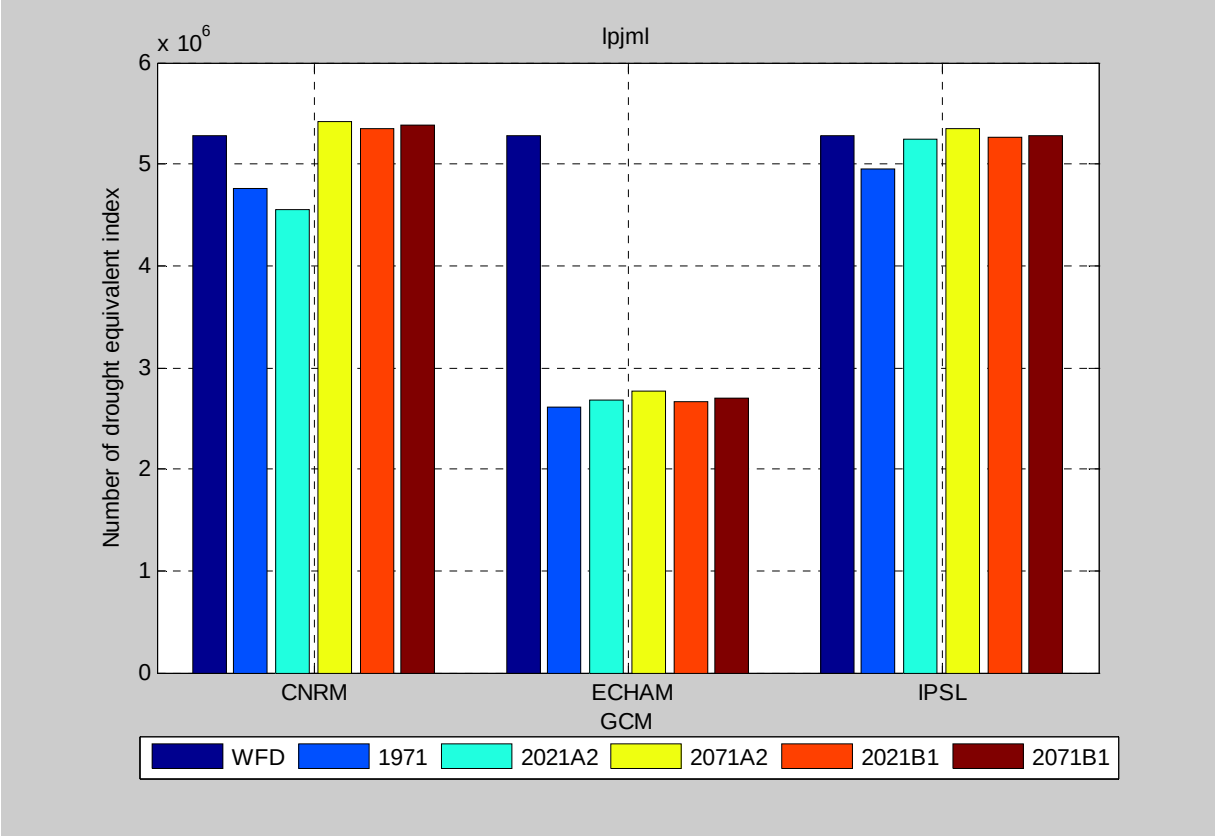

Number of drought events for control, mid and late 21st century (corrected for arid regions).

ANNEX 1.6 WATERGAP

1.6.1 Analysis of number of drought events

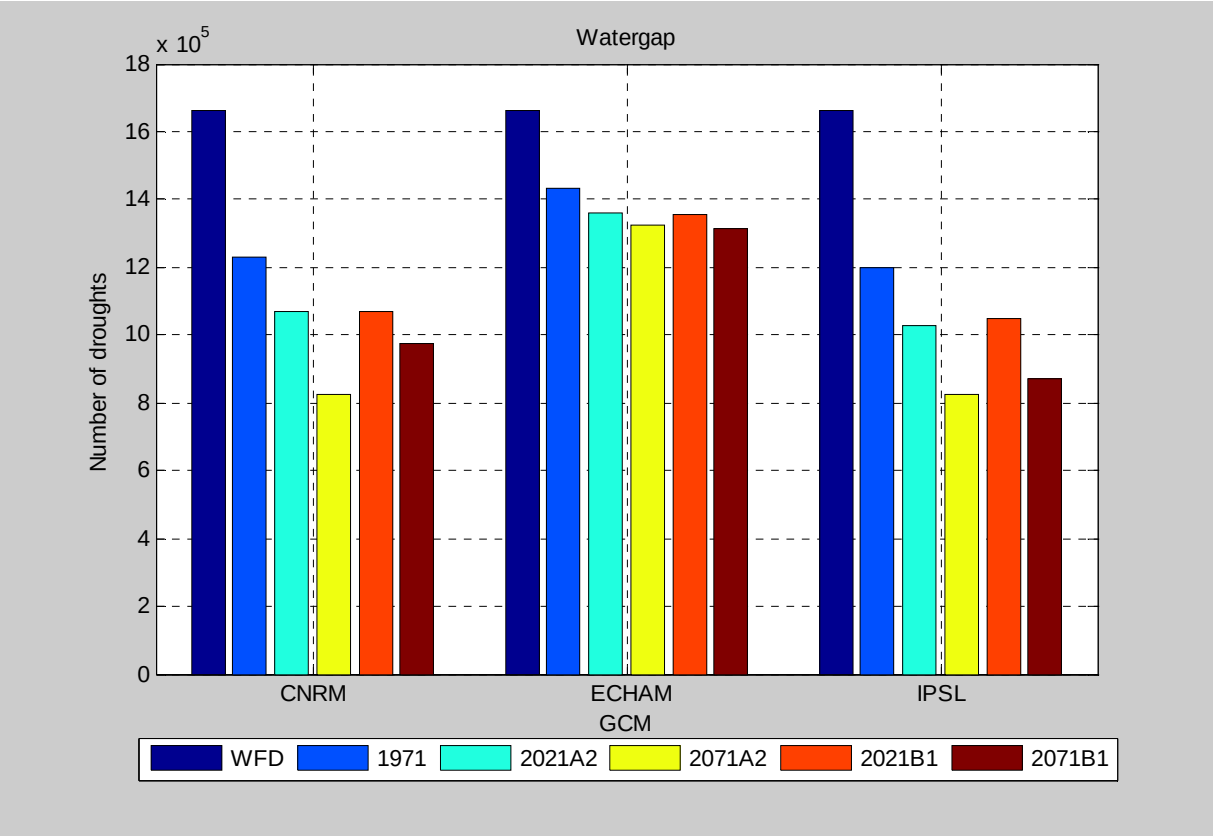

Number of drought events for control, mid and late 21st century (not corrected for arid regions).

1.6.2 Number of arid regions

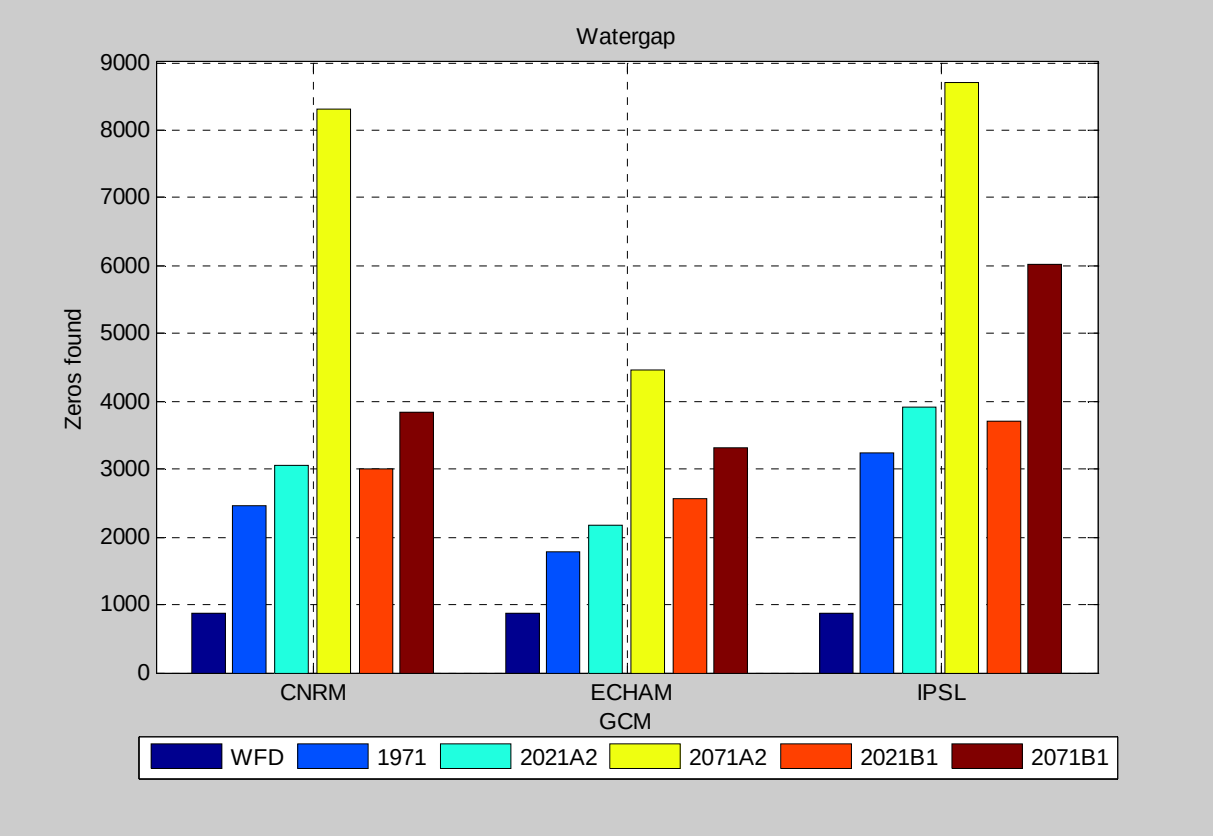

Number of Zeros.

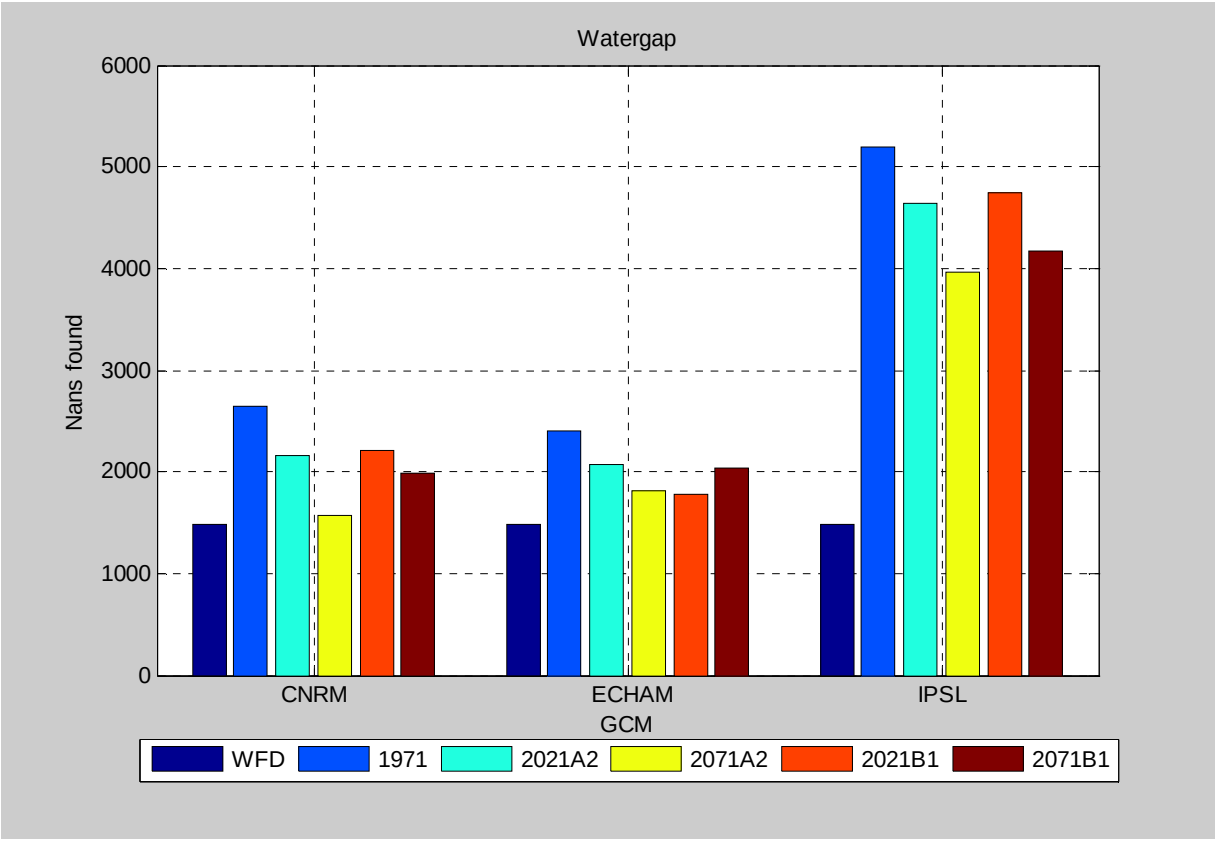

Number of Nans.

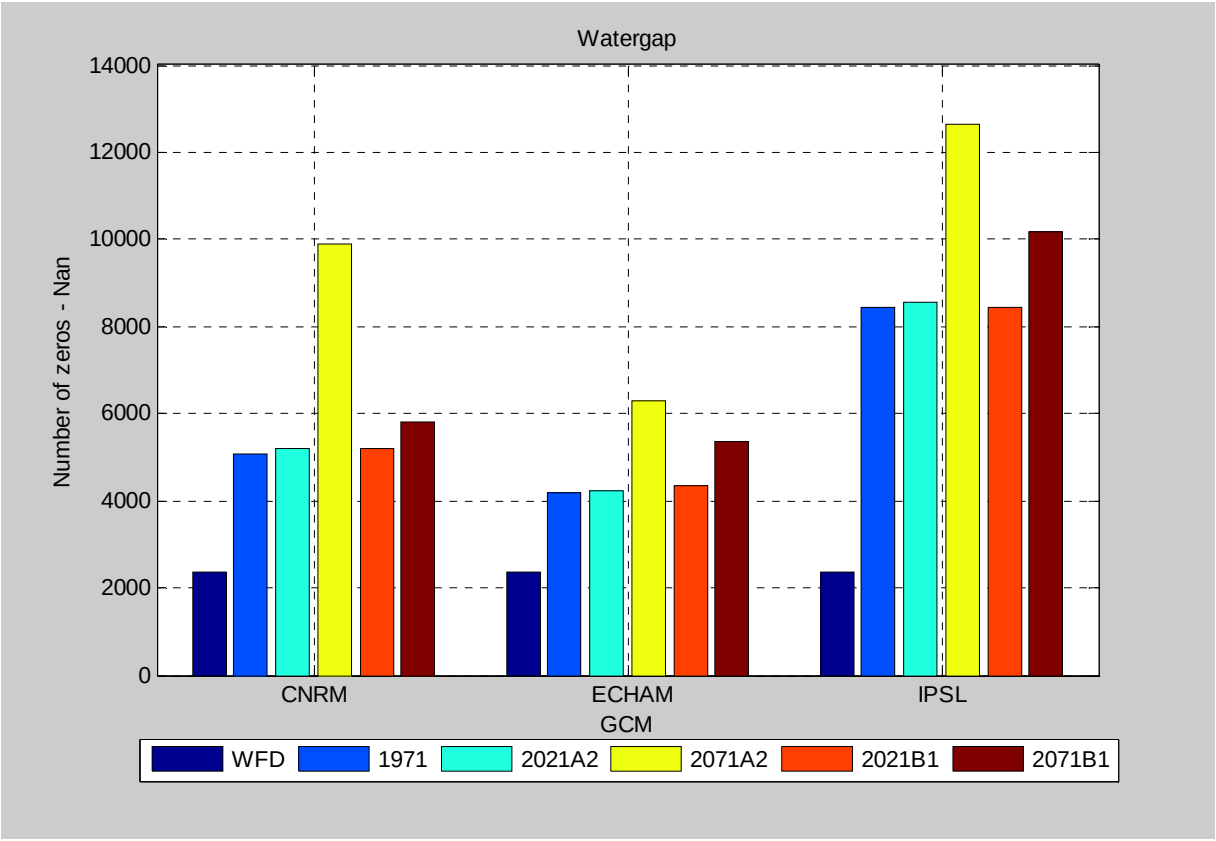

Number of arid regions (zeros + Nans) for control, mid and late 21st century.

1.6.3 PDF Number of drought events for three GCMs

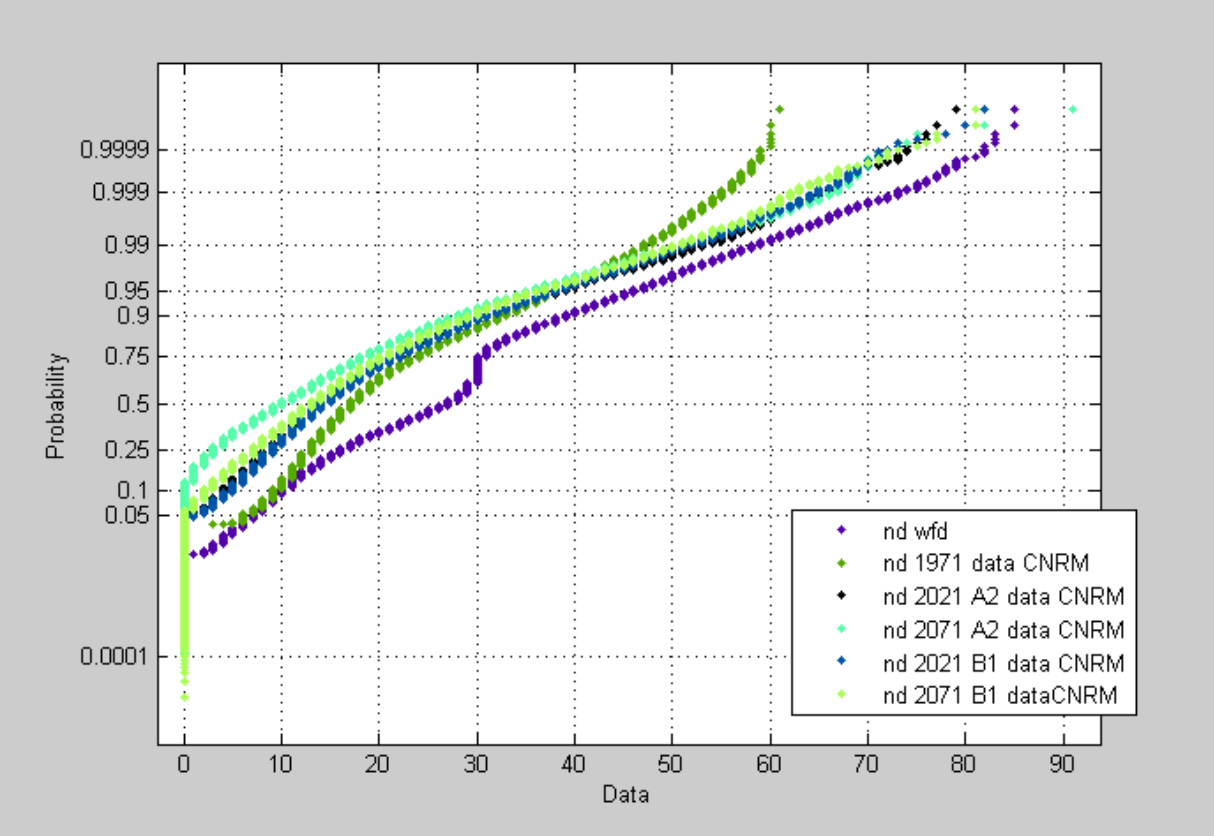

Probability density funtions of drought events for control, mid and late 21st century (not corrected for arid regions) as obtained with WaterGap and CNRM climate input.

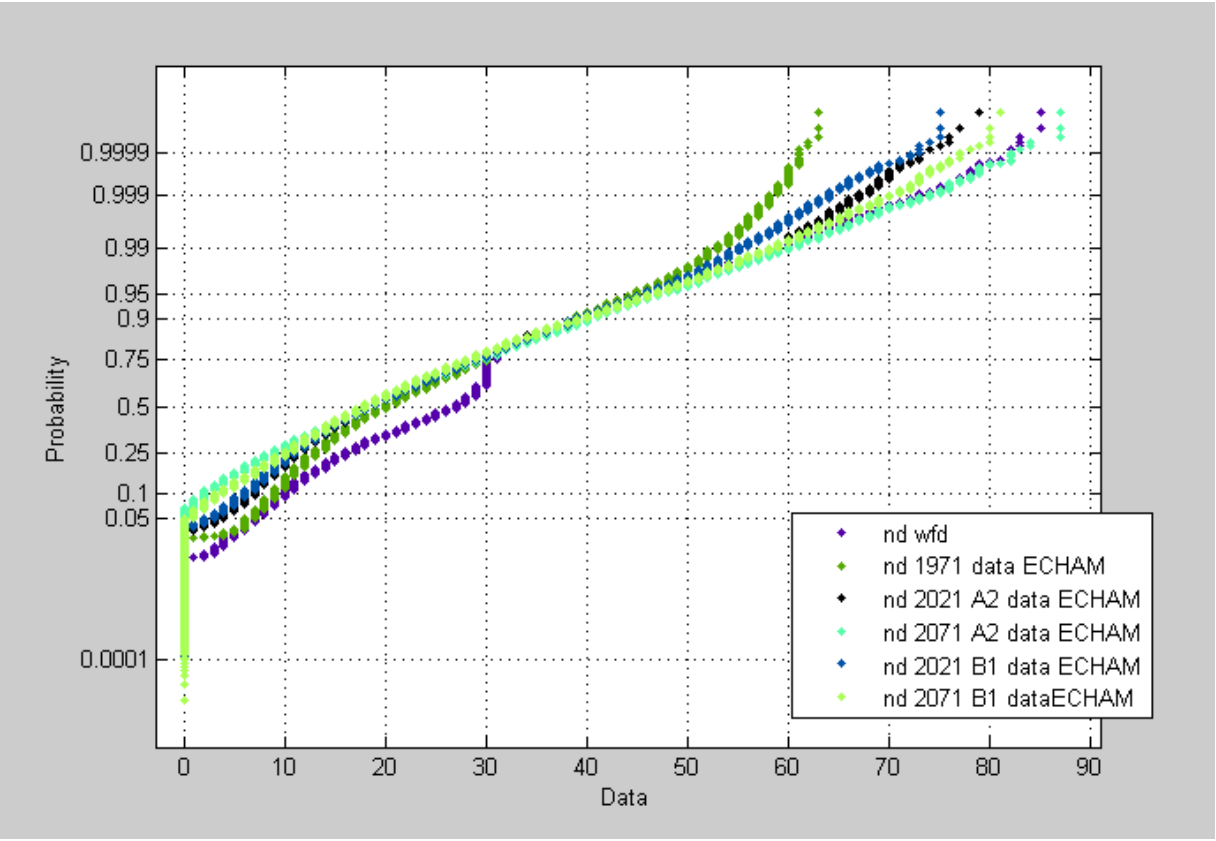

Probability density funtions of drought events for control, mid and late 21st century (not corrected for arid regions) as obtained with WaterGap and ECHAM climate input.

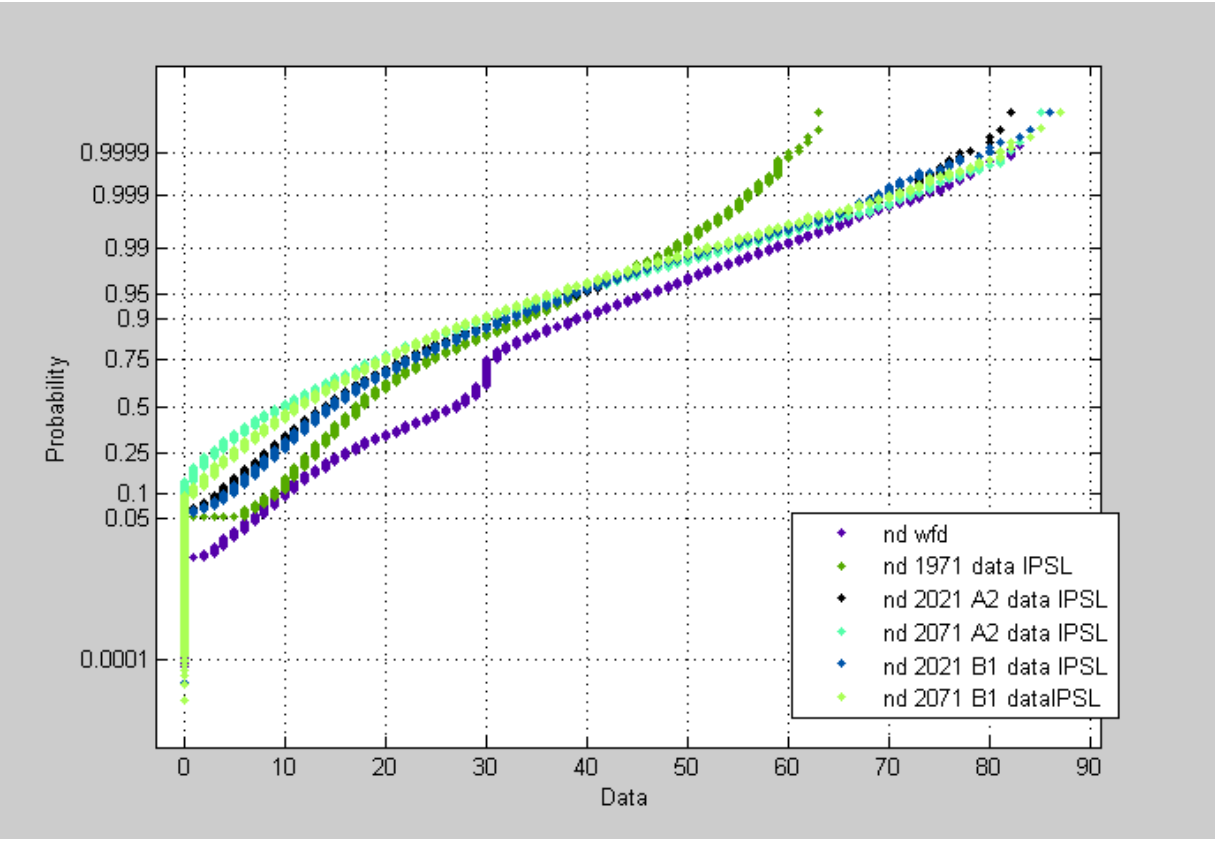

Probability density funtions of drought events for control, mid and late 21st century (not corrected for arid regions) as obtained with WaterGap and IPSL climate input.

1.6.4 Analysis of Watergap with a drought equivalent index

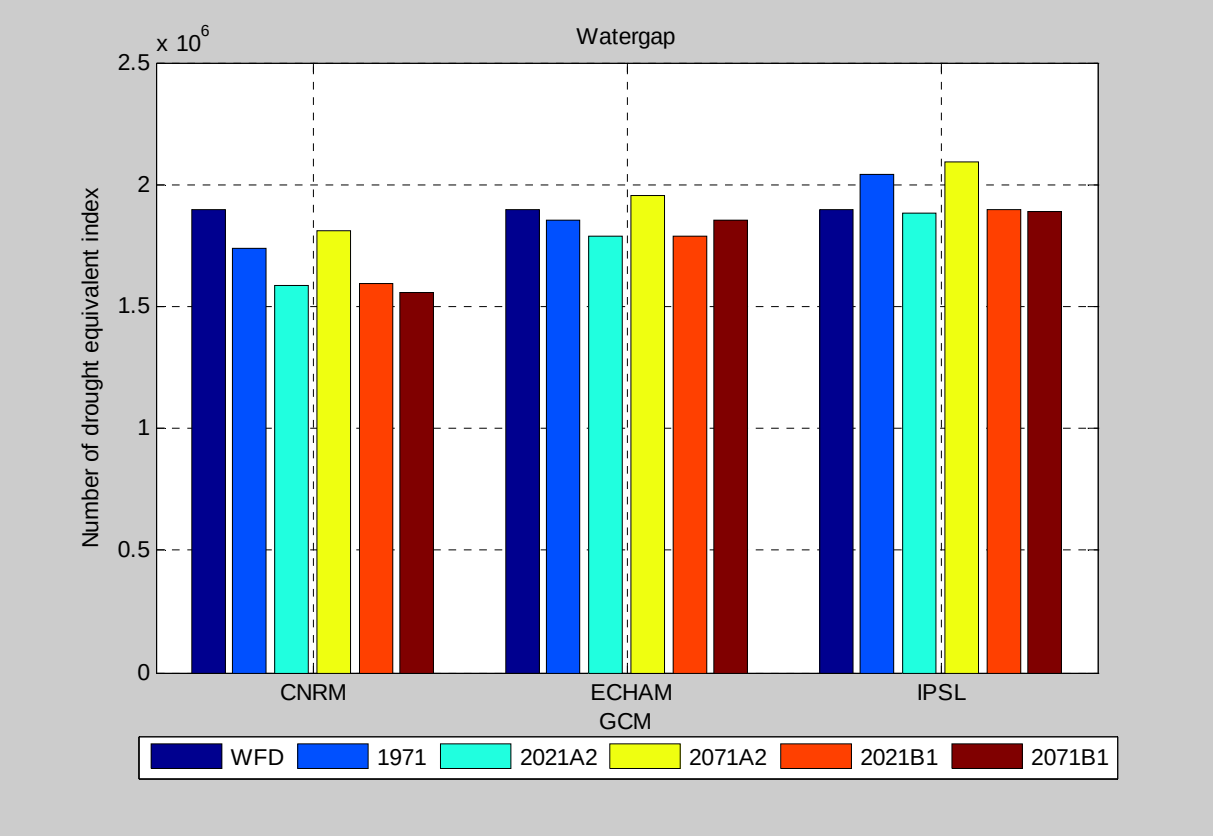

Number of drought events for control, mid and late 21st century (corrected for arid regions).

Annex 2 Analysis based on average drought duration.

ANNEX 2.1 GWAVA

1.1.1 Analysis of average drought duration

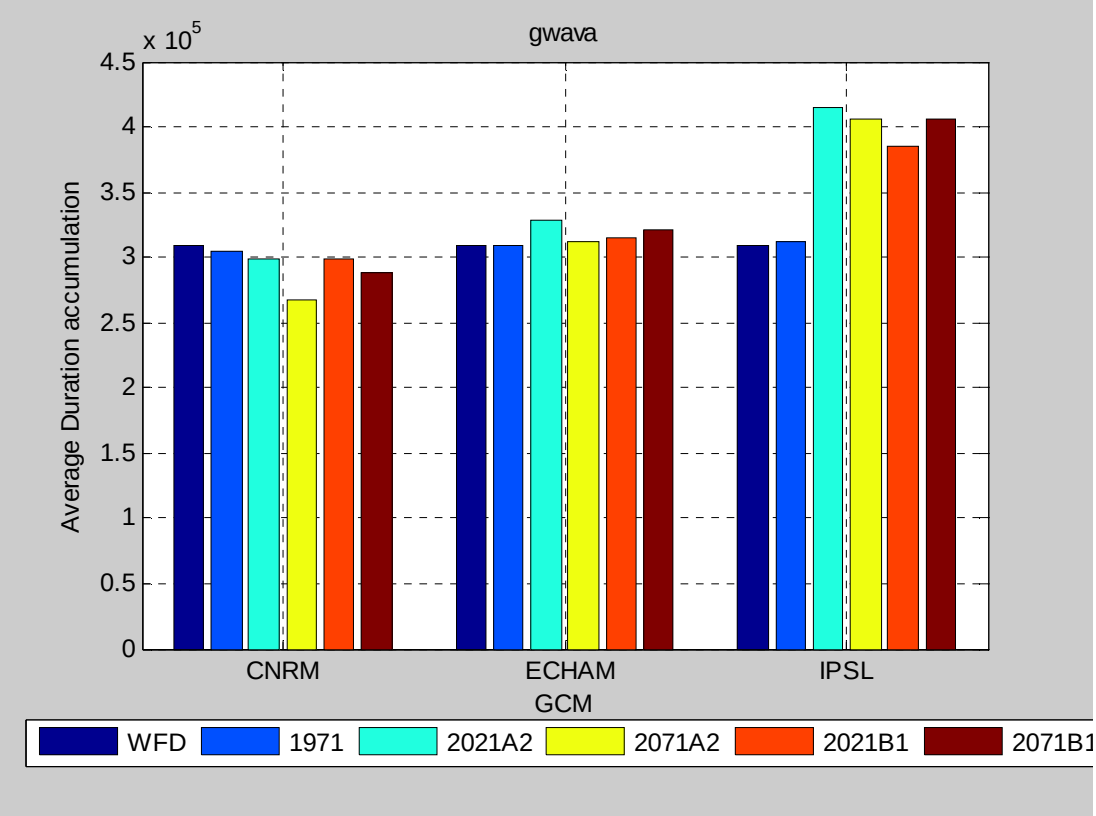

Accumulated average drought durations (for all cells) for control, mid and late 21st century (not corrected for arid regions).

2.1.2 Number of arid regions

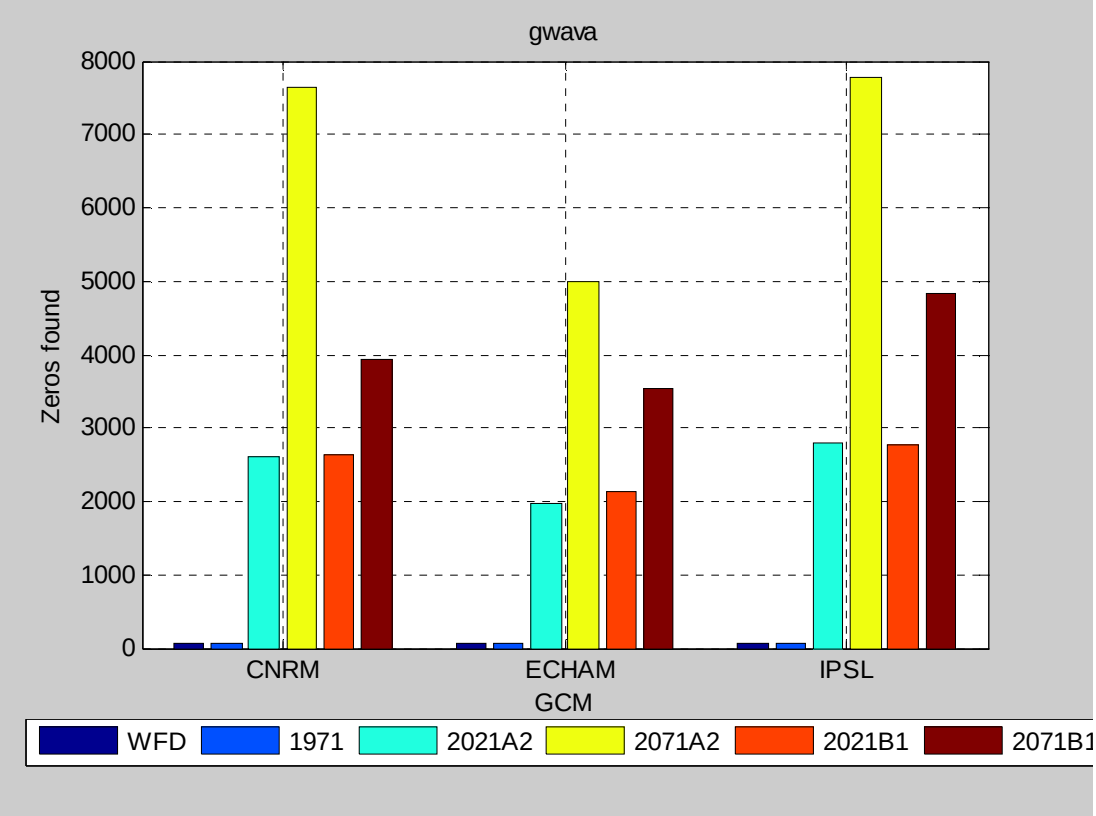

Number of Zeros.

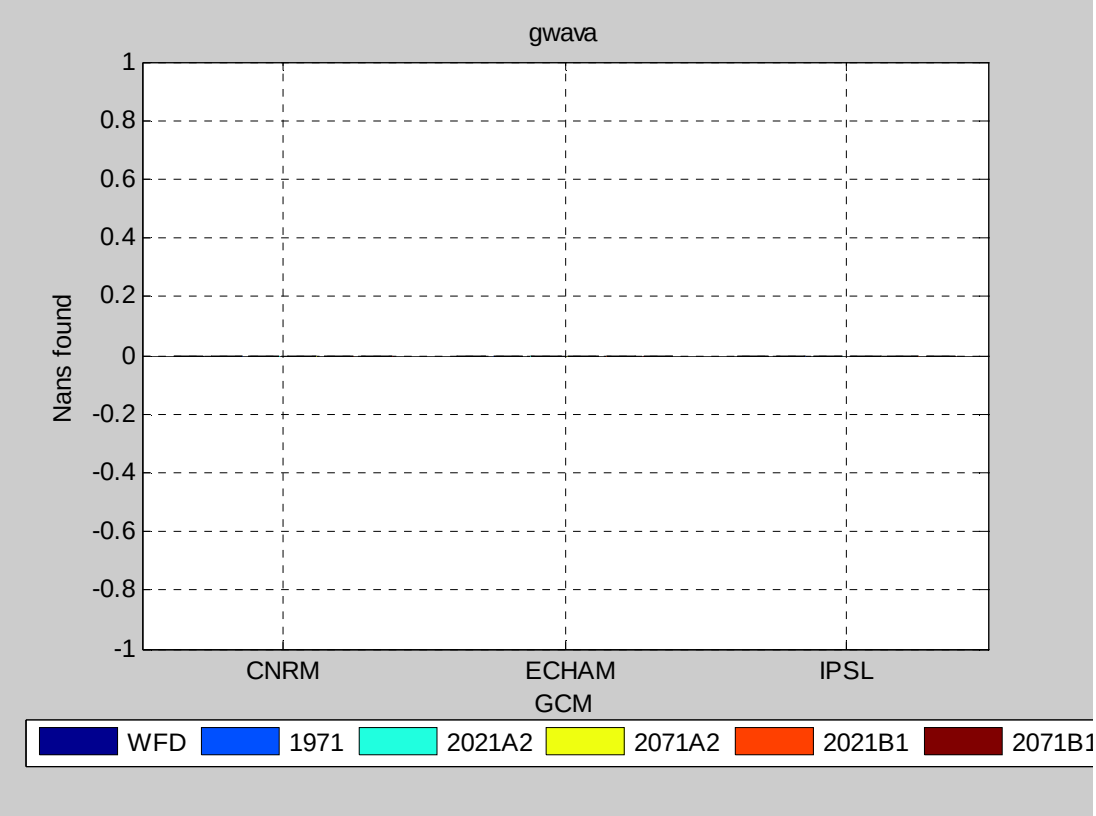

Number of Nans.

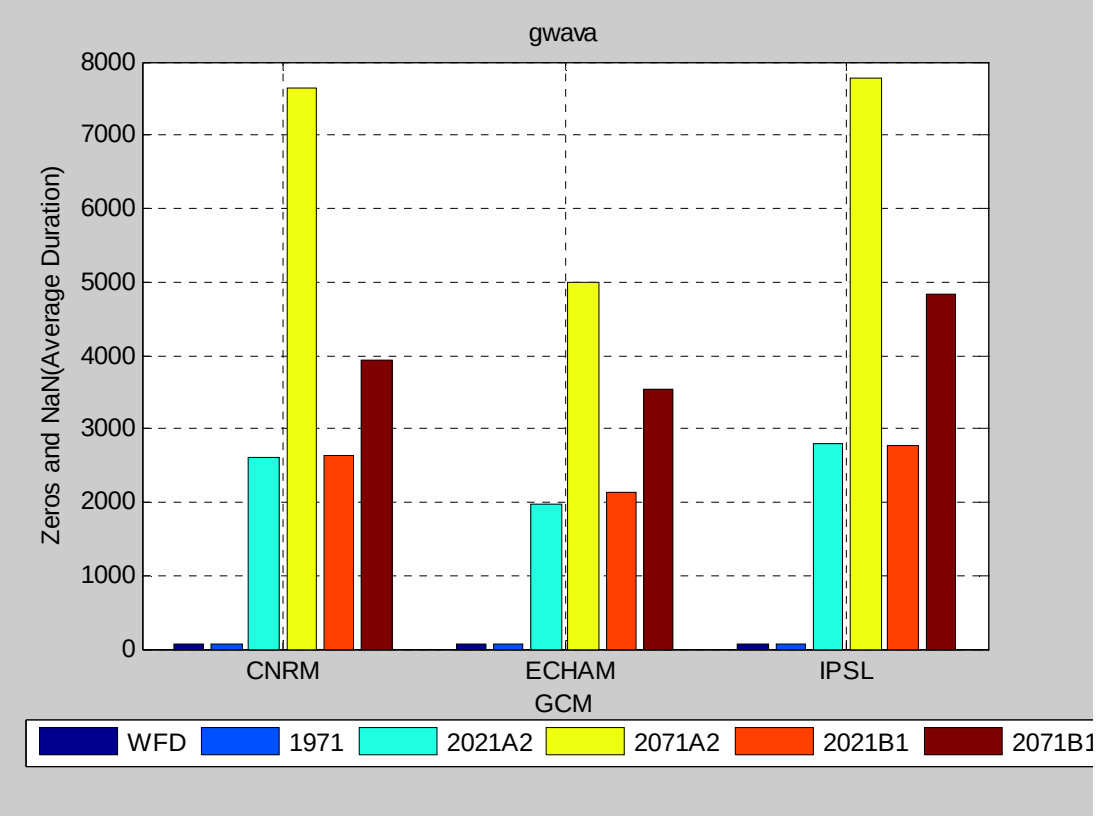

Number of arid regions (zeros + Nans) for control, mid and late 21st century.

2.1.3 PDF of average drought duration

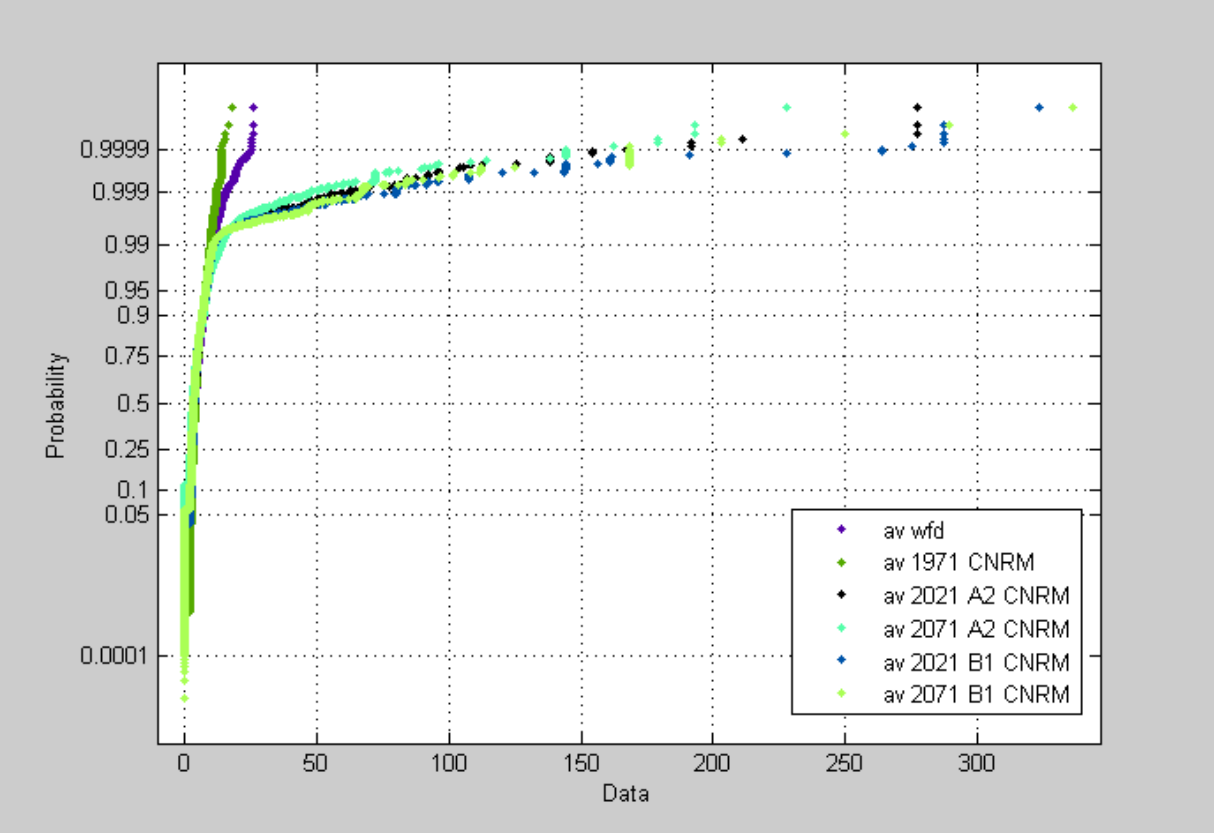

Probability density funtions of avarage drought durationsfor control, mid and late 21st century (not corrected for arid regions) as obtained with GWAVA and CNRMclimate input.

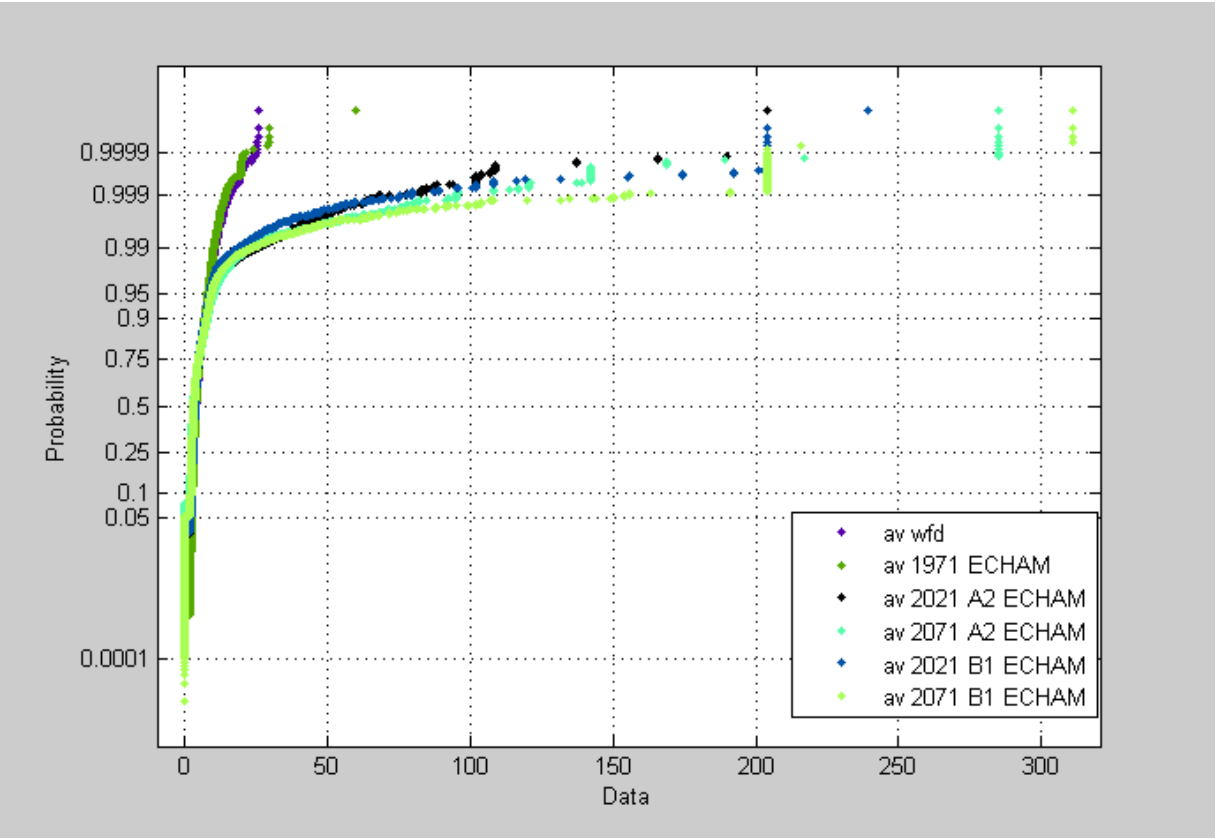

Probability density funtions of avarage drought durationsfor control, mid and late 21st century (not corrected for arid regions) as obtained with GWAVA and ECHAM climate input.

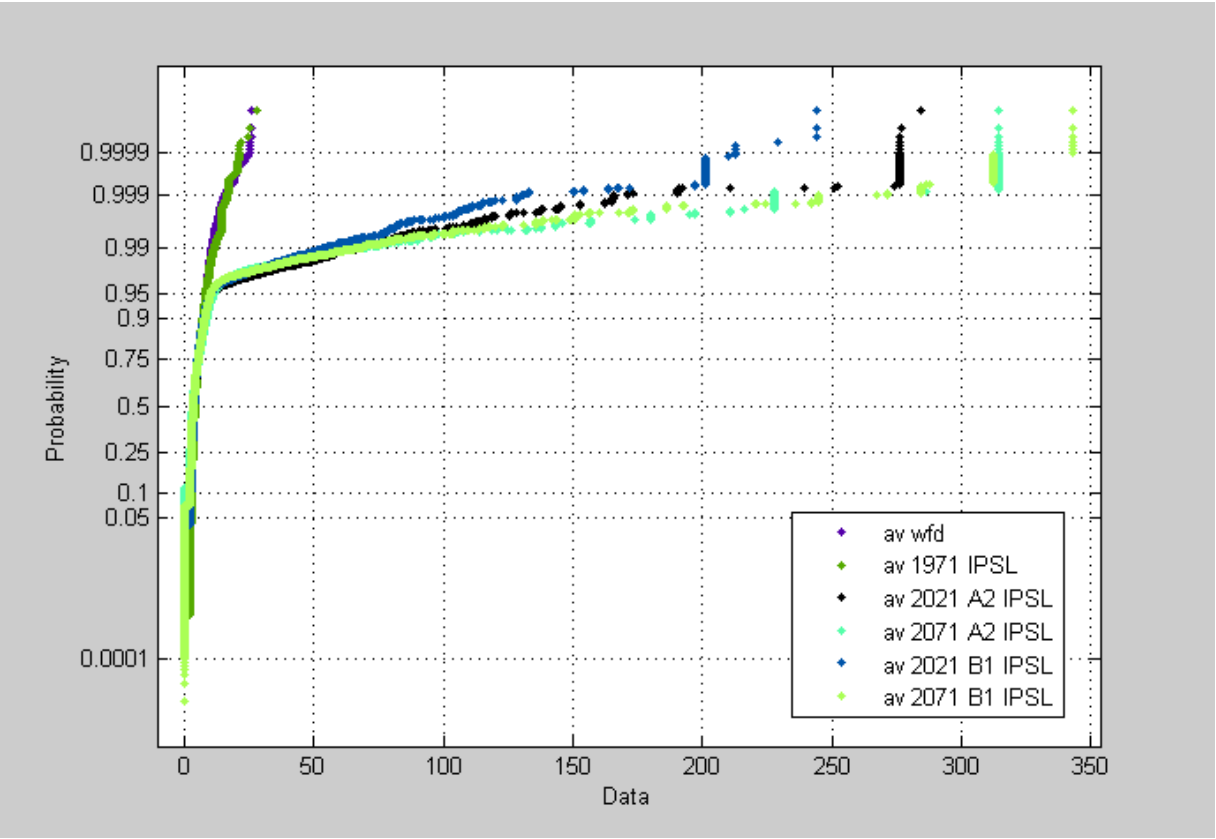

Probability density funtions of avarage drought durationsfor control, mid and late 21st century (not corrected for arid regions) as obtained with GWAVA and IPSL climate input.

2.1.4 Analysis of GWAVA with a drought equivalent index

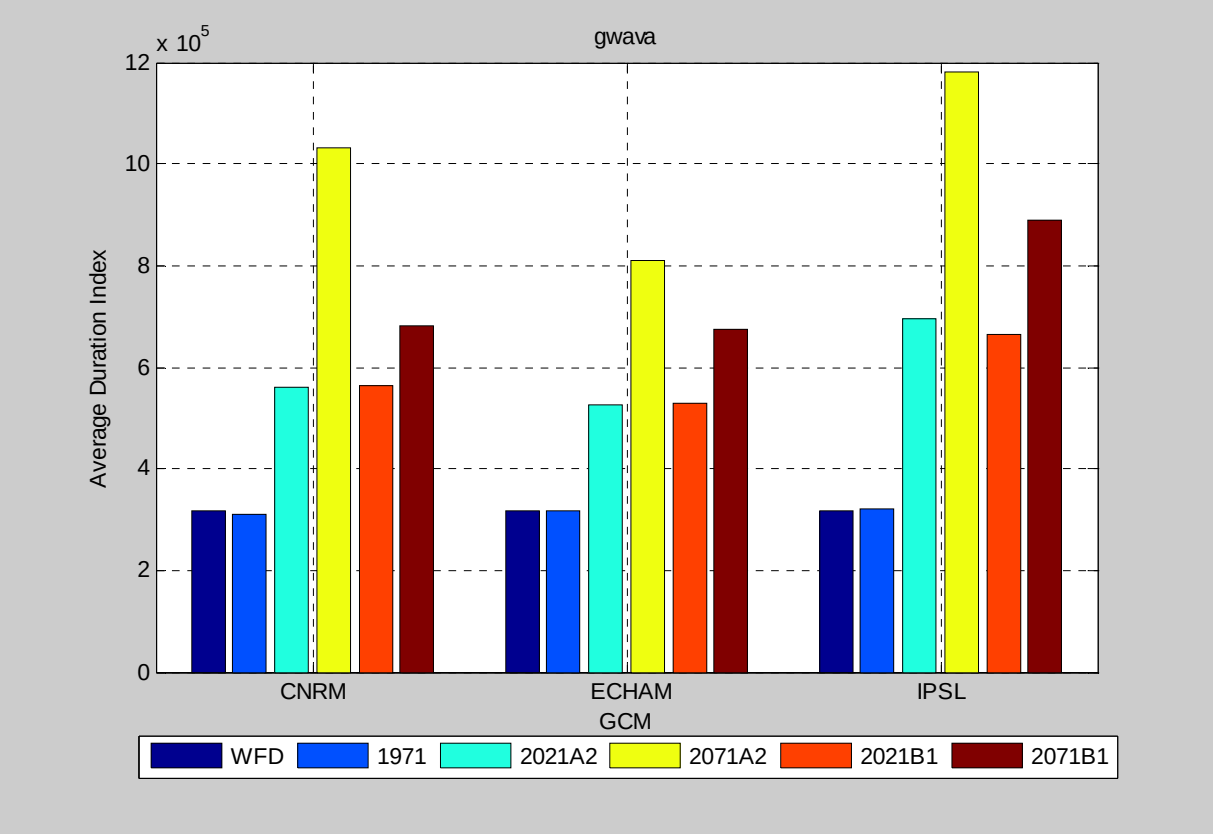

ANNEX 2.2 H08

2.2.1 Analysis of average drought duration

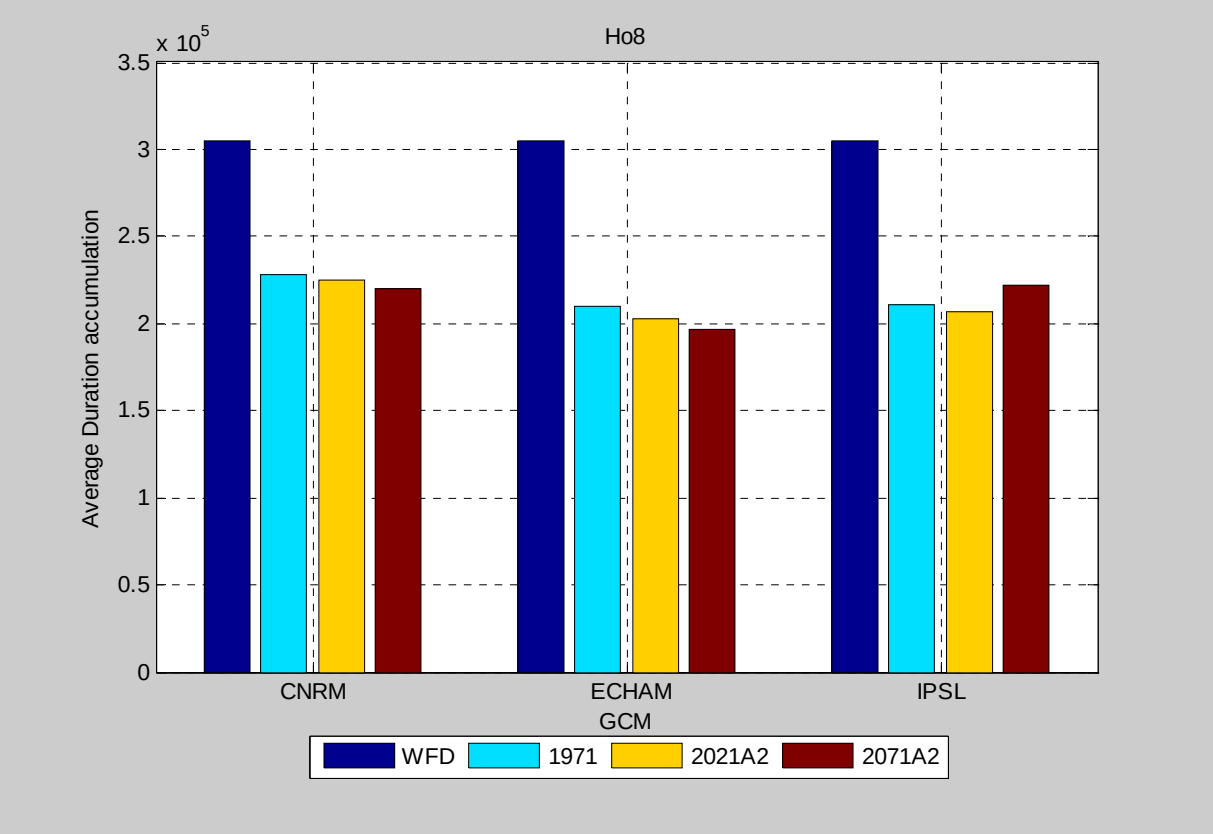

Accumulated average drought durations (for all cells) for control, mid and late 21st century (not corrected for arid regions).

2.2.2 Number of arid regions

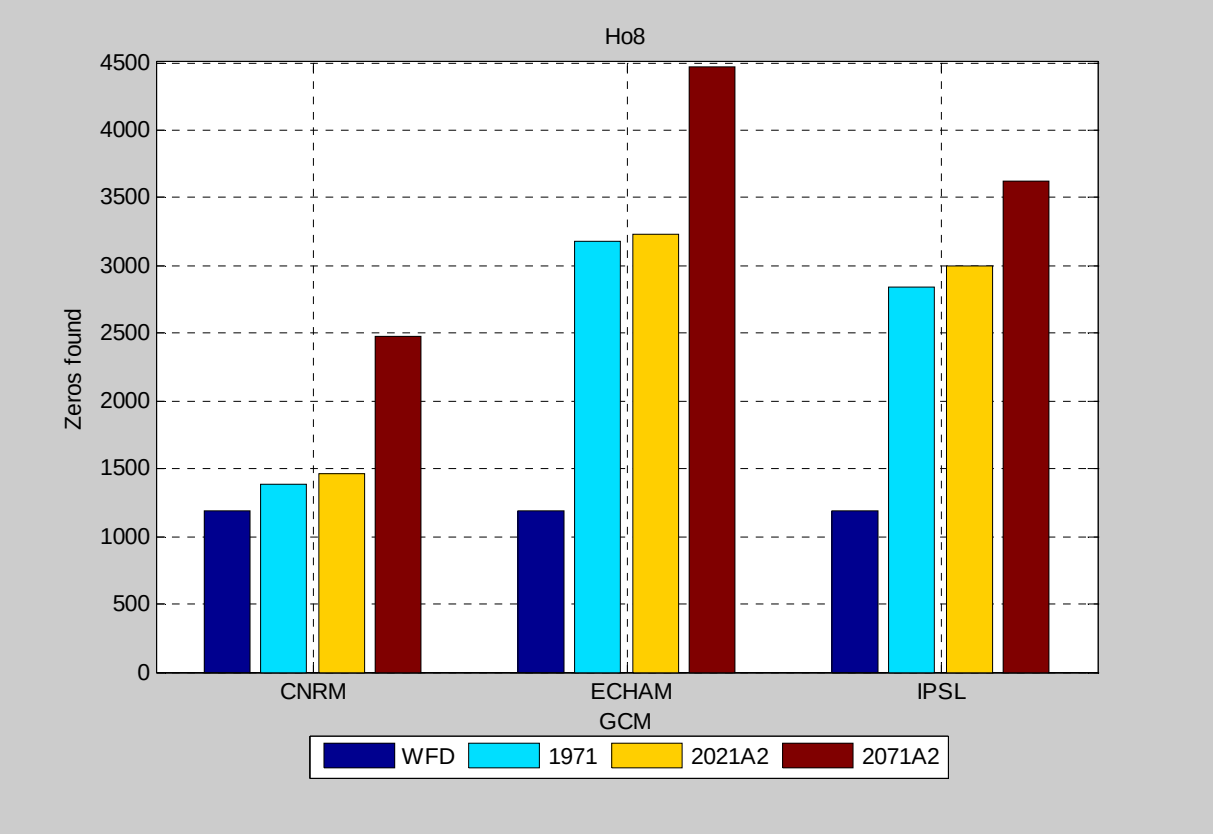

Number of Zeros.

2.2.3 PDF of average drought duration

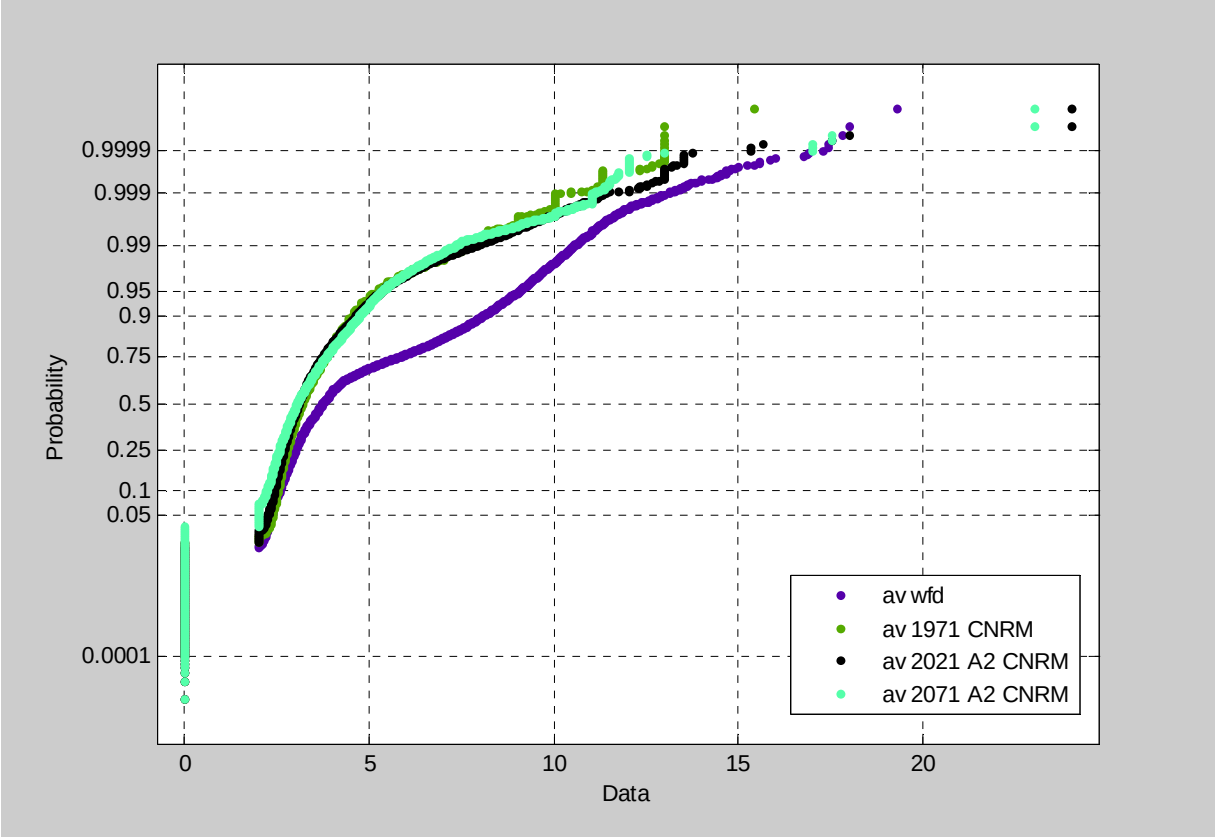

Probability density funtions of avarage drought durationsfor control, mid and late 21st century (not corrected for arid regions) as obtained with H08 and CNRM climate input.

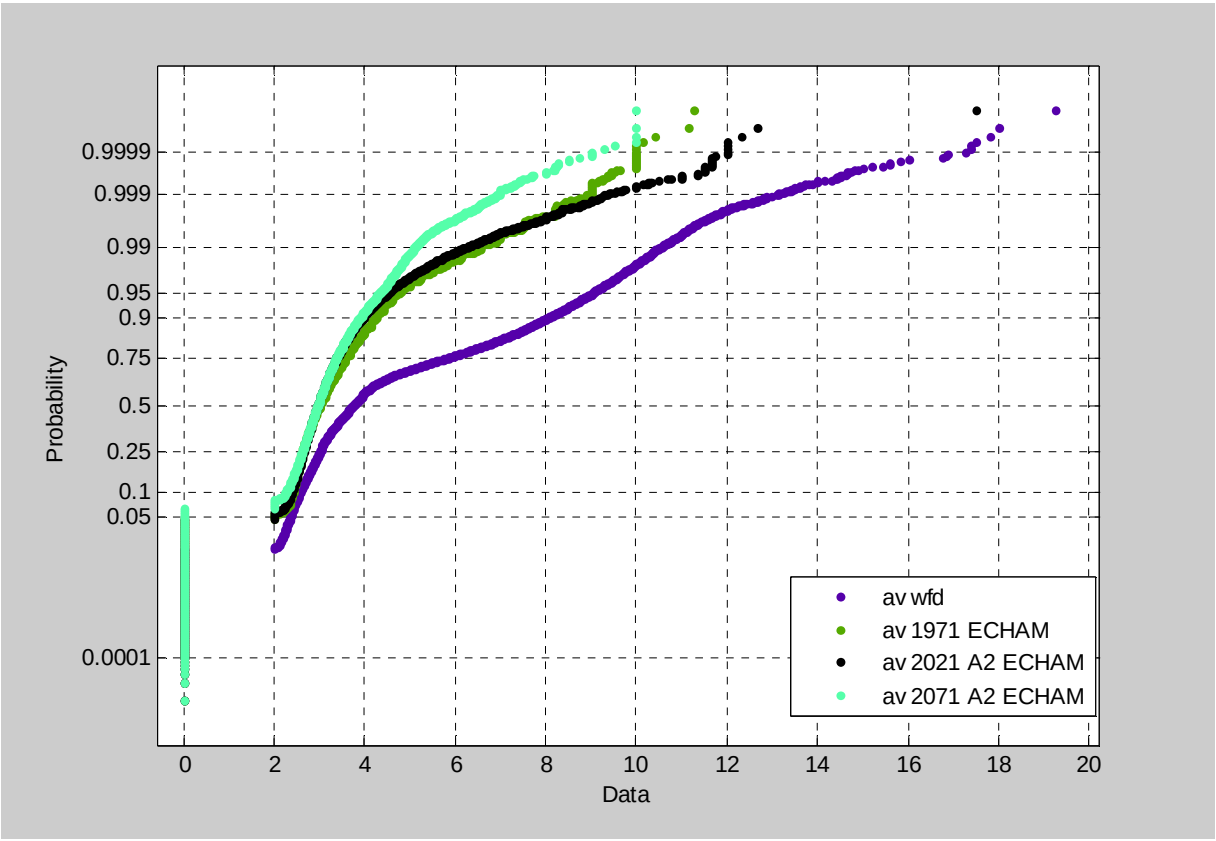

Probability density funtions of avarage drought durationsfor control, mid and late 21st century (not corrected for arid regions) as obtained with H08 and ECHAM climate input.

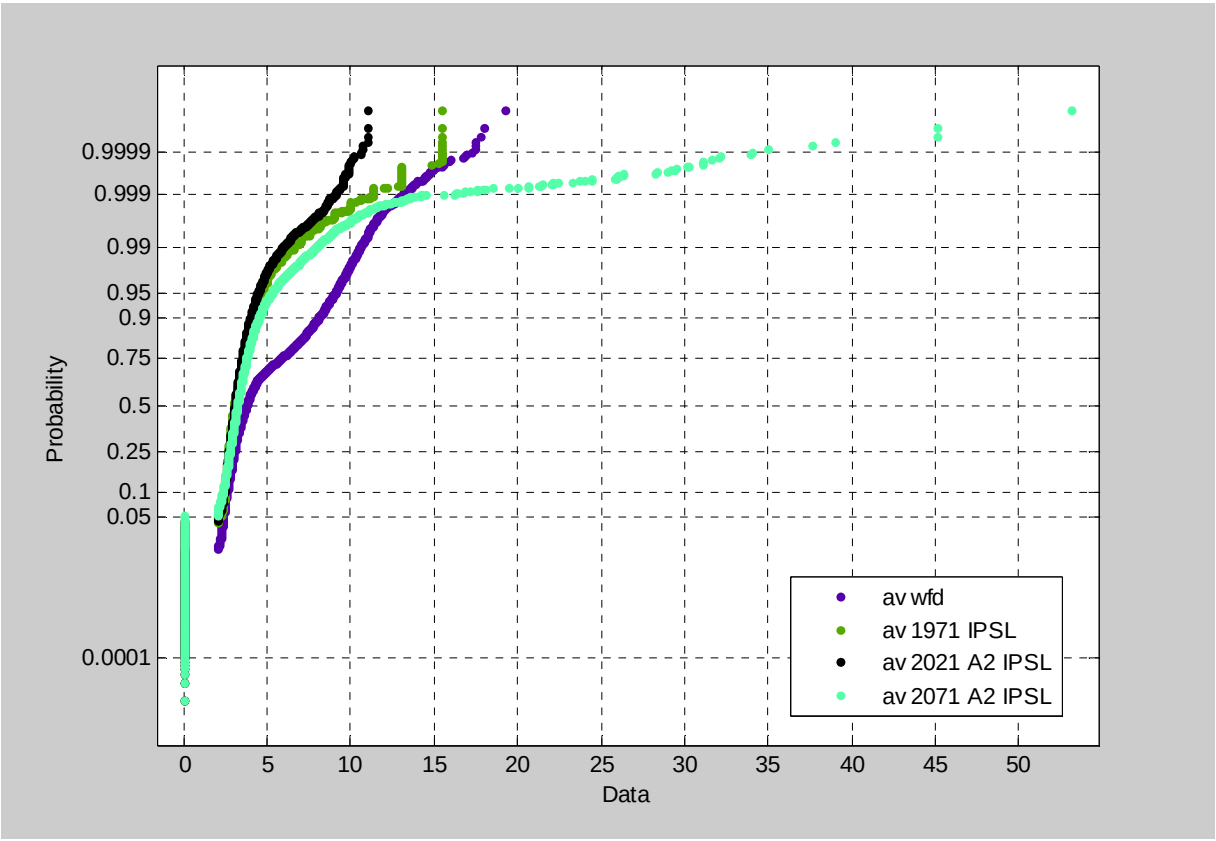

Probability density funtions of avarage drought durationsfor control, mid and late 21st century (not corrected for arid regions) as obtained with H08 and IPSL climate input.

2.2.4 Analysis of H08 with a drought equivalent index

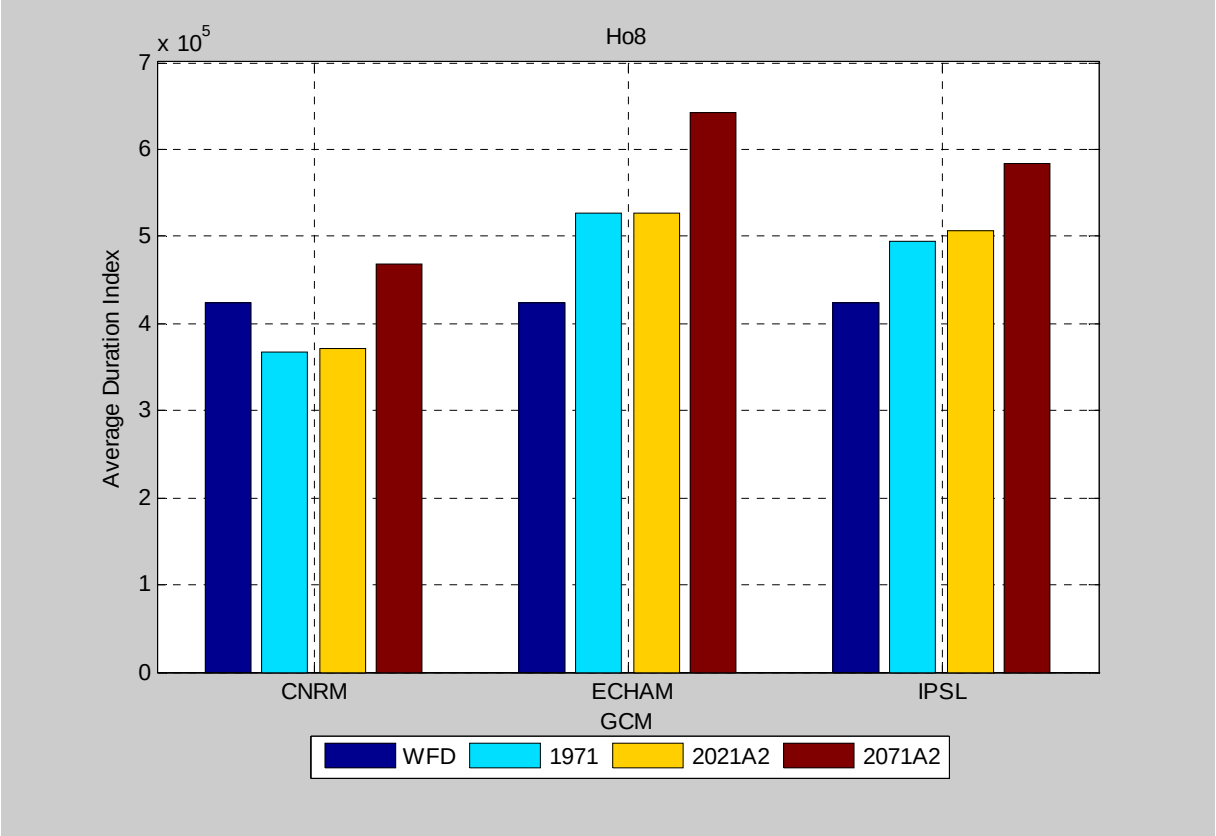

ANNEX 2.3 LPJML

2.3.1 Analysis of average drought duration

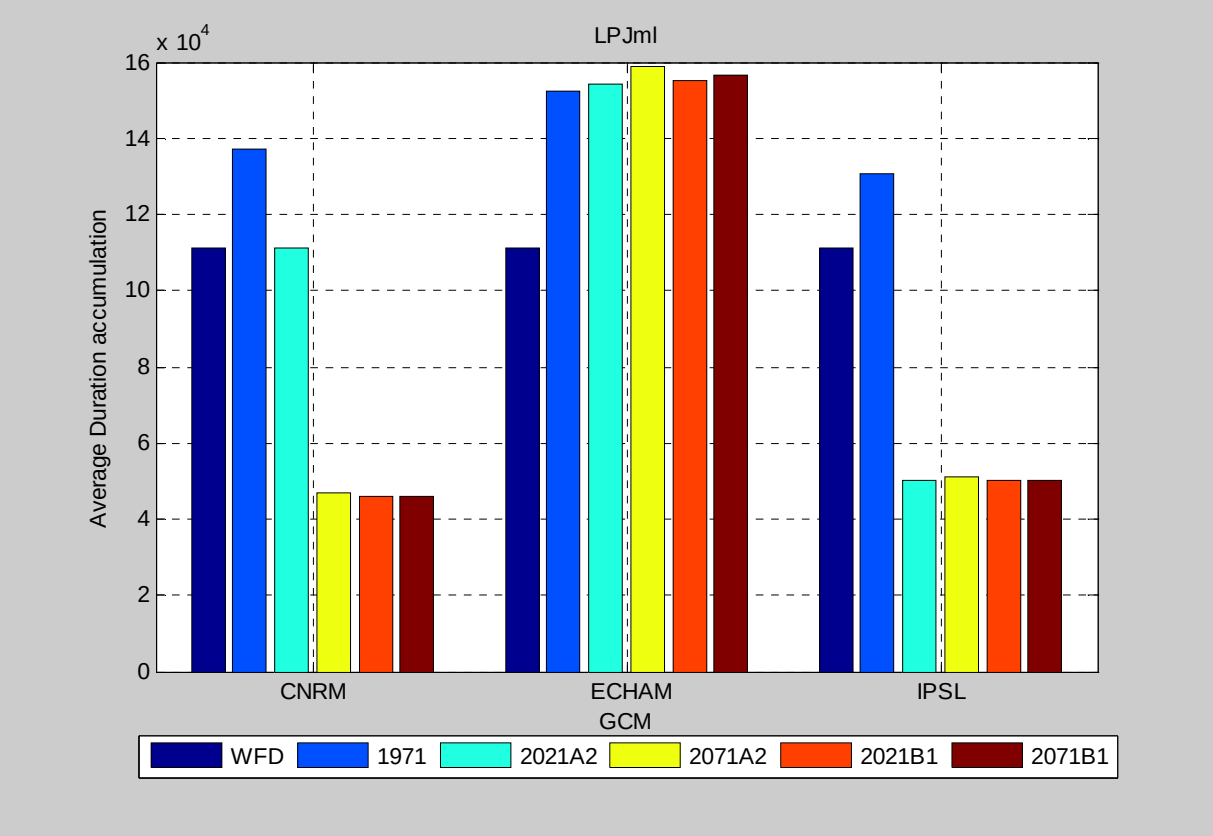

Accumulated average drought durations (for all cells) for control, mid and late 21st century (not corrected for arid regions).

2.3.2 Number of arid regions

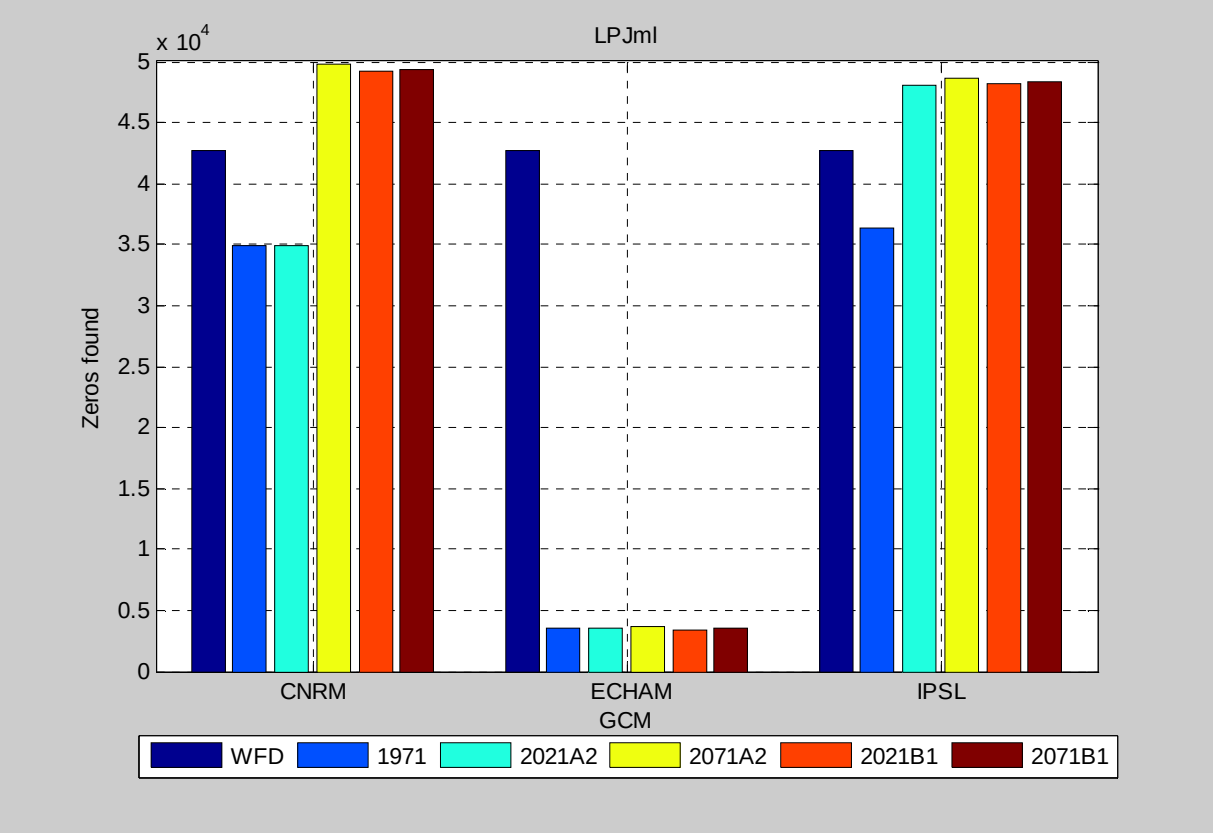

Number of Zeros.

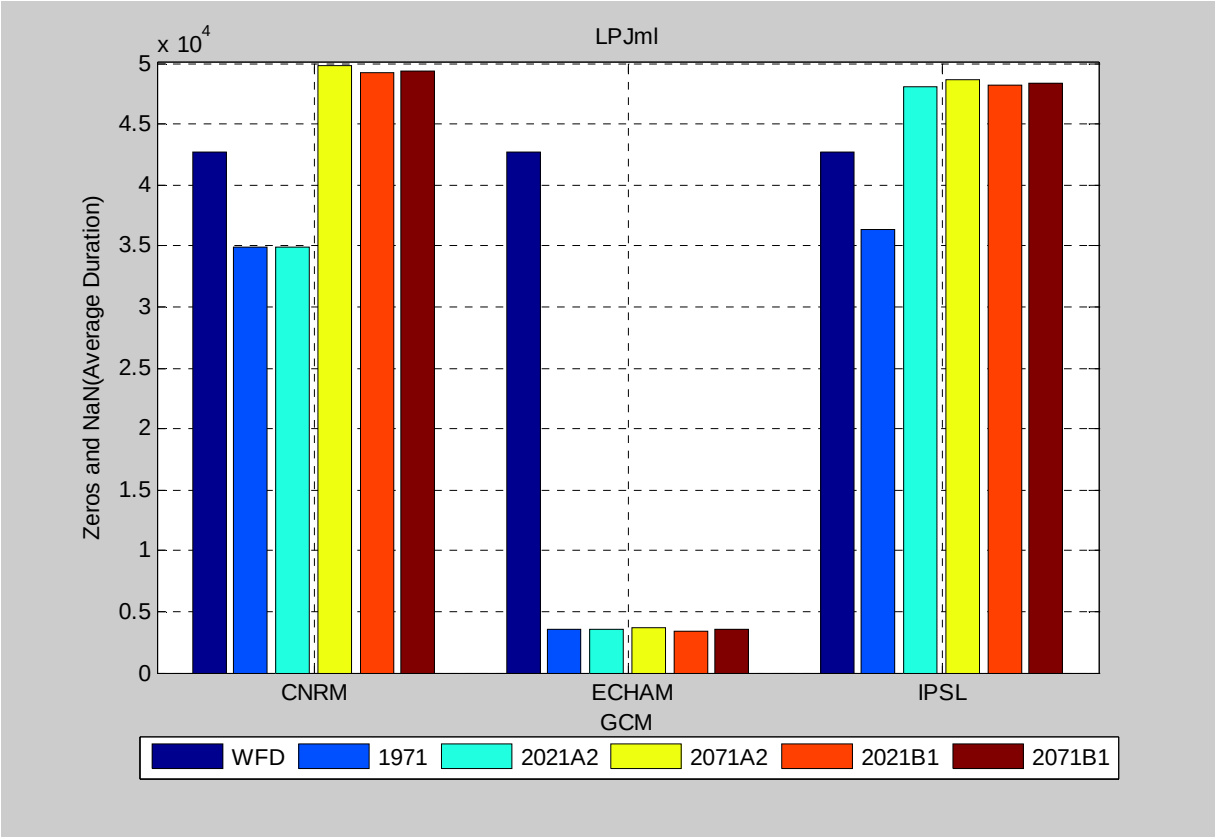

Number of arid regions (zeros + Nans) for control, mid and late 21st century.

2.3.3 PDF of average drought duration

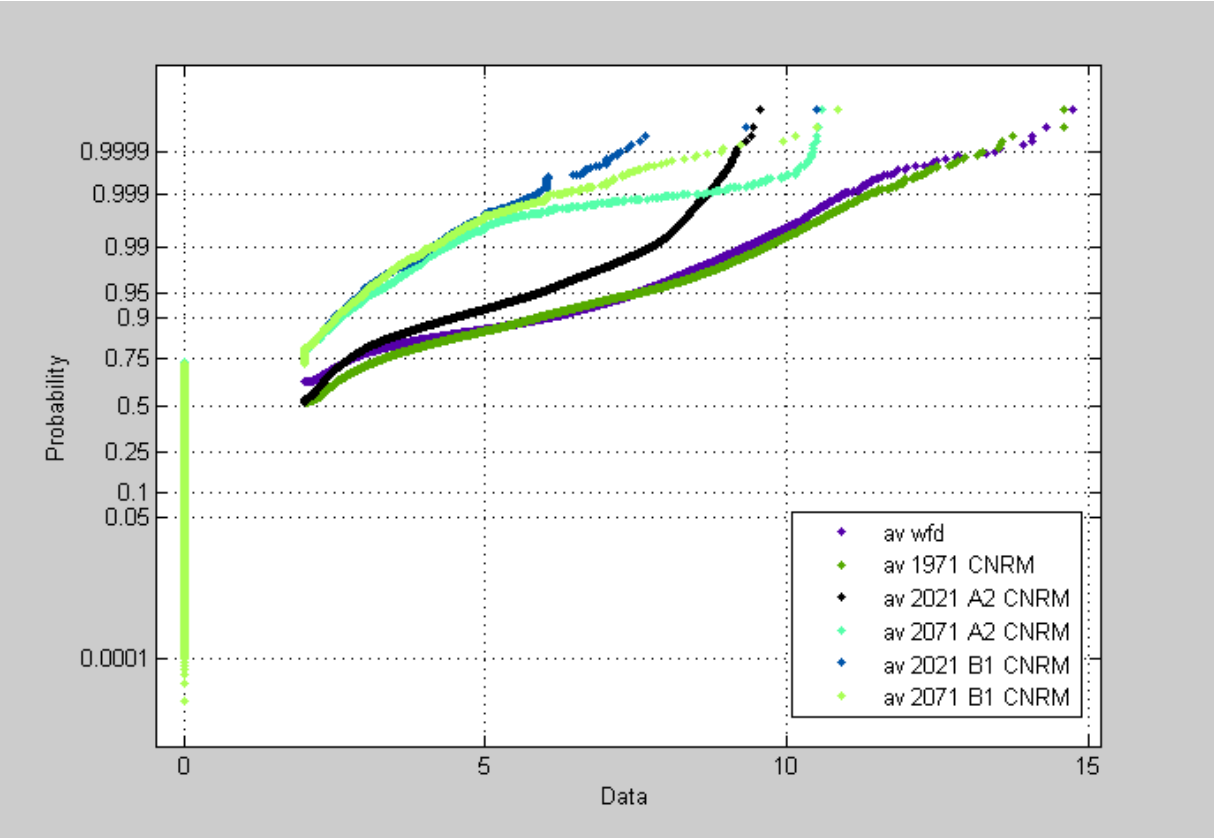

Probability density funtions of avarage drought durationsfor control, mid and late 21st century (not corrected for arid regions) as obtained with LPJlm and CNRM climate input.

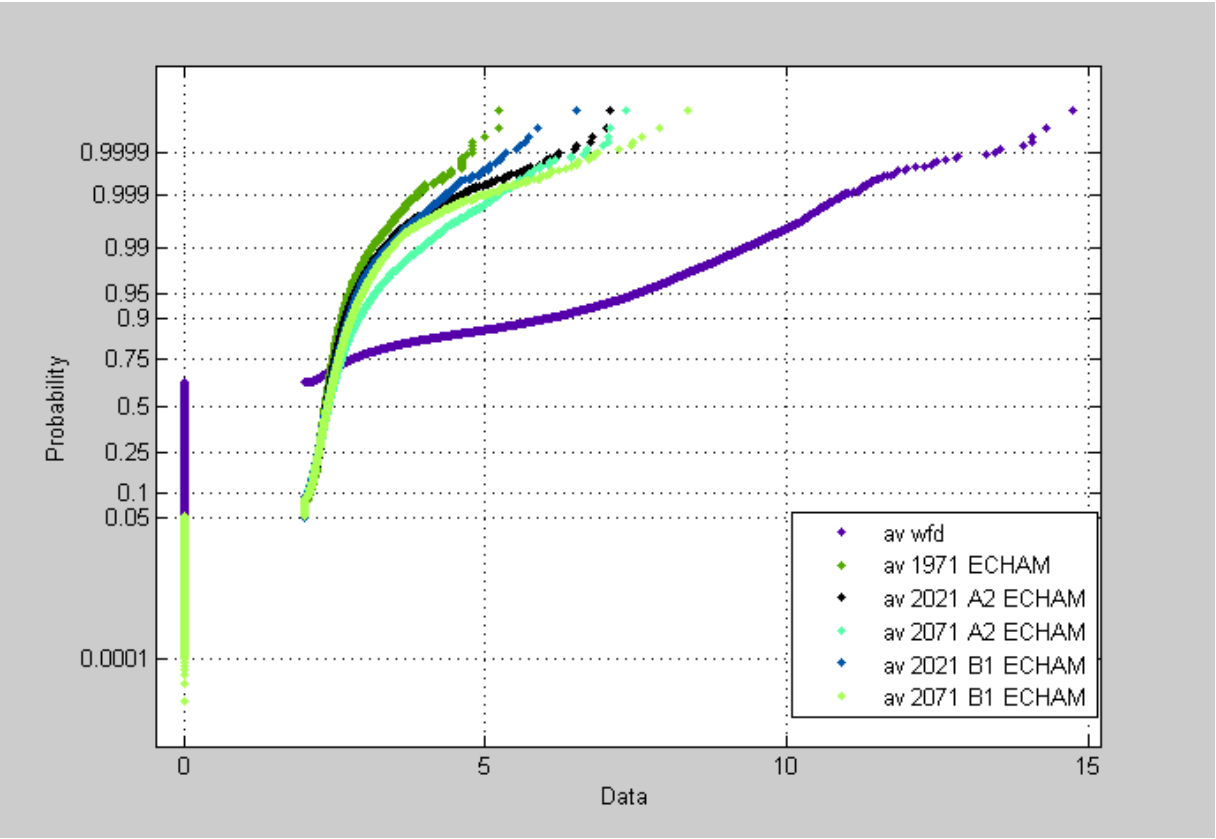

Probability density funtions of avarage drought durationsfor control, mid and late 21st century (not corrected for arid regions) as obtained with LPJlm and ECHAM climate input.

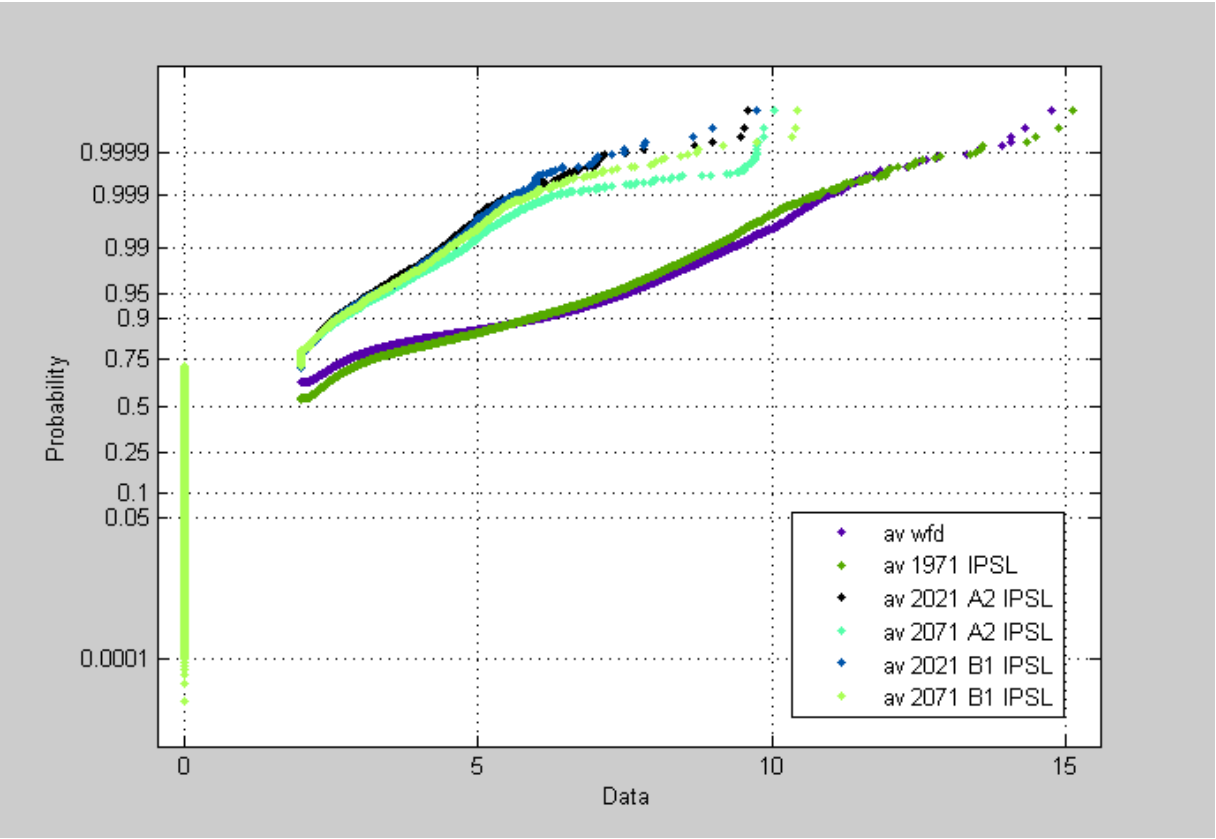

Probability density funtions of avarage drought durationsfor control, mid and late 21st century (not corrected for arid regions) as obtained with LPJlm and IPSL climate input.

2.3.4 Analysis of LPJml with a drought equivalent index

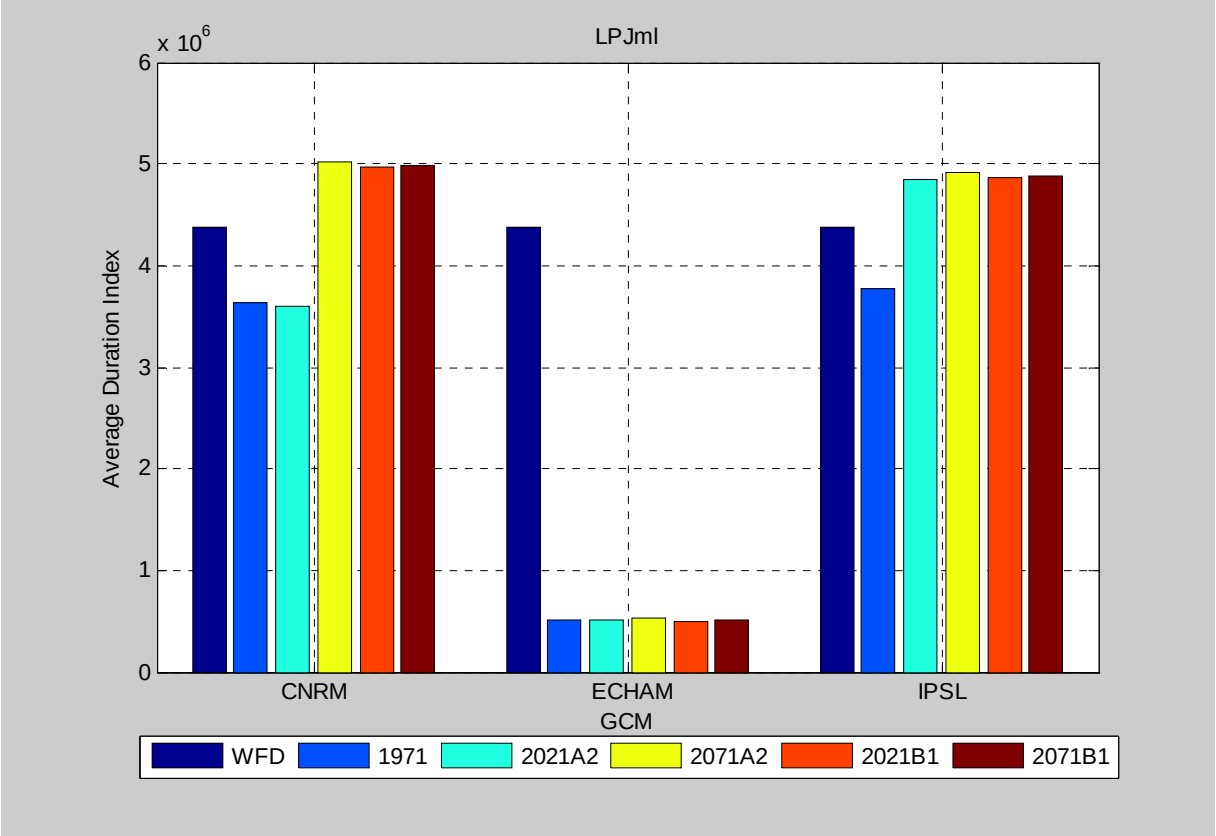

ANNEX 2.4 MacPDM

2.4.1 Analysis of average drought duration

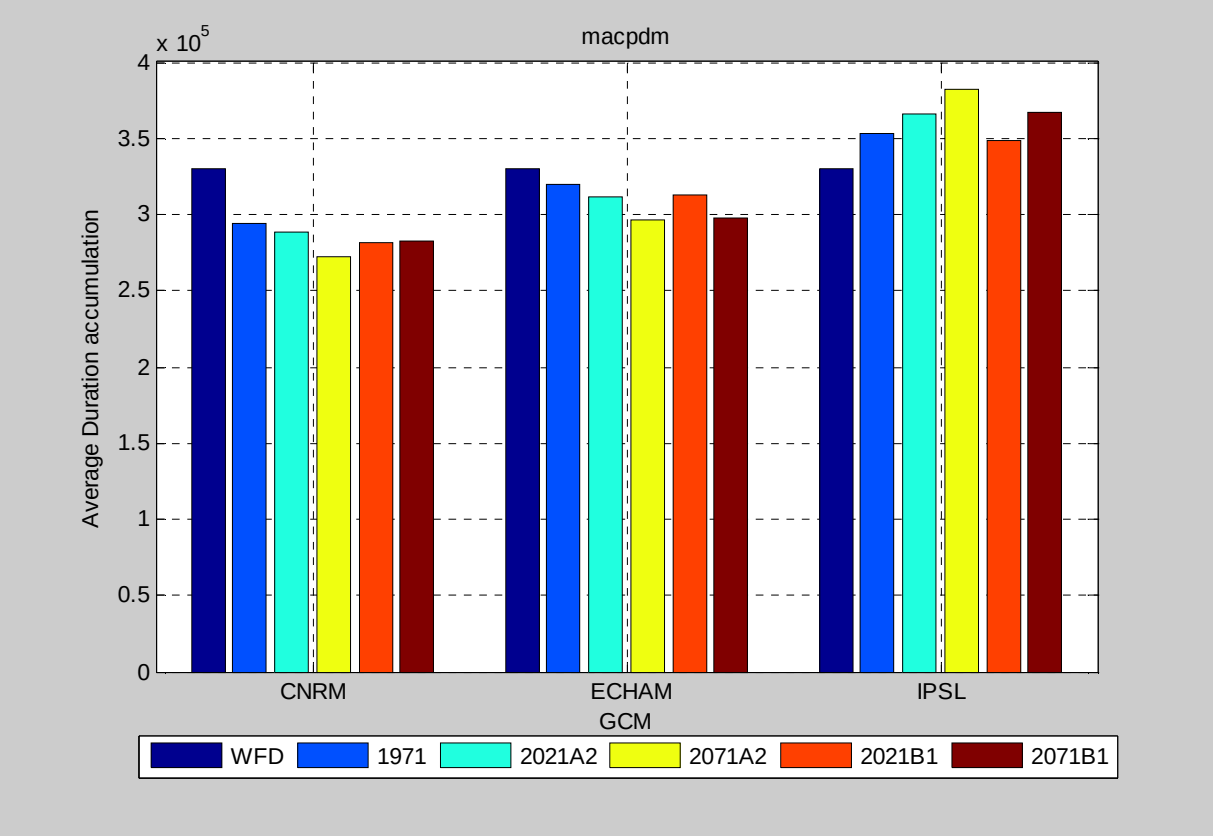

Accumulated average drought durations (for all cells) for control, mid and late 21st century (not corrected for arid regions).

2.4.2 Number of arid regions

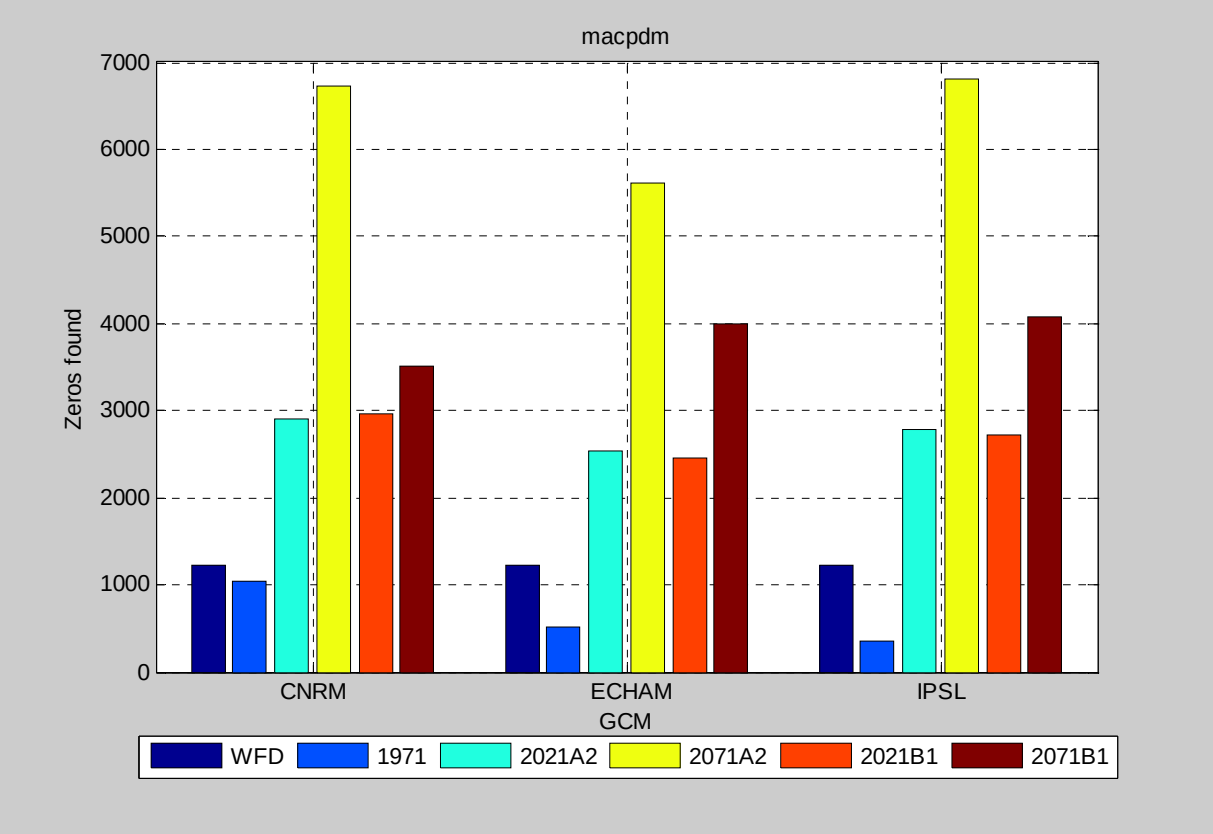

Number of Zeros.

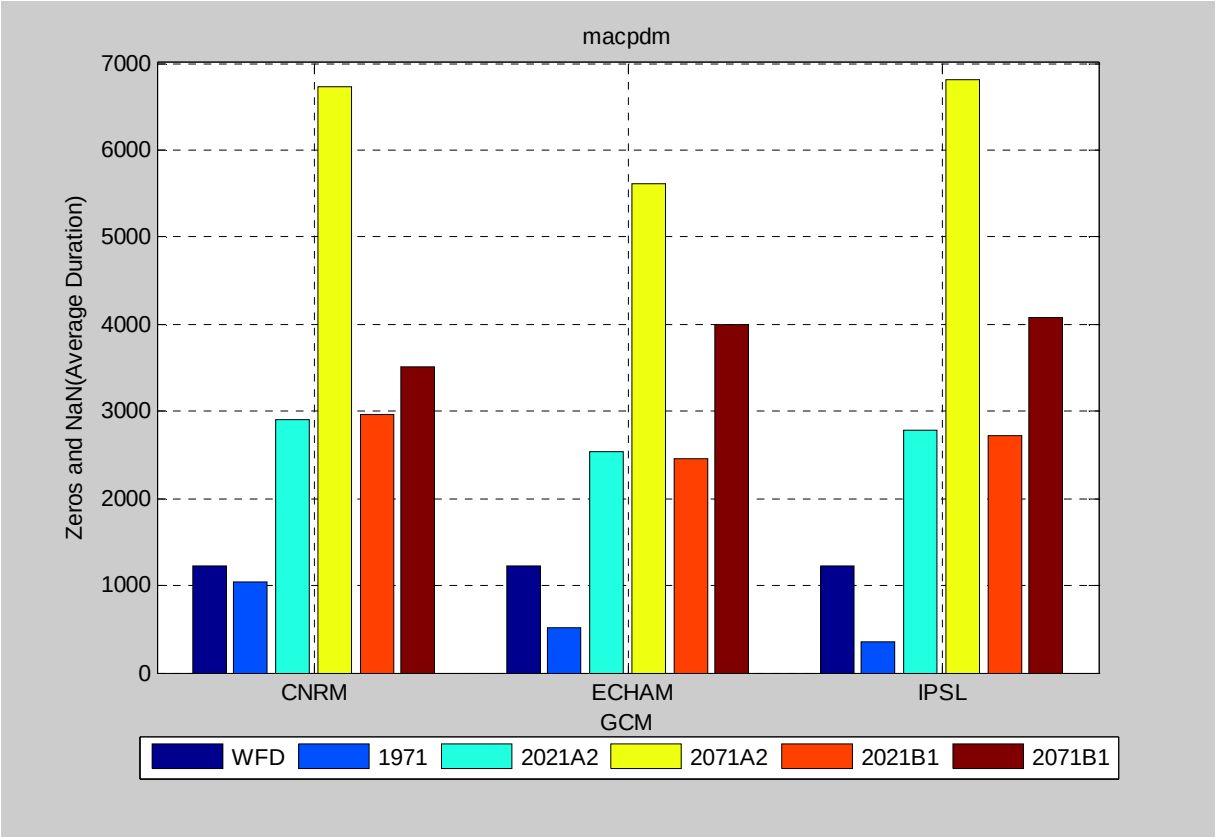

Number of arid regions (zeros + Nans) for control, mid and late 21st century.

2.4.3 PDF of average drought duration

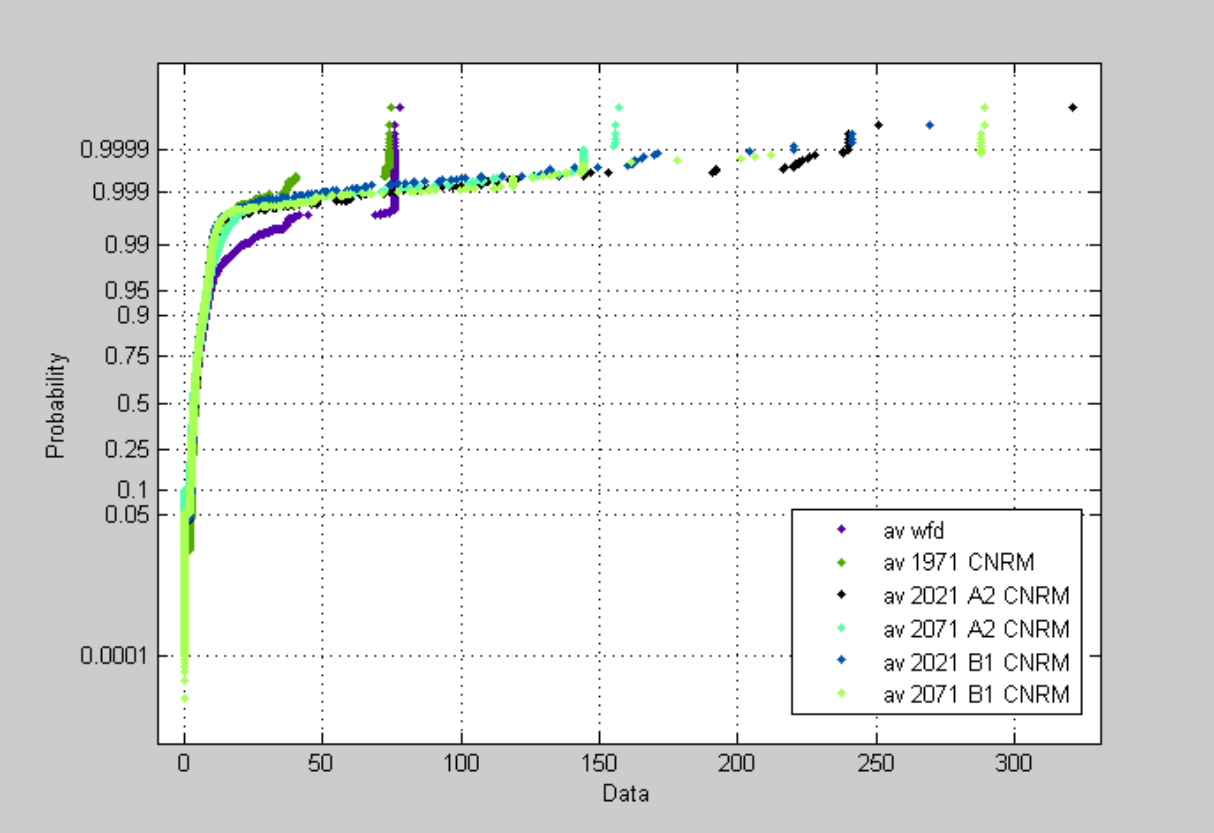

Probability density funtions of avarage drought durationsfor control, mid and late 21st century (not corrected for arid regions) as obtained with MACPDM and CNRM climate input.

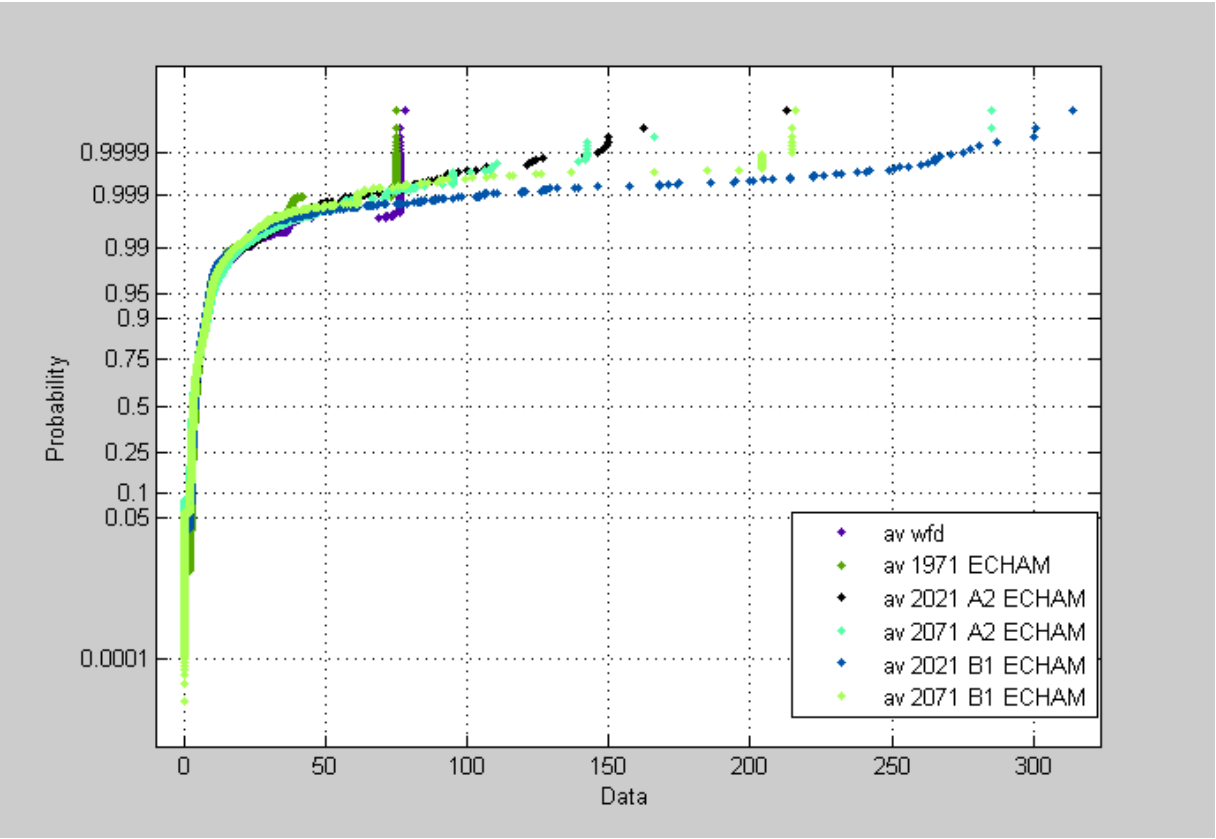

Probability density funtions of avarage drought durationsfor control, mid and late 21st century (not corrected for arid regions) as obtained with MACPDM and ECHAM climate input.

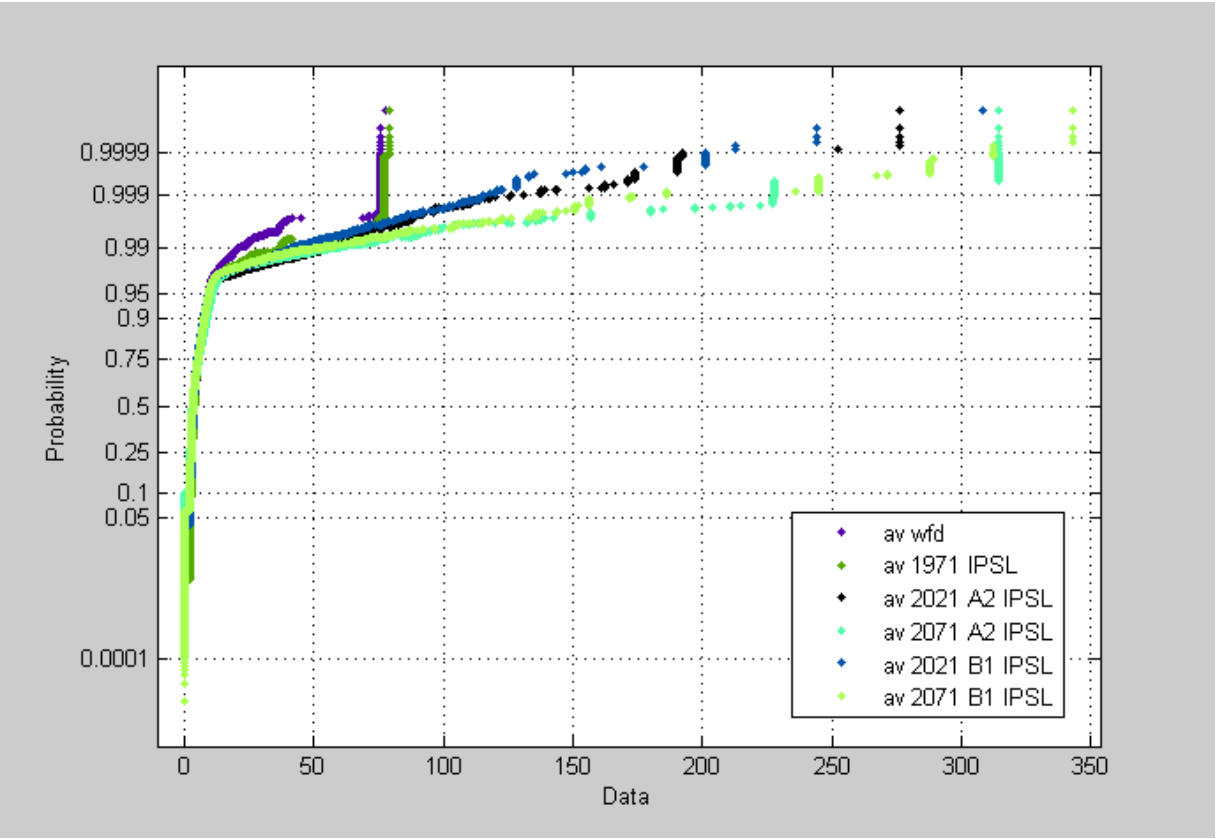

Probability density funtions of avarage drought durationsfor control, mid and late 21st century (not corrected for arid regions) as obtained with MACPDM and IPSL climate input.

2.4.4 Analysis of MacPDM with a drought equivalent index

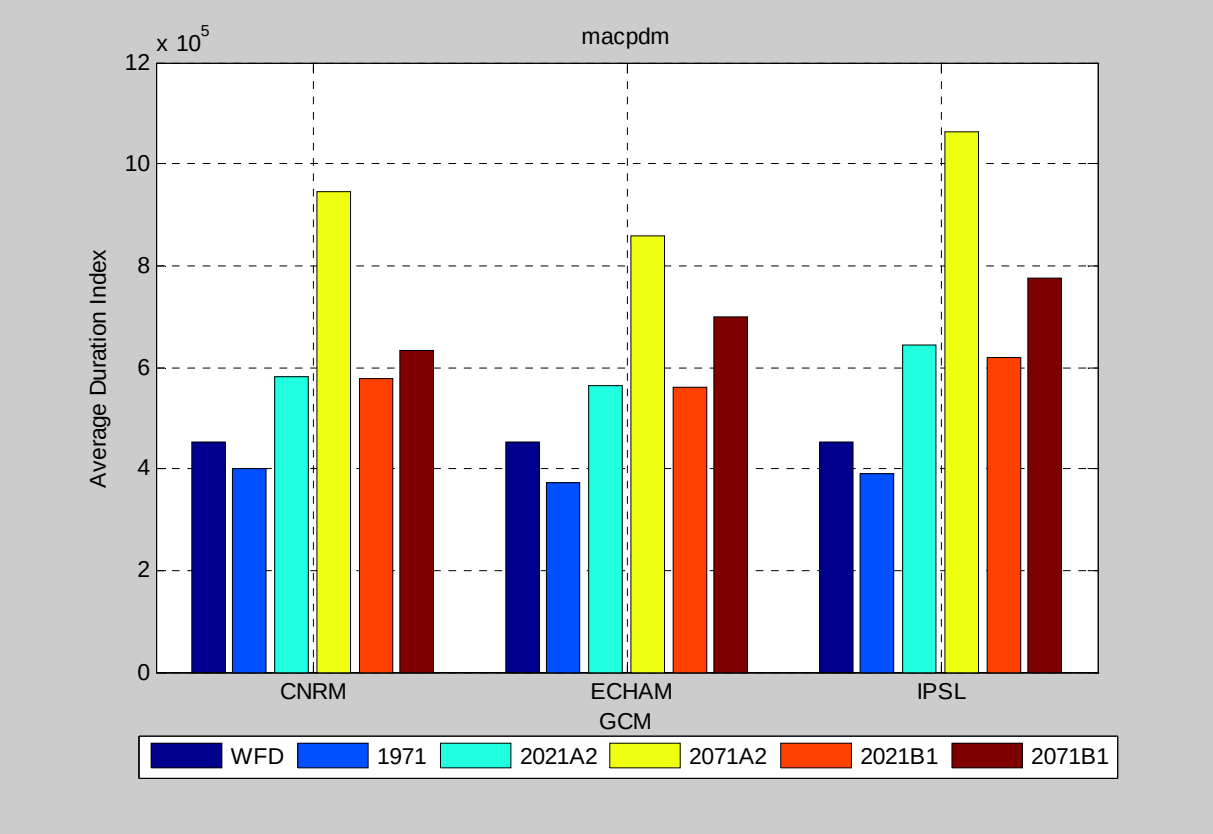

ANNEX 2.5 MPI-HM

2.5.1 Analysis of average drought duration

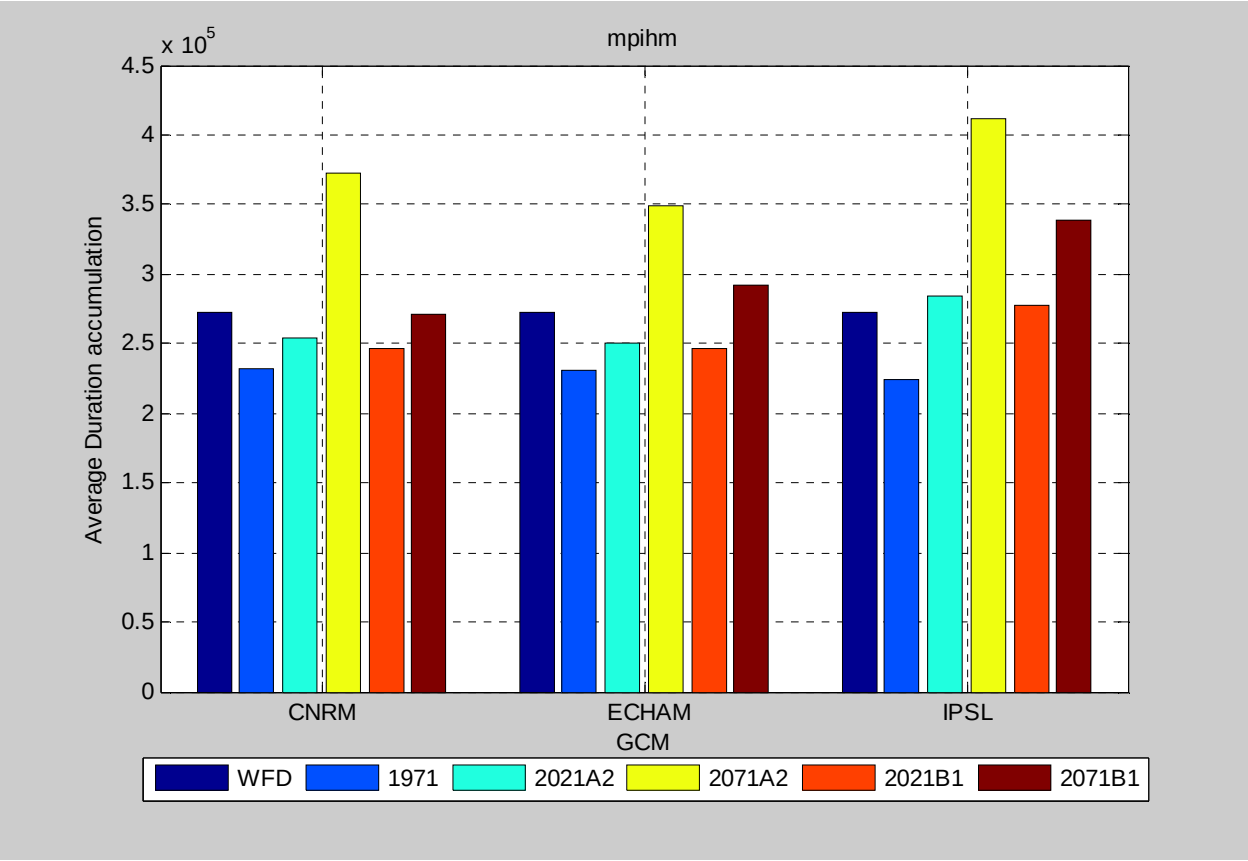

Accumulated average drought durations (for all cells) for control, mid and late 21st century (not corrected for arid regions).

2.5.2 Number of arid regions

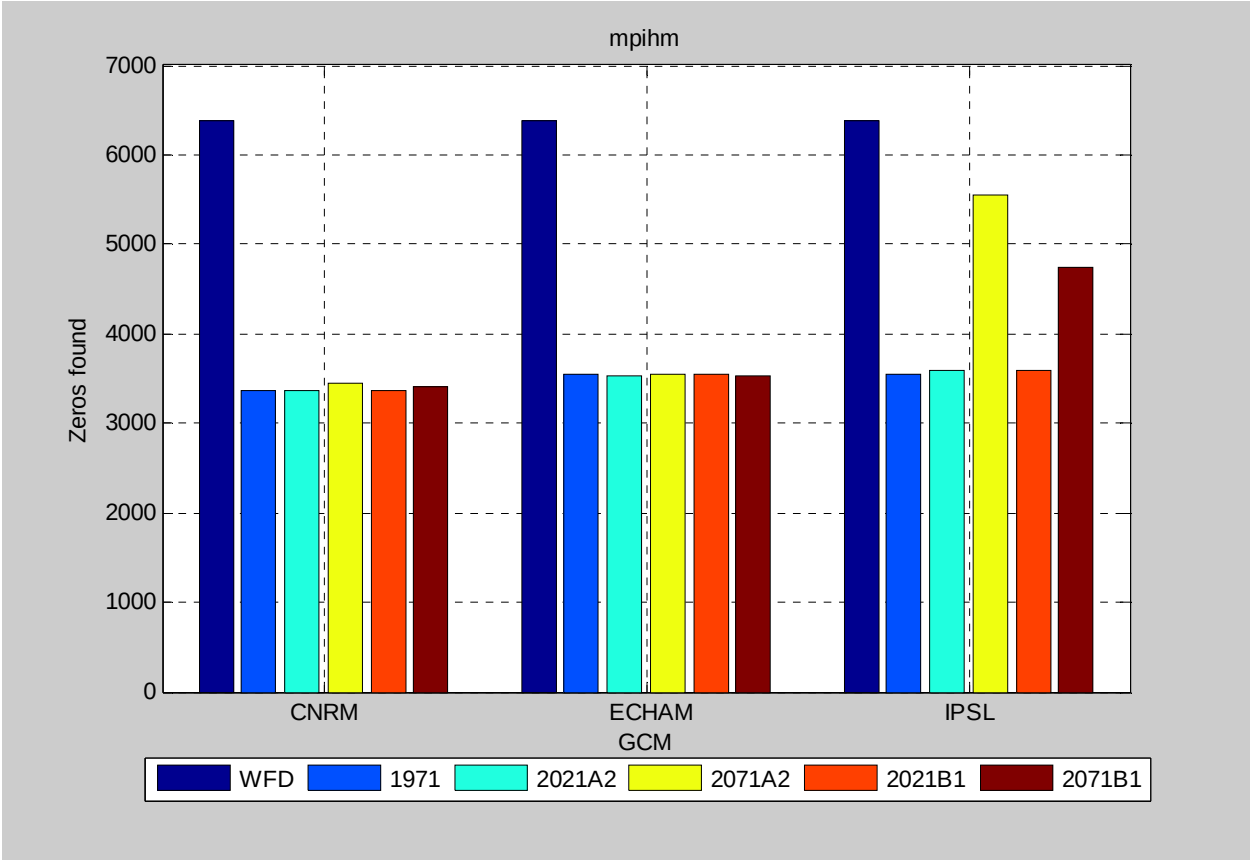

Number of Zeros.

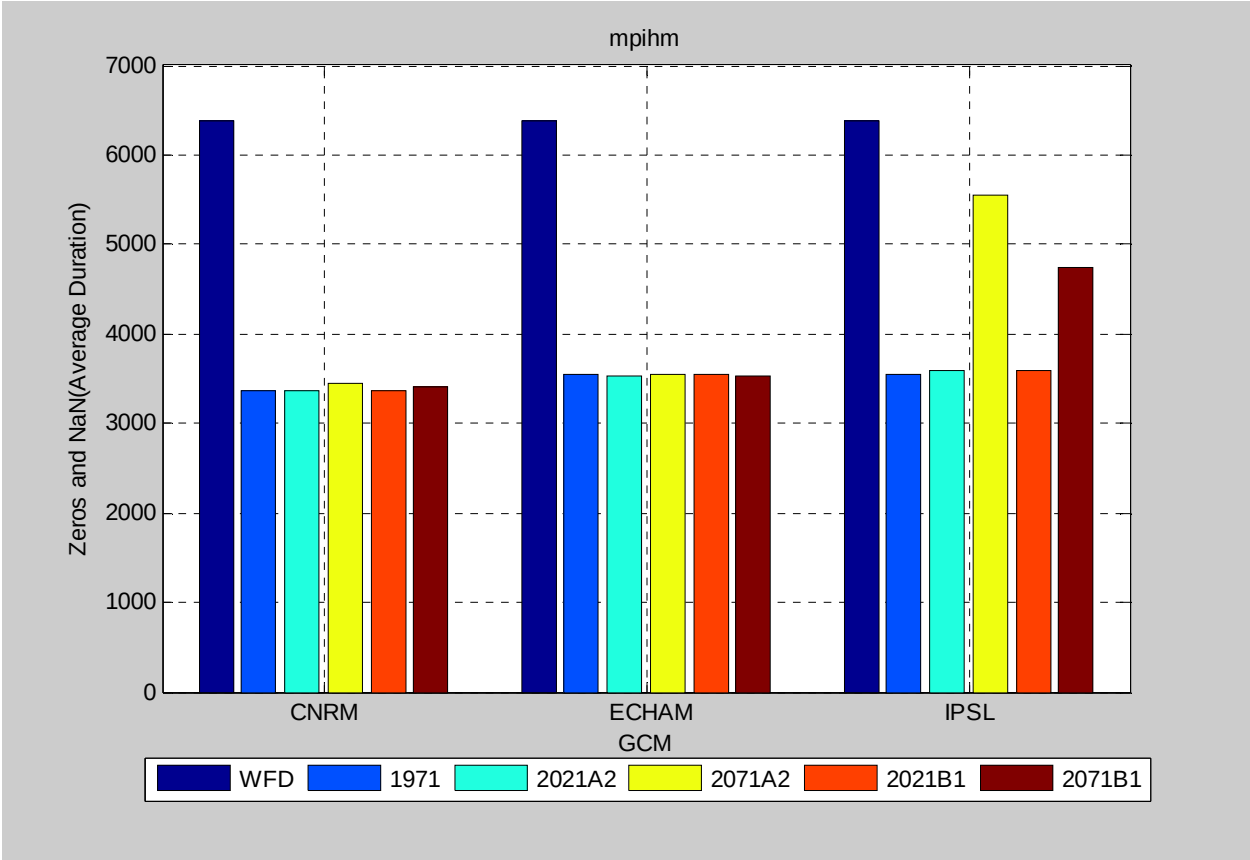

Number of arid regions (zeros + Nans) for control, mid and late 21st century.

2.5.3 PDF of average drought duration

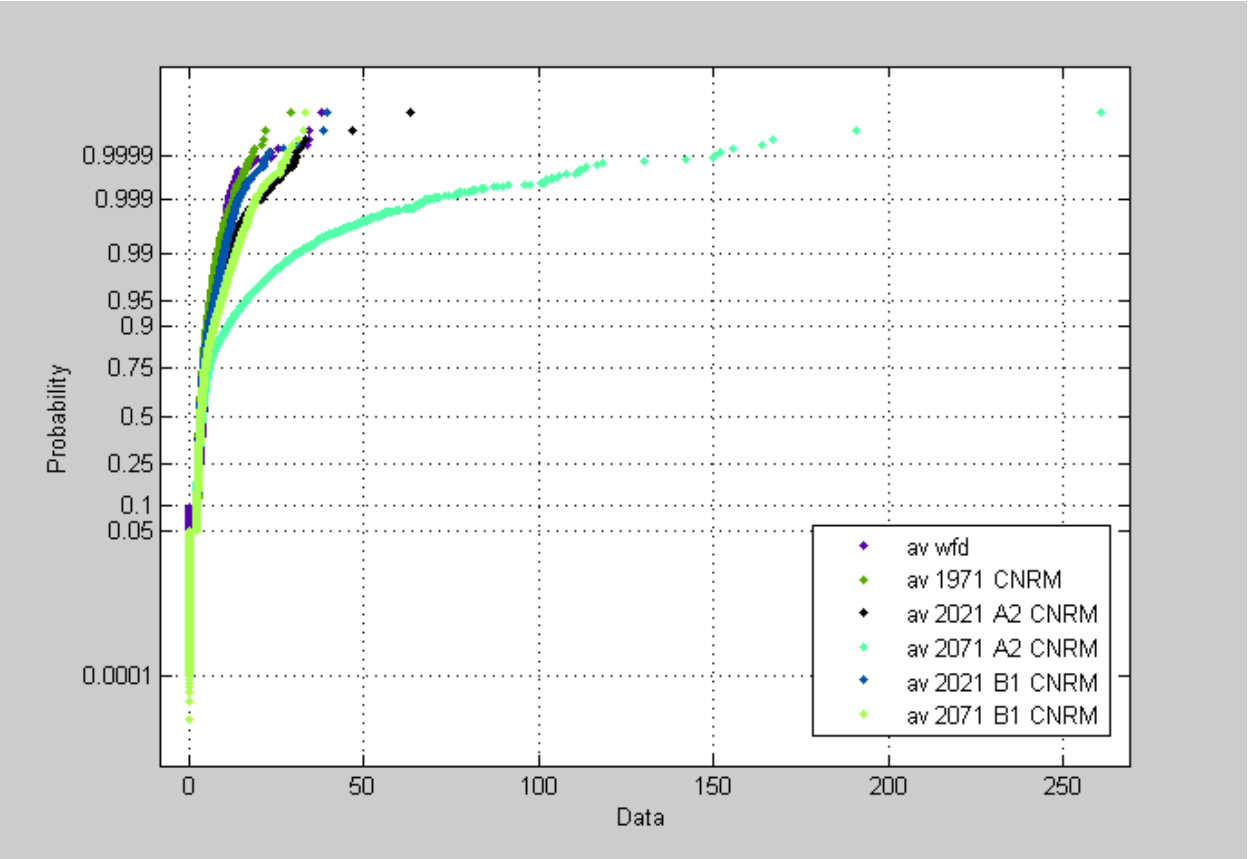

Probability density funtions of avarage drought durationsfor control, mid and late 21st century (not corrected for arid regions) as obtained with MPI-HM and CNRM climate input.

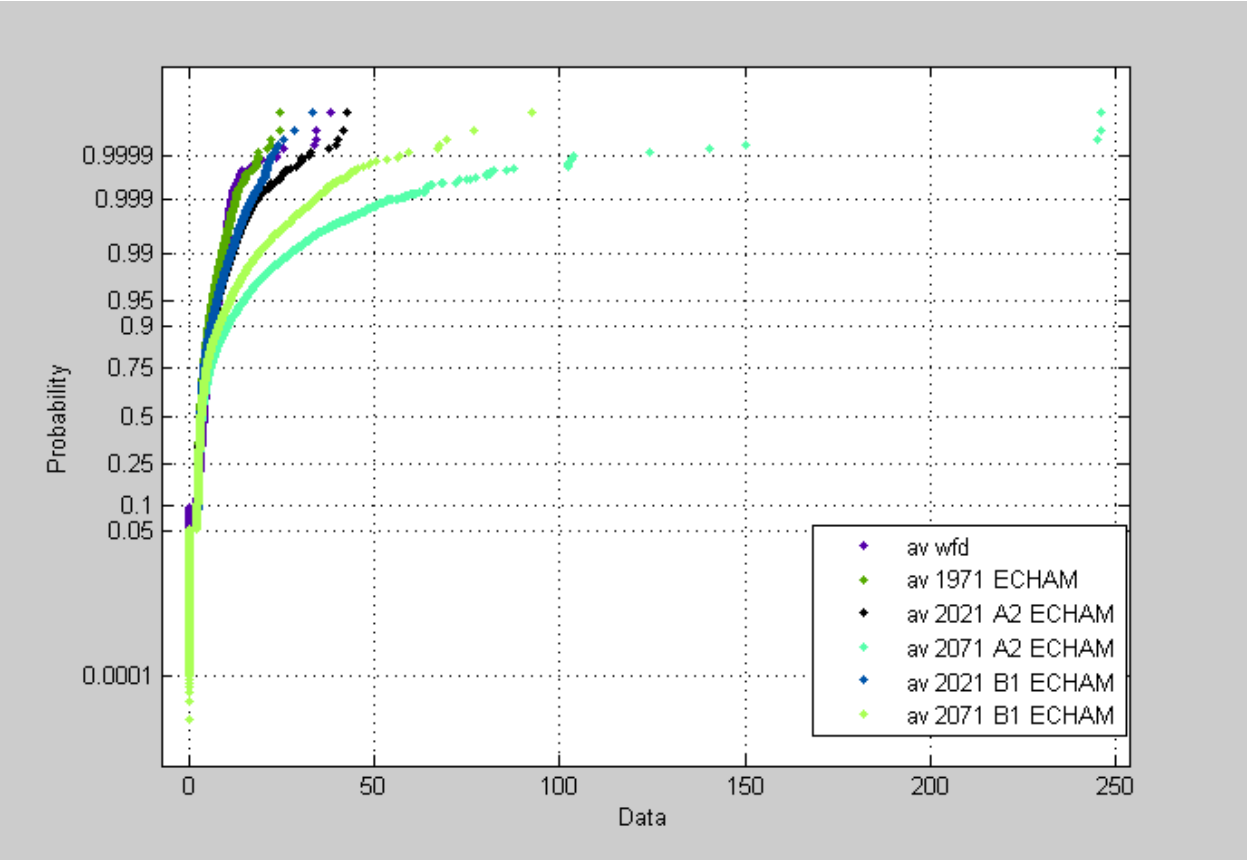

Probability density funtions of avarage drought durationsfor control, mid and late 21st century (not corrected for arid regions) as obtained with MPI-HM and ECHAM climate input.

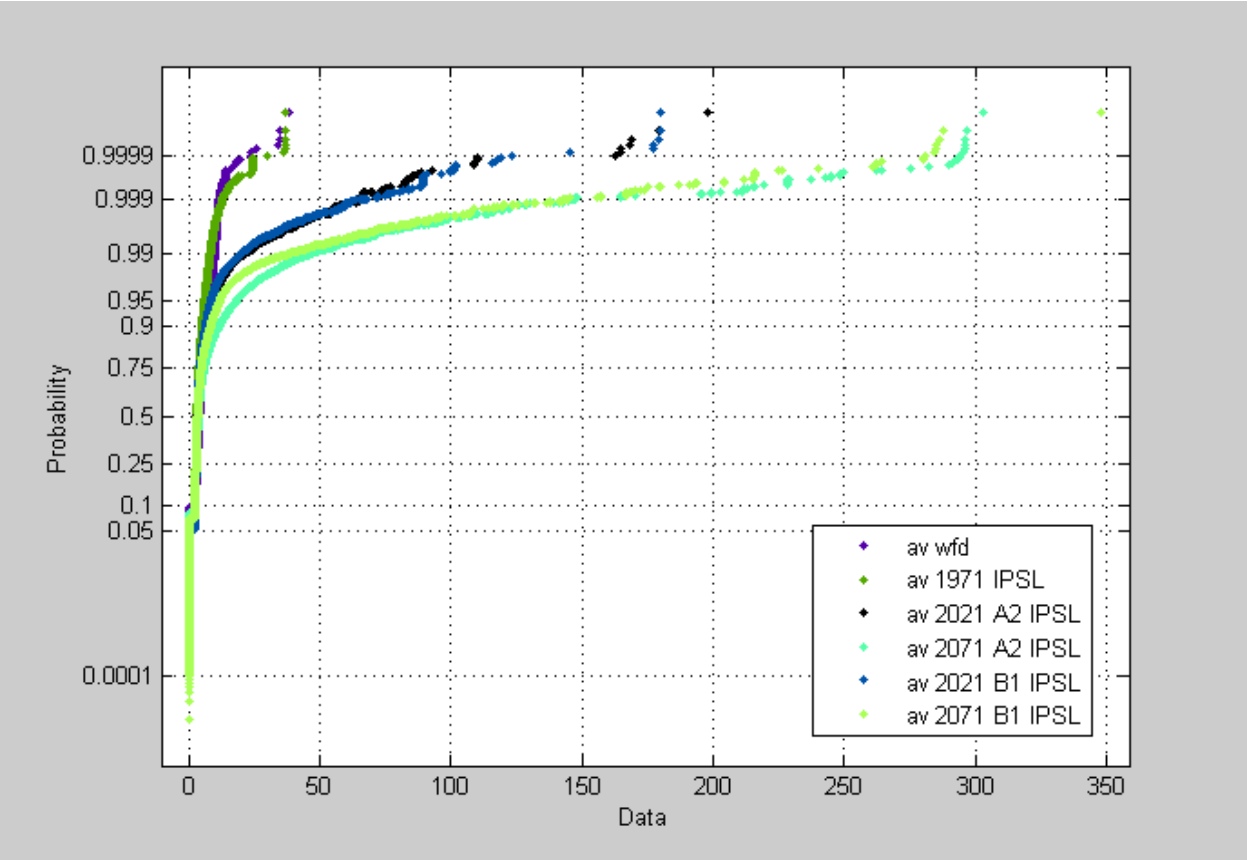

Probability density funtions of avarage drought durationsfor control, mid and late 21st century (not corrected for arid regions) as obtained with MPI-HM and IPSL climate input.

2.5.4 Analysis of MPI-HM with a drought equivalent index

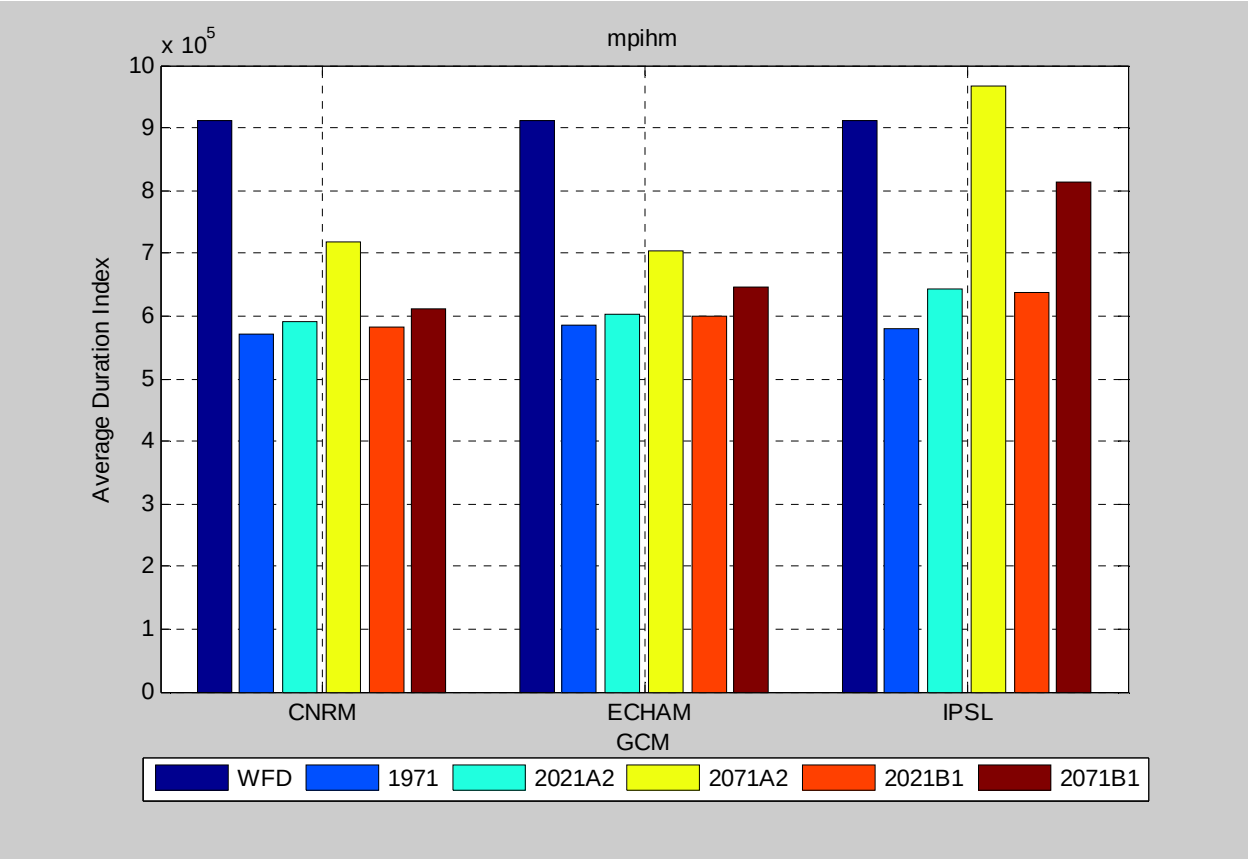

ANNEX 2.6 WATERGAP

2.6.1 Analysis of average drought duration

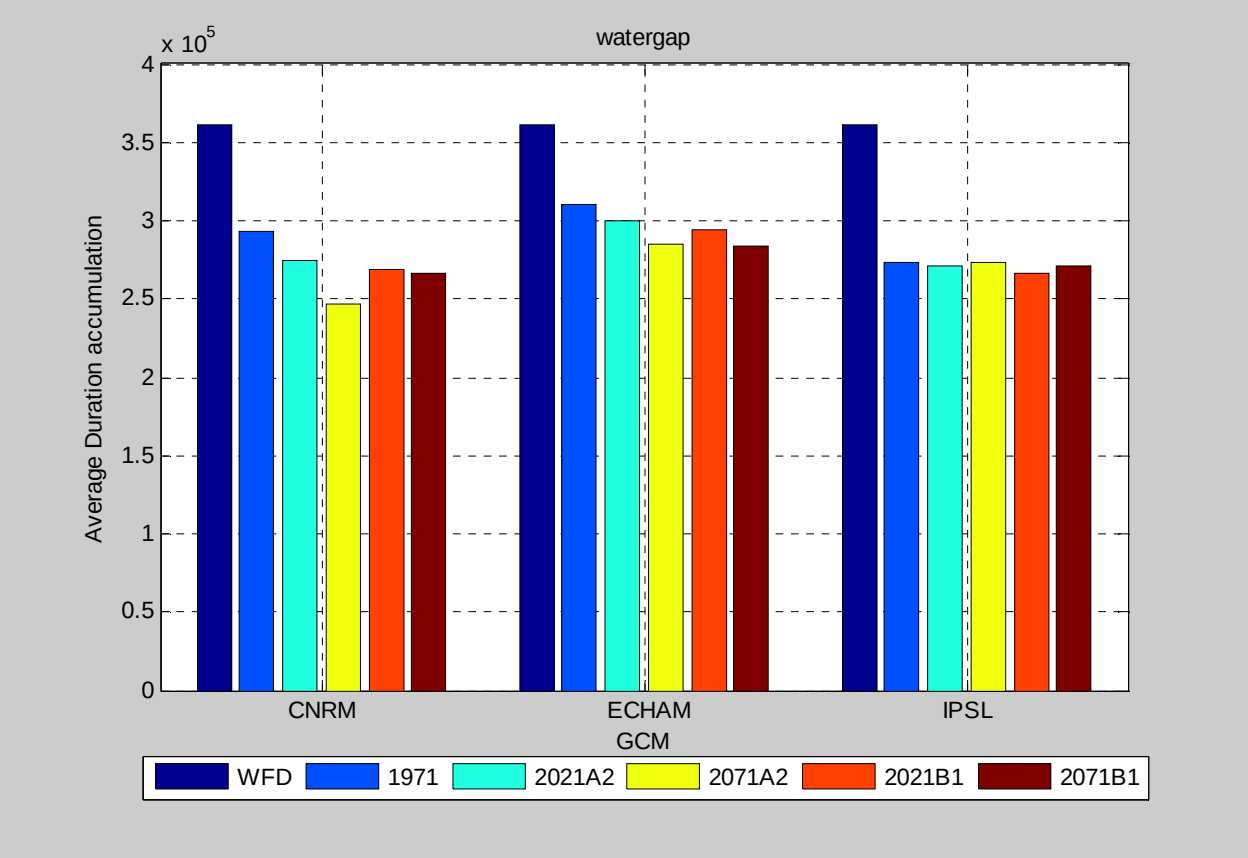

Accumulated average drought durations (for all cells) for control, mid and late 21st century (not corrected for arid regions).

2.6.2 Number of arid regions

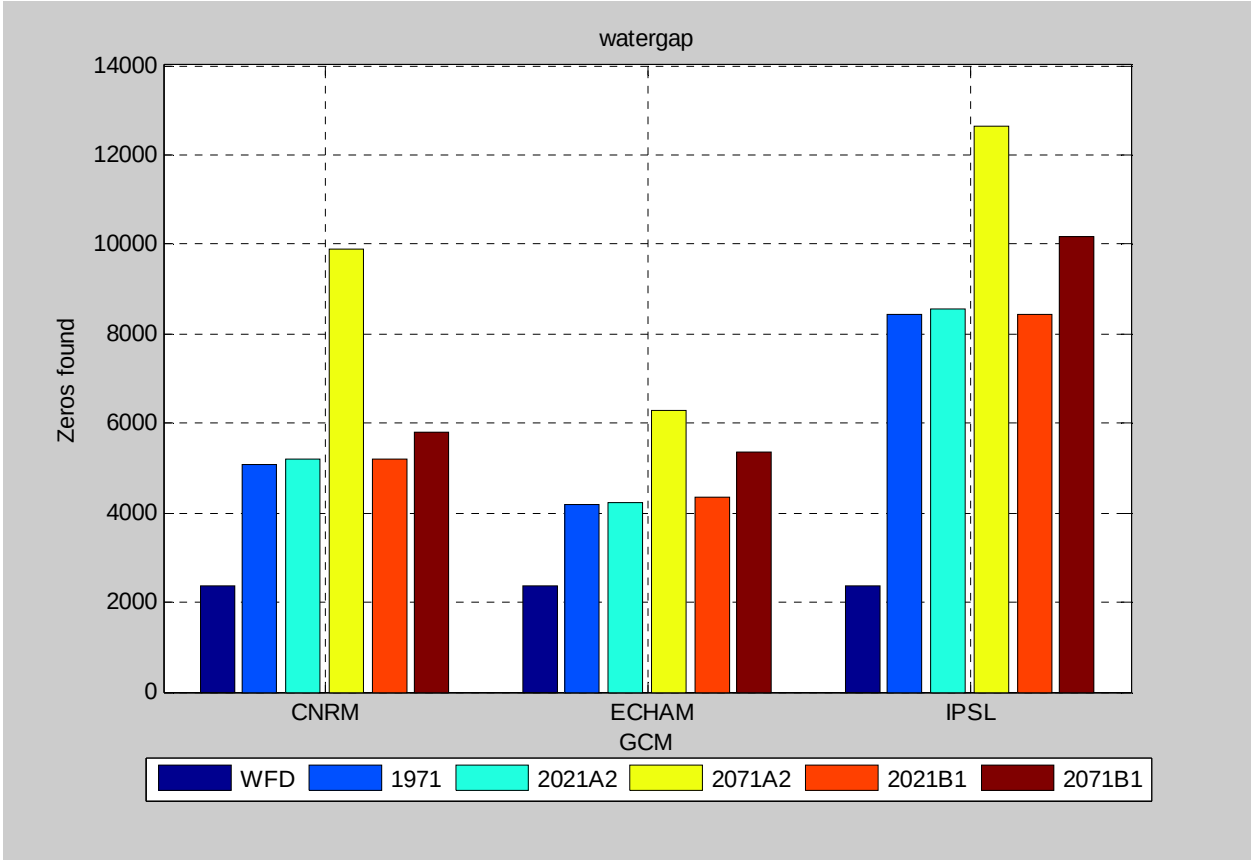

Number of Zeros.

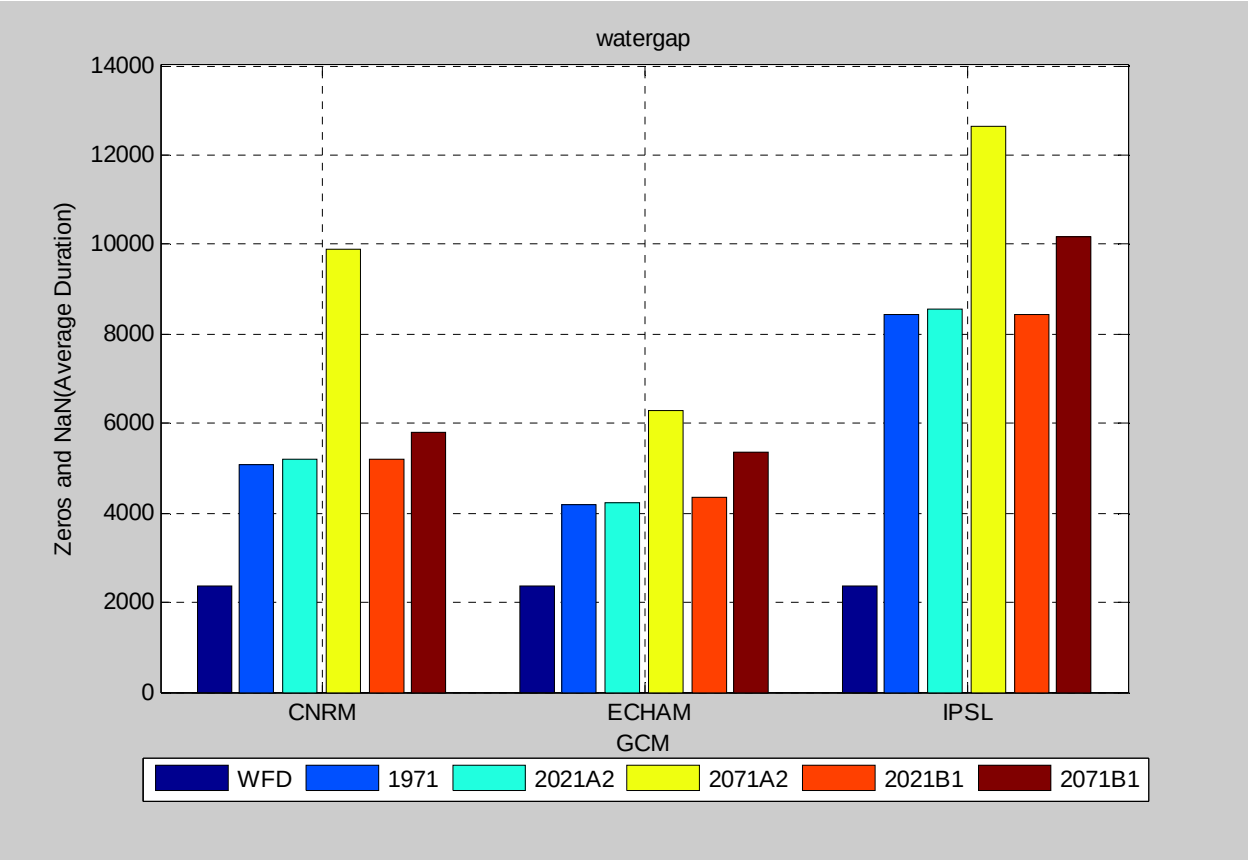

Number of arid regions (zeros + Nans) for control, mid and late 21st century.

2.6.3 PDF of average drought duration

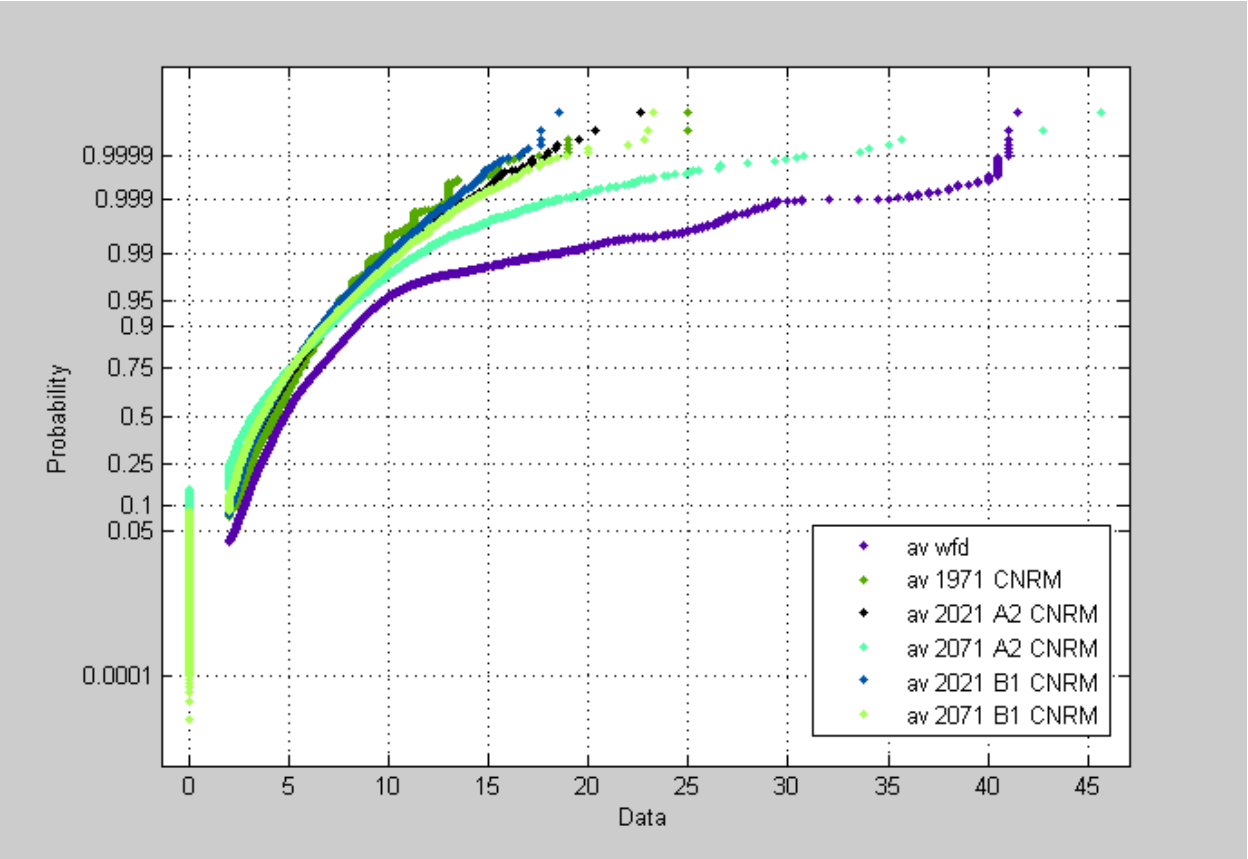

Probability density funtions of avarage drought durationsfor control, mid and late 21st century (not corrected for arid regions) as obtained with WaterGap and CNRM climate input.

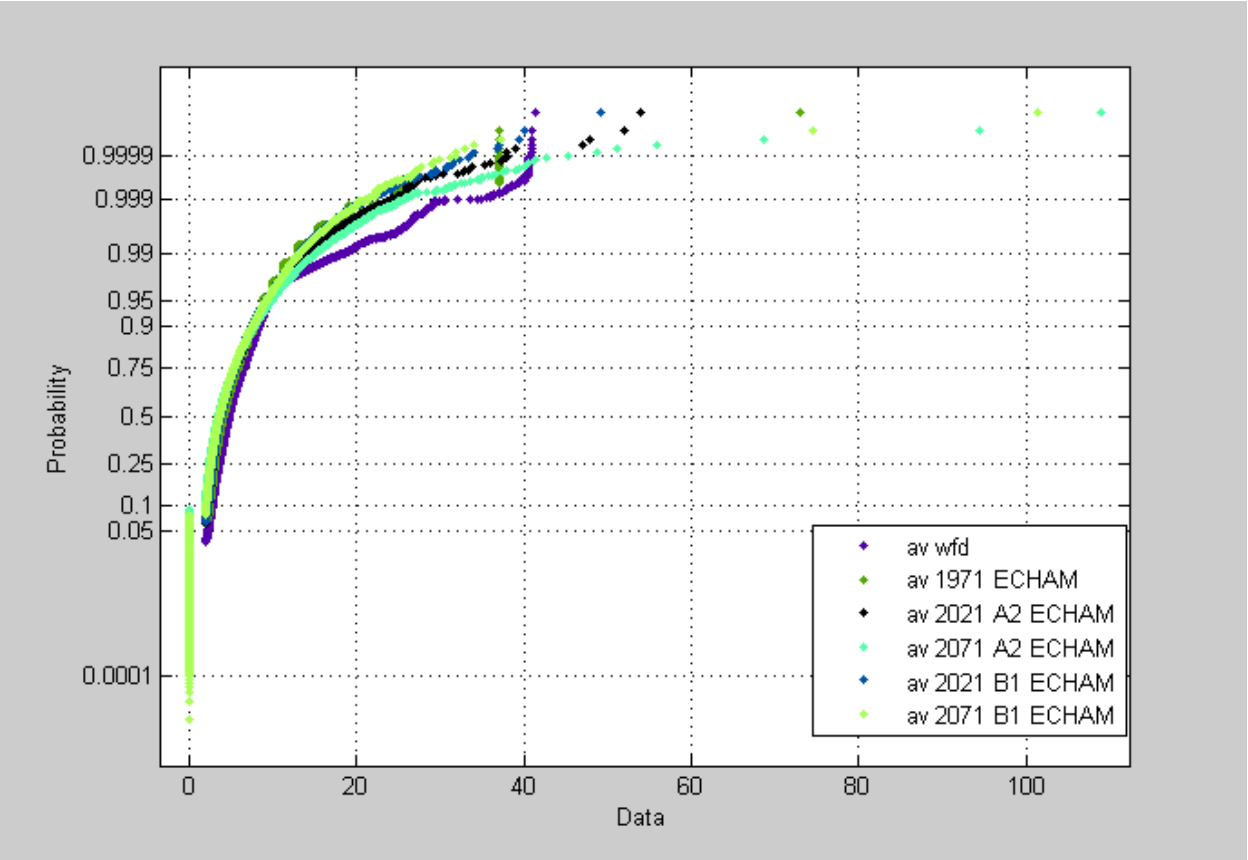

Probability density funtions of avarage drought durationsfor control, mid and late 21st century (not corrected for arid regions) as obtained with WaterGap and ECHAM climate input.

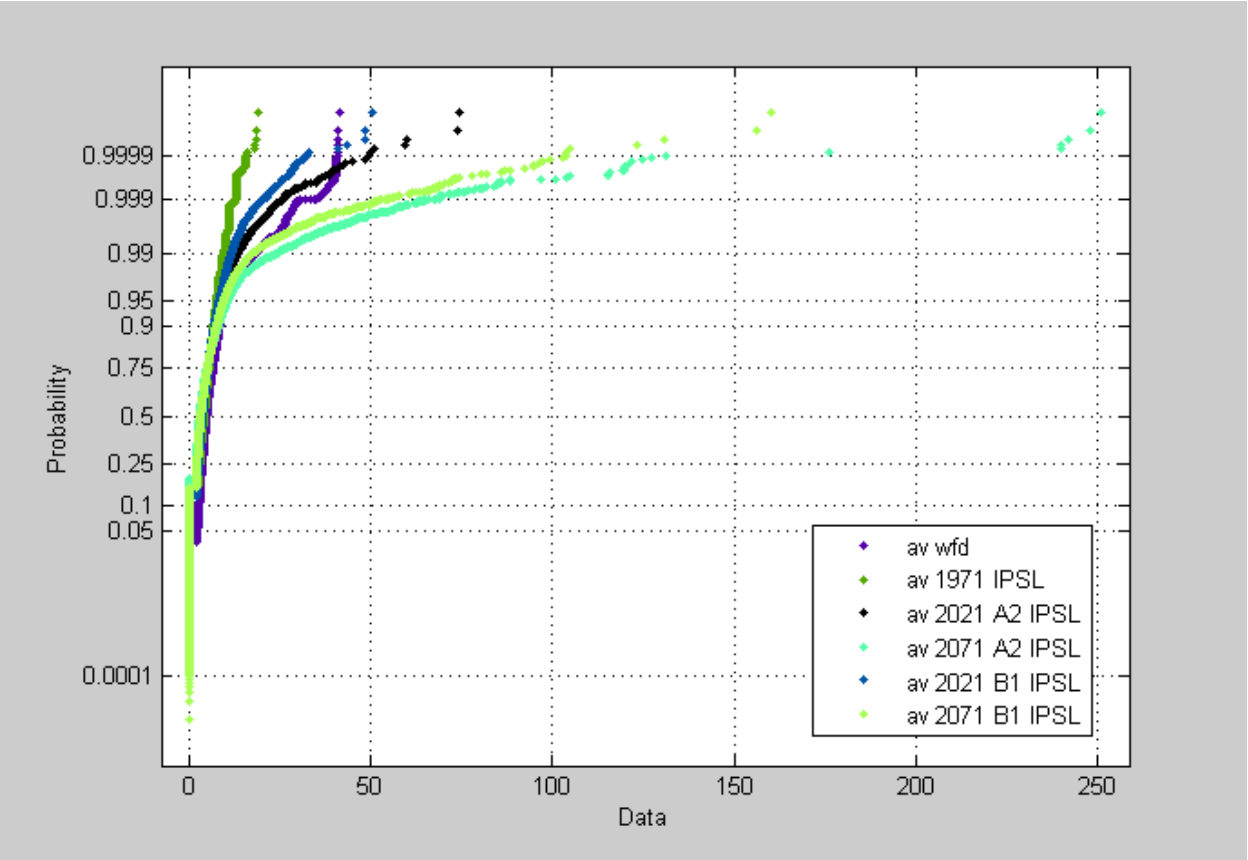

Probability density funtions of avarage drought durationsfor control, mid and late 21st century (not corrected for arid regions) as obtained with WaterGap and IPSL climate input.

2.6.4 Analysis of WaterGap with a drought equivalent index